Technische Universität München

Institut für Organische Chemie und Biochemie
Lehrstuhl für Biotechnologie

The effect of oxidative stress on *C. elegans*

Caroline Kumsta

Vollständiger Abdruck der von der Fakultät für Chemie der Technischen Universität München zur Erlangung des akademischen Grades eines

Doktors der Naturwissenschaften (Dr. rer. nat)

genehmigten Dissertation.

Vorsitzende: Univ.-Prof. Dr. S. Weinkauf

Prüfer der Dissertation:

1. Univ.-Prof. Dr. J. Buchner
2. Ass. Prof. U. Jakob, Ph.D.,
   University of Michigan, USA
3. Univ.-Prof. Dr. Th. Kiefhaber

Die Dissertation wurde am 25.09.2008 bei der Technischen Universität München eingereicht und durch die Fakultät für Chemie am 21.10.2008 angenommen.

Table of Contents

Abbreviations

2D	two-dimensional
ACN	acetonitrile
ATP	adenosine 5’-triphosphate
bp	basepair
BSA	bovine serum albumin
CAT	catalase
C. elegans	*Caenorhabditis elegans*
CGC	Caenorhabditis Genomic Center
C_P	peroxidatic cysteine
C_R	resolving cysteine
CS	citrate synthase
Cys	cysteine
Da, kDa	dalton, kilo dalton
DAB	denaturing alkylating buffer
ddH_2O	double distilled water
DIC	differential interference contrast
DNA	deoxyribonucleic acid
DTT	dithiothreitol
E. coli	*Escherichia coli*
ERK	extracellular signalregulated kinase
F	filial generation
Fwd	forward
g	gravitational force
GSH	glutathione

h	hours
H_2O_2	hydrogen peroxide
IAM	iodoacetamide
IEF	isoelectric focusing
ICAT	isoptope coated affinity ag
IGF-1	insulin growth factor 1
JNK	c-Jun amino-terminal kinase
m, cm, μm, nm	meter, centimeter, micrometer, nanometer
M, mM, μM	molar, millimolar, micromolar
MAPK	p38 mitogen activated protein kinase
min	minutes
MLS	mean lifespan
MnSOD	manganese superoxide dismutase
NF- κB	nuclear factor κ B
NGM	nematode growth medium
$^1O_2$	singlett oxygen
$^{\bullet}O_2^-$	superoxide radical
$^{\bullet}OH$	hydroxyl radical
P	parental generation
PAGE	polyacrylamide gel electrophoresis
PCR	polymerase chain reaction
pI	isoelectric point
PI(3)K	phosphoinositide 3-kinase
PRX	peroxiredoxin
Rev	reverse
RNA	ribonucleic acid

ROS	Reactive oxygen species
SE	standard error
SDS	sodium dodecyl sulfate
SL	spliced leader
SOD	superoxide dismutase
SOH	sulfenic acid
SO_2H	sulfinic acid
SRX	sulfiredoxin
TCA	trichloraceticacid
TRX	thioredoxin
UV	ultraviolet
V	volt
v/v	volume per volume
WT	wild type
w/v	weight per volume
Zn	zinc

Index of Figures

Index of Tables

1 Introduction and Outline

1.1 The riddle of the sphinx

In Greek mythology, the Sphinx sat outside of Thebes and would grant passage only to those travelers who solved her riddle: “What goes on four legs in the morning, on two legs at noon, and on three legs in the evening?” The answer, for gerontologists, is easy: “A man. In childhood he creeps on hands and knees, in manhood he walks upright, and in old age he walks with the aid of a cane.” The fascination of aging as life progresses is as old as mankind. The real riddle remains, however: “What is aging and why do we age?”

Aging can be defined as the decline of fitness and an increase in mortality as time goes by. In fact, the risk of death doubles every eight years for humans (Olshansky and Carnes 1997). Whereas most species’ mortality increases exponentially with age, aging is not a universal process (Kirkwood and Austad 2000). There are some species, such as sea turtles and some amphibians that do not exhibit an age-dependent decline in strength, agility or reproductive capability (Hayflick 2000). Even though their intrinsic risk of mortality does not increase over time, these animals are not immortal and still die of disease, poor environmental conditions and predation. These non-aging animals present unique research opportunities to validate various aging theories.

Over the last 150 years, scientists have been trying to explain why aging occurs. The extent of postulated theories became evident when the Russian biologist Zhores Medvedev catalogued more than 300 theories of aging (Medvedev 1990). Many of these theories are not mutually exclusive, and, in an attempt for a better classification, were recently summarized in three evolutionary theories of aging (Kirkwood and Austad 2000).

1.2 Evolutionary aging theories

Evolutionary aging theories are distinct from many other aging theories because they address the question “why do we age” rather than explaining the mechanistic process of aging. The theories on “how we age” address the cellular changes that occur in the lifetime of an organism and are summarized as mechanisms of senescence.

1.2.1 Mutation accumulation theory

The mutation accumulation theory was first postulated by Peter Medawar in 1952 and states that lethal genes that act late in life (after reproduction capability ceases) do not fall under evolutionary selection (Medawar 1952). Especially in the wild, where animals generally do not live long enough to grow old, deleterious mutations that exert their effects only late in life are able to accumulate because natural selection has limited opportunity to directly influence the mechanisms of aging. Hence, the force of selection weakens with increasing age (Kirkwood and Austad 2000). To illustrate in humans, Huntington’s disease is a lethal late-onset neurodegenerative disorder that is passed on to the next generation before the onset of the disease and is, therefore, not evolutionarily selected against.

1.2.2 Antagonistic pleiotropy theory

The antagonistic pleiotropy theory postulated by George C. Williams (1957) extends Medawar’s mutation accumulation theory and suggests that genes with beneficial effects early in life can have deleterious pleiotropic effects later on (Williams 1957). These genes are therefore even favored by natural selection. An example is the tumor suppressor gene p53, which acts to prevent cancer in younger individuals but might actually impair the cell’s capability for renewal later in life. If the force of natural selection is extended to later stages of life, it is conceivable that aging could be delayed. In accordance, selective breeding experiments in *Drosophila melanogaster,*

where mating is repressed until a later stage, give rise to strains that reproduce late in life and have an extended lifespan (Rose and Charlesworth 1980).

1.2.3 Disposable soma theory

Reproduction comes at a huge metabolic cost, and there seems to be a general correlation between reduced fecundity and long life (Kirkwood and Austad 2000). The disposable soma theory, postulated by Thomas Kirkwood in 1979, advocates that organisms have to balance their metabolic resources between cellular maintenance and reproduction (Kirkwood and Holliday 1979). A good illustration is the mouse, which does not live long enough to grow old in the wild due to predation or environmental conditions. From an evolutionary standpoint, it is not favorable to invest valuable resources into repair and maintenance mechanisms, because the lifespan of the mouse is so limited. Instead, investing this energy in increased reproduction will be advantageous for the survival of the mouse population. Because an organism then invests its resources into reproduction, mutations and other cellular damage can accumulate in somatic cells. The disposable soma theory therefore suggests that aging involves somatic damage. This implies that long-lived species have better repair systems than short-lived species. This prediction was validated in comparative biological studies that showed that the long-lived rodent species *Peromyscus leucopus* has more antioxidant enzymes, lower generation of reactive oxygen species and less oxidative damage than the relatively short-lived *Mus musculus*. The disposable soma theory suggests that mechanisms of senescence exist in postmitotic cells that lead to the aging of an organism. These mechanisms of senescence are often described as separate aging theories that attempt to explain the cellular changes that occur over the lifetime of an organism.

1.2.4 Mechanisms of senescence

The process of senescence is complex and could be the result of one or many mechanisms. The “error catastrophe theory” suggests that errors in proteins involved in transcription and translation will lead to further errors, which will ultimately lead to an error crisis that disrupts cellular function (Goel and Ycas 1976). The “genome maintenance theory” advocates that accumulating mutations will affect normal gene regulation and will lead to genomic instability (Medvedev 1990). Genomic and chromosomal instability could also be caused by “telomere shortening” that occurs with each cell division and contributes to replicative senescence (Counter et al. 1992). The “glycation theory” proposes that the nonenzymatic reaction of glucose and other reducing sugars with proteins and nucleic acids leads to structural and functional changes of proteins (Medvedev 1990). Along the same lines, the free radical theory of aging postulates that reactive oxygen species (ROS) react with biomolecules, such as DNA, lipids and proteins, leading to structural and functional changes that contribute to cellular senescence (Harman 1956). It is possible that any number of these senescence mechanisms occur simultaneously and that cumulative effects increase functional decline and promote aging. For instance, accumulation of mutations in the genome as well as errors in proteins that affect transcription and translation could be a consequence of damage by ROS. Hence, the major challenge in gerontological research is the separation of the mechanisms that *cause* aging from the events that take place due to these aging mechanisms.

1.3 Free radical theory of aging

One of the most popular theories on the mechanisms of aging is the free radical theory of aging. Denham Harman (1956) suggested that the progressive decline in the functional capacity of aging organisms is a consequence of the accumulation of

oxidative damage caused by reactive oxygen species (ROS) (Harman 1956). Several lines of correlative evidence support this theory. It has been shown, for instance, that the extent of oxidative damage to macromolecules and the rate of ROS generation increase with the age of an organism and that this increase is inversely related to the mean lifespan of that species (Stadtman et al. 1992). Accordingly, the levels of oxidatively modified proteins in fibroblasts from individuals with the age-accelerating genetic disease progeria are shown to be significantly higher than age-matched control. Strong evidence for the free radical theory of aging also stems from long-lived mutants of *Drosophila melanogaster* and *Caenorhabditis elegans* with downregulated insulin/IGF-1 like signaling. These longevity mutants are resistant to oxidative, heat and ultraviolet stress, conditions that are known to either cause or be accompanied by the accumulation of toxic ROS (Sampayo et al. 2003). This increased stress resistance appears to be due to the up-regulation of the ROS-detoxifying enzyme MnSOD (Manganese Superoxide Dismutase) (Honda and Honda 1999). In accordance, a decline of the ROS-detoxifiying enzyme MnSOD is reported in patients suffering from progeria (Macmillan-Crow and Cruthirds 2001). The direct administration of antioxidants, however, does not increase maximum lifespan even though oxidative damage is decreased (Blokhina et al. 2003). In this case, it is likely that the presence of cellular redox regulating systems that balance oxidants and antioxidants alleviate the effects of the excess antioxidants.

Currently it is still unclear whether accumulating ROS are directly implicated in the aging process. It is undeniable, however, that increased concentrations of ROS have deleterious effects on most cellular macromolecules and that potent redox balancing systems exist to counteract this threat. A more complete understanding of the accumulation of ROS and the cellular responses to oxidative stress should provide significant insights into aging.

1.4 Oxidant production and oxidative stress

Reactive oxygen species (ROS) such as superoxide radicals ($^{\bullet}O_2^-$), hydrogen peroxide (H_2O_2) and hydroxyl radicals ($^{\bullet}OH$) arise during normal metabolism, mostly due to incomplete electron transfer in the respiratory chain (Apel and Hirt 2004). The cell can cope with low levels of ROS due to a number of detoxifying enzymes and redox balancing systems (Storz and Imlay 1999). These strategies of general oxidative defense can become inadequate under conditions where increased levels of ROS are encountered. When the concentration of ROS becomes too high to be properly removed by the general oxidative response, the cell suffers from a condition termed oxidative stress (Figure 1.1). Oxidative stress can be endogenously caused by defects in energy metabolism, such as impaired glycolysis or the damage to cellular antioxidant systems (Stadtman 2001; Aliev et al. 2002). Then, the redox homeostasis gets shifted towards more oxidizing conditions and ROS further accumulate.

The accumulation of ROS under oxidative stress conditions can lead to severe DNA, lipid and protein damage (Dean et al. 1997; Imlay 2003). The predominant cellular targets of ROS are the amino acids of proteins. The most sensitive amino acids are the sulfur-containing methionine and cysteine residues, whose side chains undergo a variety of largely reversible oxidative modifications (Storz and Imlay 1999; Hoshi and Heinemann 2001; Fratelli et al. 2004). Irreversible oxidative side chain modifications include oxidation of aromatic amino acids and carbonylations, which often lead to the inactivation of the affected proteins and increase the susceptibility to proteolysis and aggregation (Naskalski 1994; Yan and Sohal 2001). Such protein damage has been implicated to be the leading cause in a variety of pathologies including neurodegenerative disease, cancer, atherosclerosis, diabetes, heart disease and

aging (Finkel and Holbrook 2000; Kovacic and Jacintho 2001; Aliev et al. 2002; Kyselova et al. 2002) (Figure 1.1).

1.5 Oxidants in cellular signaling

Besides the damaging effect of ROS to various cellular components, ROS also act as specific messenger molecules and trigger the activation of several signaling pathways in response to oxidative stress. In response to oxidant injury, three signaling pathways are activated: (i) extracellular signal-regulated kinase (ERK), (ii) c-Jun amino-terminal kinase (JNK) and (iii) p38 mitogen activated protein kinase (MAPK). In addition, the phosphoinositide 3-kinase (PI(3)K/Akt) pathway, the nuclear factor κ B signaling (NF-κB) system, tumor suppressor protein p53 and the heat shock response are also activated by ROS (for review (Finkel and Holbrook 2000)). These signaling pathways are not exclusively activated by oxidative stress and can also function in normal growth and metabolism.

Very little is known about the sensoring mechanisms and the initiating events of these pathways in response to oxidants. In the case of the ERK and the PI(3)K/Akt signaling pathways, activation is mainly achieved by the stimulation of growth factor receptors, where the oxidants are thought to mimic the actions of natural ligands (Blanc et al. 2003). Another way of modulating the signaling capacity of these receptors is by phosphorylation. Endogenous oxidative stress treatment was shown to increase phosphorylation of the growth factor receptors. This could be due to oxidant-mediated inactivation of specific phosphatases that are required for dephosphorylation (Stone and Yang 2006).

The NF-κB pathway is activated by ROS, which leads to an increase in nuclear translocation of NF-κB and, thus, modulation of the transcription of downstream targets. Paradoxically, NF-κB can also be directly inactivated by the oxidation of a

cysteine residue. This oxidative modification disturbs the DNA binding domain, which leads to a decrease in transcription of NF-κB inducible genes (Bowie and O'Neill 2000). Similar posttranslational modifications also modulate the DNA binding activity of the tumor suppressor protein p53. Glutathionylation of the Zn-center of p53 was shown to occur both *in vitro* and *in vivo* and leads to inactivation of p53 (Liu et al. 2008). In contrast to the NF-κB pathway, the ROS-mediated increase in p53 leads to a further increase in ROS concentration. ROS-induced activation of p53, JNK and p38 are commonly linked to apoptosis, and this positive feedback loop might be important for the induction of the apoptotic response. The heat shock response, ERK, PI(3)K/Akt and NF-κB signaling, on the other hand, trigger survival pathways by the induction of many genes that are involved in scavenging ROS or act as chaperones (Finkel and Holbrook 2000).

Taken together, the generation of high concentrations of ROS can perturb normal redox balance and shift cells into a state of oxidative stress. At low concentrations ROS are also important in the activation of various response pathways that can ultimately lead to the important decision of survival of the cell or apoptosis. The maintenance of ROS homeostasis is critical for normal metabolism, and investigating the specific action of ROS in these various pathways is important for the understanding of normal cell differentiation, host defense and disease states such as cancer, artherosclerosis and aging (Figure 1.1).

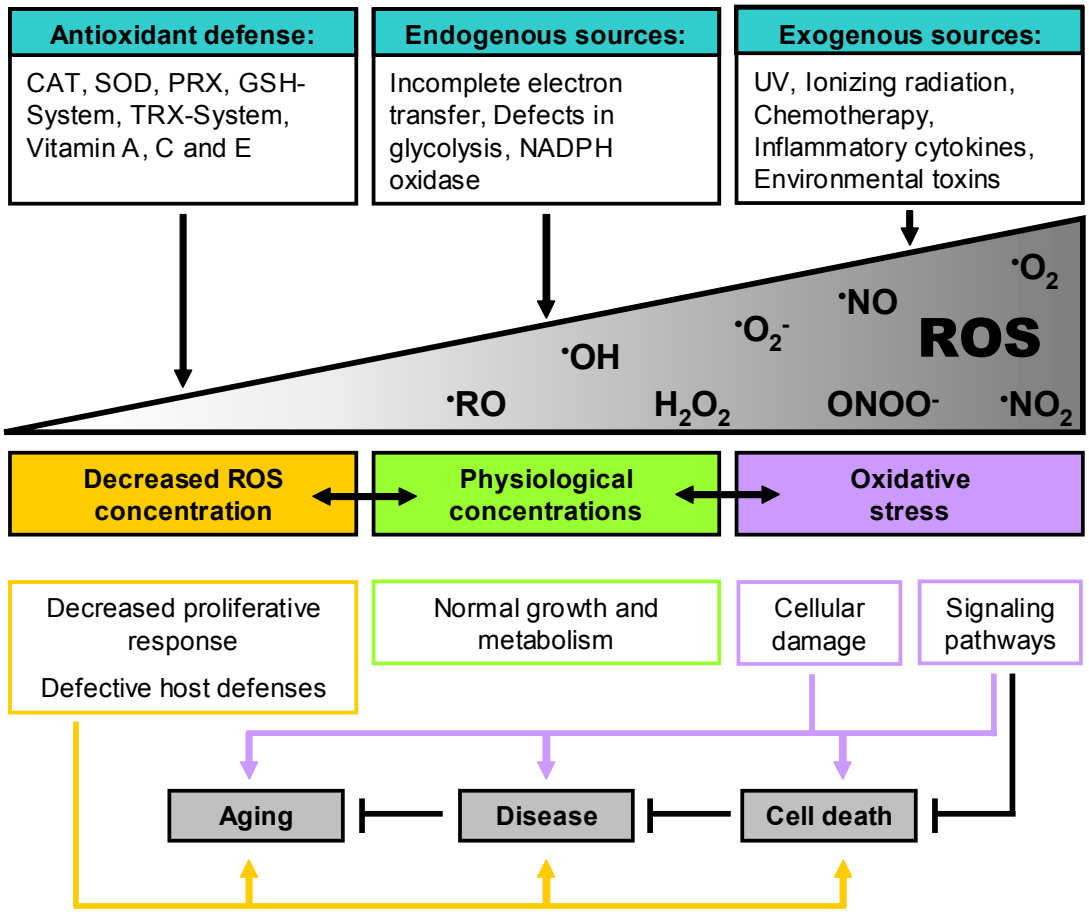

Figure 1.1: The sources of and responses to cellular reactive oxygen species (ROS)

ROS are generated endogenously due to incomplete electron transfer in the mitochondria, or exogenously by a number of environmental sources. The antioxidant defense counteracts the accumulation of cellular ROS to maintain homeostatic ROS concentrations. Antioxidant systems include enzymes such as catalase (CAT), superoxide dismutase (SOD) and peroxiredoxins (PRX), redox balancing systems such as the glutathione (GSH)-system, the thioredoxin (TRX) system and non-enzymatic components such as various vitamins. If intracellular ROS levels become too low, proliferation and host defense might be disturbed. If the ROS concentration becomes too high, the cell suffers from oxidative stress and cellular damage can occur. Simultaneously, ROS can function in various signaling pathways. Both increased and decreased ROS levels may have either damaging or potentially protective functions for the cell and, consequently the organism. Figure modified from (Finkel and Holbrook 2000).

1.6 Antioxidant defense

To maintain physiological concentrations of ROS, many antioxidant enzymes and redox balancing systems have evolved. The enzymatic defense systems that directly destroy ROS include superoxide dismutase (SOD), catalases (CAT), peroxiredoxins (PRX) and peroxidases. The thioredoxin (TRX) system and the glutathione (GSH) system, on the other hand, preserve redox homeostasis by maintaining a highly reducing environment in the cytosol (Deneke 2000) (Figure 1.1). The tripeptide glutathione (GSH) is very versatile in its protective role against oxidative stress. Besides being an important redox buffer component, GSH is also able to directly scavenge hydroxyl radicals ($^{\bullet}OH$) and singlet oxygen ($^1O_2$). Superoxide radicals ($^{\bullet}O_2^-$) are dismutated by SOD to hydrogen peroxide (H_2O_2) (Jefferies et al. 2003). H_2O_2 can then be detoxified by catalase, peroxiredoxins and glutathione peroxidase. Catalase, one of the most efficient enzymes known, reduces two molecules of H_2O_2 to a molecule of water and oxygen. CAT is a tetrameric heme containing enzyme that does not consume any reducing equivalents in the removal of H_2O_2 (Michiels et al. 1994). In eukaryotes, this energy efficient mechanism occurs mainly, but not exclusively, in peroxisomes where CAT oxidizes substrates such as phenols, formaldehyde and alcohol in a peroxidation reaction (Schrader and Fahimi 2006). *C. elegans* deficient in peroxisomal CAT *(ctl-2)* are short-lived (Petriv and Rachubinski 2004) and prokaryotes and certain human cell types that lack CAT are hypersensitive to oxidative stress. In contrast, the lack of cytosolic catalase in *C. elegans (ctl-1),* as well as catalase knock-out mice, do not display any apparent phenotypes (Reaume et al. 1996). It is possible that other antioxidant proteins, such as the high abundant peroxiredoxins can compensate for the loss of catalase and play an equally important role as H_2O_2 scavengers.

1.7 Peroxiredoxins

Peroxiredoxins (PRX) are a highly conserved family of antioxidant enzymes, which have been identified in bacteria, yeast, plants and mammals (Hofmann et al. 2002). Although PRX are mainly cytosolic proteins, isoforms exclusively expressed in mitochondria, chloroplasts, peroxisomes, or associated with nuclei and membranes have been identified in different organisms (Hofmann et al. 2002).

PRX reduce H_2O_2, peroxynitrite and various organic hydroperoxides, thereby help to maintain intracellular redox balance and protect organisms from oxidative stress. Their moderate catalytic efficiency (10^5 $M^{-1}s^{-1}$) compared with glutathione peroxidases (10^8 $M^{-1}s^{-1}$) and catalase (10^6 $M^{-1}s^{-1}$) is compensated for by their high cellular abundance (Hillar et al. 2000; Hofmann et al. 2002). PRXs constitute 0.1-0.8 % of all soluble proteins in mammalian cells. They are the third most abundant proteins in erythrocytes and among the ten most highly expressed proteins in *E. coli* (Moore et al. 1991; Link et al. 1997; Chae et al. 1999).

Structurally, PRX possess a thioredoxin fold with a few additional secondary structure features present as insertions (Wood et al. 2003b). Peroxiredoxins can be divided into three different classes, 1-Cys PRX, atypical 2-Cys PRX and typical 2-Cys PRX. All peroxiredoxins share the same basic catalytic mechanism, where the conserved active-site cysteine, termed the peroxidatic cysteine (C_P) is oxidized by the substrate to a sulfenic acid (SOH) (Ellis and Poole 1997). The mechanism of C_P regeneration though is different among the three classes. 1-Cys PRX contain only the conserved peroxidatic cysteine and are regenerated by a thiol-containing electron donor, whose identity is still unknown (for review (Wood et al. 2003b; Rhee et al. 2005)). 2-Cys PRX contain two conserved cysteines, where C_P in the N-terminus is catalytically active and the resolving cysteine (C_R) in the C-terminus. In atypical 2-Cys PRX,

which are monomeric proteins, reaction of the resolving cysteine with the sulfenic acid of C_P results in intramolecular disulfide bond formation, which can be resolved by thioredoxin (Seo et al. 2000).

Typical 2-Cys PRX, such as PrxI, II from yeast and PrxII from humans are obligate homodimers. The sulfenic acid is resolved by an intermolecular disulfide bond C_P-SOH of one subunit and C_R present on the other polypeptide chain. The dimer of typical 2-Cys PRX is domain swapped; the C-terminus of one subunit reaches across the dimer interface to interact with the other subunit for disulfide bond formation (Hirotsu et al. 1999; Alphey et al. 2000; Schroder et al. 2000). Reduction of this disulfide bond is carried out by one of the cell specific disulfide oxidoreductases, such as thioredoxin or AhpF (Poole et al. 2000; Bryk et al. 2002).

Eukaryotic PRX have been implicated in a range of other cellular functions besides ROS detoxification, such as the regulation of peroxide-mediated signaling cascades, regulation of NF-κB activity and apoptosis (Delaunay et al. 2002; Kang et al. 2004; Veal et al. 2004). They are overexpressed in disease states such as cancer and neurodegenerative diseases and appear to play neuroprotective roles in models of Parkinson's and Alzheimer's disease (Kinnula et al. 2002; Krapfenbauer et al. 2003; Hattori and Oikawa 2007).

1.7.1 Oligomerization is dependent on the redox-state

Typical 2-Cys PRX, from here on referred to as PRX, function as head-to-tail arranged homodimers. In addition, studies showed that PRX are also present as homopolymeric complexes under native conditions. X-ray crystal structures for a number of different 2-Cys PRX have shown that they exist either as (α_2) homodimers or as toroid shaped complexes consisting of pentameric arrangement of dimers $(\alpha_2)_5$. Electron microscopy of mammalian PrxII revealed discrete complexes with apparent

ten-fold symmetry that also formed higher order multimers by stacking into columns of various lengths (for review (Wood et al. 2003b)). Purified yeast PrxI elutes from a size exclusion column in stable complexes ranging from 40 kDa dimers to high molecular weight complexes of more than 1000 kDa (Jang et al. 2004).

Various factors were shown to promote PRX oligomerization, such as ionic strength, low pH, high magnesium or calcium concentration and elevated temperature (Wood et al. 2003b). The most important factor, however, seems to be the redox state of the active site cysteine C_P of PRX. Analytical ultracentrifugation experiments of several bacterial PRX showed that the reduced form of C_P stabilizes the decameric forms of PRX (Wood et al. 2002), while studies with human PrxII suggested that the overoxidation of the peroxidatic cysteine to sulfinic acid drives the formation of high molecular weight oligomers (Moon et al. 2005).

1.7.2 Peroxiredoxins undergo structural changes upon overoxidation

Eukaryotic peroxiredoxins are highly susceptible to inactivation through "overoxidation" in the presence of high H_2O_2 concentrations. Overoxidation is the formation of a sulfinic acid (SO_2H) at the peroxidatic cysteine. In the reduced, fully folded conformation, C_P is located within a helix forming a highly conserved peroxidatic active site. The pyrrolidine ring of a conserved proline near C_P limits the solvent and peroxide accessibility of C_P-SOH and shields it from further oxidation (Wood et al. 2003a; Wood et al. 2003b). The resolving cysteine C_R is located 14 Å apart, oriented in the opposite direction and partially buried. The condensation reaction requires substantial conformational changes to allow disulfide bond formation of C_P-SOH and C_R-SH. This local unfolding of the C_P loop makes it solvent exposed and accessible for disulfide bond formation. In the presence of high peroxide concentrations, however, this solvent-accessibility also makes C_P prone to further oxidation to C_P-SO_2H (Figure 1.2). Interestingly, the overoxidation seems to be

unique to eukaryotic PRX (Wood et al. 2003a). Structural comparisons of eukaryotic PRXs with bacterial AhpC, which appears to be resistant to overoxidation, suggested that structural stabilization of the C-terminus might promote overoxidation in eukoryotic PRX. Eukaryotic PRX contain a GGLG loop motif and an additional α-helix with a conserved YF motif in the C-terminus (Figure 1.2 and Figure 1.3). In the reduced state, both GGLG loop and the extended C-terminus appear to cover the active site helix that contains the catalytic C_P. The C-terminus of eukaryotic PRXs is thus, structurally much more rigid than the C-terminus of bacterial AhpC. In eukaryotes, two local unfolding events are required to allow disulfide bond formation: unfolding of the α-helical loop that contains C_P and unfolding of the extended C-terminus with YF motif. This additional motif is proposed to slow down the local unfolding and subsequent disulfide bond formation and thus might allow for further oxidation of the peroxidatic cysteine (Wood et al. 2003a; Wood et al. 2003b).

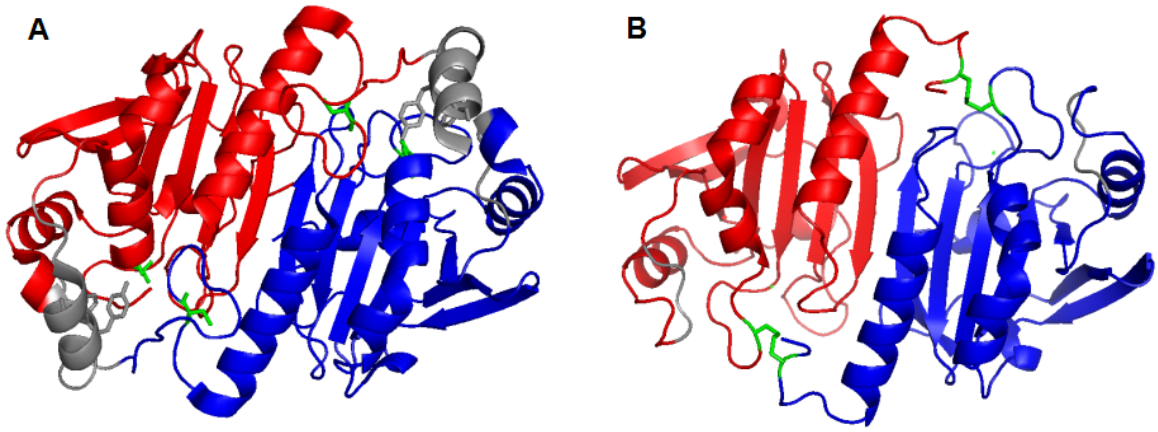

Figure 1.2: Crystal structure of human PrxII

The different polypeptide chains of the domain swapped homodimer are colored in red and blue, respectively. The peroxidatic and resolving cysteines are depicted in green. ***A)*** *The peroxidatic cysteine is overoxidized to a sulfinic acid, the extended C-terminal α-helix is fully folded and depicted in grey.* ***B)*** *The peroxidatic cysteine forms a disulfide bond with the resolving cysteine on the other polypeptide chain, the C-terminal α-helix unfolded to allow disulfide bond formation.*

In agreement with these structural considerations, C-terminally truncated yeast PrxI mutants are resistant towards overoxidation. HeLa cells expressing a truncated version of human PrxII, do not show any PrxII high molecular weight complexes upon treatment with H_2O_2, which supports the notion that overoxidation is the driving force of oligomerization (Moon et al. 2005). Moreover, the assembly into high molecular weight oligomers is also reduced when overoxidation of C_P is blocked by mutagenesis of C_P to serine but not by mutagenesis of C_R.

The association of AhpC into decamers was shown to be largely dependent on the redox-state. In the reduced state, where the C_P containing loop is fully folded, the association of AhpC into the decameric form is enhanced. The crystal structure of human PrxII revealed that the overoxidized C_P loop maintains a fold very similar to that of reduced PrxII and strengthens the dimer-dimer interface. Overoxidation of PrxII might therefore promote oligomerization.

1.7.3 Overoxidation as the redox switch for peroxiredoxin's dual activity

Yeast cells deficient in PrxI/II were shown to be highly sensitive to heat stress. The expression of a catalytically inactive PrxI in these cells, however, restores most of the resistance to the heat stress (Jang et al. 2004), suggesting that PRX has a cytoprotective function that is independent of the peroxidase activity. Subsequent *in vitro* studies revealed that yeast PrxI as well as human PrxII possess molecular chaperone activity and protect thermally-unfolded citrate synthase from aggregation (Jang et al. 2004; Moon et al. 2005). Since elevated temperatures were shown to enhance oligomerization of PRX, Jang et al. functionally analyzed the different molecular weight species of PRX. They were able to show that the dimer and decamer of PrxI exclusively functions as a peroxidase, whereas high molecular weight complexes have chaperone activity but no peroxidase activity (Jang et al. 2004). Since overoxidation of C_P to C_P-SO_2H is thought to be one of the major driving

forces of PRX oligomerization, C_P was therefore proposed to act as a highly efficient redox sensor. Upon overoxidation, C_P induces structural changes of PRX, which support the assembly of high molecular weight complexes that exhibit chaperone activity (Jang et al. 2004; Moon et al. 2005). It remains to be shown whether this functional switch is a general feature of PRXs.

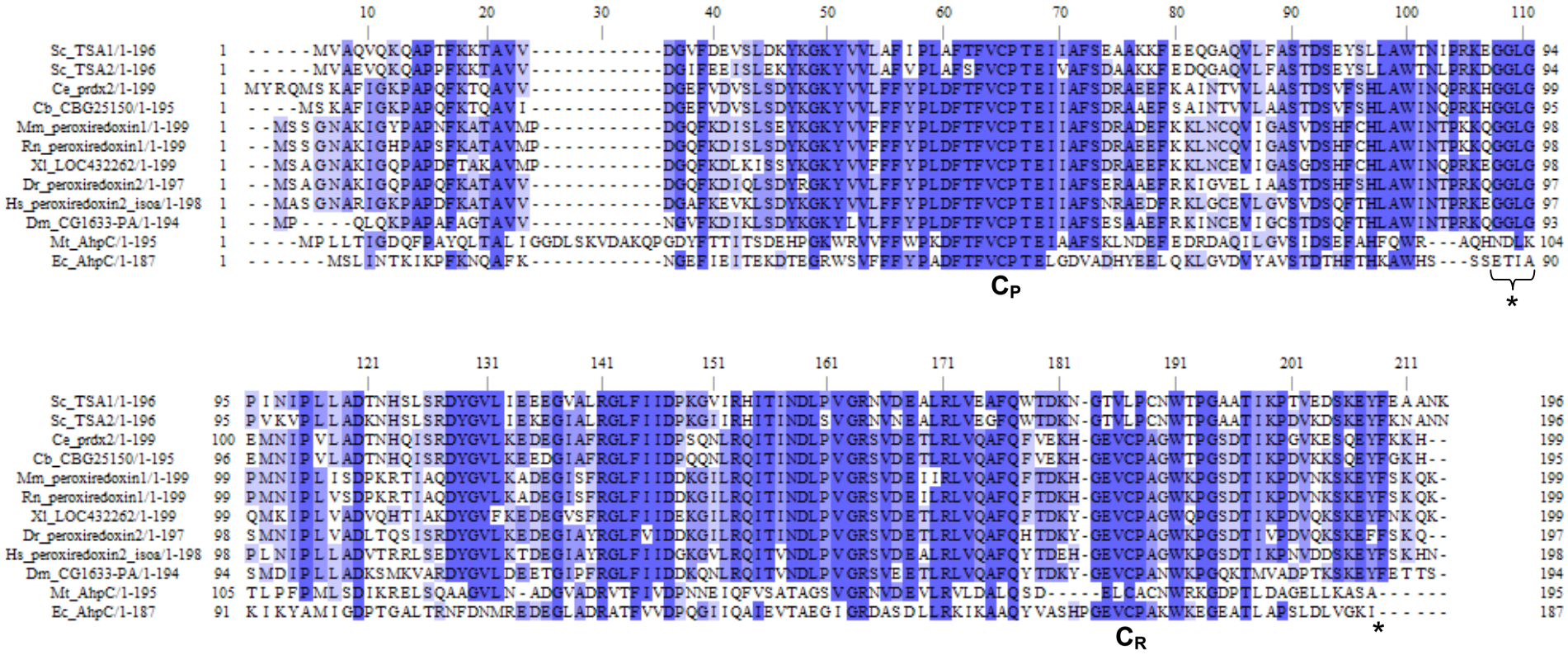

Figure 1.3: Sequence alignment of typical 2-Cys Peroxiredoxins

The sequence alignment of typical 2-Cys PRXs from S. cerevisiae *(TSA1 and TSA2),* C. elegans*,* C. briggsae, Mus musculus, Rattus norwegicus*,* Xenopus laevi, Danio rerio, Homo sapiens, Drosophila melanogaster *and* Mycobaterium tumofaciens *and* Escherichia coli *is shown and color coded by conservation. The peroxidatic and the resolving cysteines are indicated by* C_P *and* C_R *respectively. The asterisks (*) show the evolutionarily new features, the GGLG motif and the extended C-terminus wih the FY motif. The bacterial species lack these motifs.*

1.7.4 Overoxidation of peroxiredoxin's C_P is not an irreversible process

Protein sulfinic acids cannot be reduced by the typical oxidoreductases, such as thioredoxin or glutaredoxin and were long thought to be irreversible. However, pulse-chase experiments have shown that the generation of the sulfinic acid form of PRX is reversible without new protein synthesis or the removal of the sulfur atom (Woo et al. 2003a; Woo et al. 2003b).

Biteau et al. discovered Sulfiredoxin (SRX) as the enzyme that appears to be responsible for the ATP-dependent sulfinic acid reduction in yeast (Biteau et al. 2003). SRX constitute a family of proteins conserved in lower and higher eukaryotes. They are absent from prokaryotes, where PRXs have been shown to be about a 100-fold more resistant to overoxidation (Wood et al. 2003a). In the presence of Srx1 and upon the removal of H_2O_2, the high molecular weight complexes of overoxidized yeast PrxI dissociate into low-molecular weight complexes (Jang et al. 2004). Regeneration of reduced C_P restores the peroxidase activity and lowers the level of chaperone activity to the basal level. SRX seems therefore to contribute to regulating the peroxidase and chaperone function of PRX. The identification of a second reductase family underscores the importance of the reduction of the sulfinic acid species in cellular function. To this date only very little is known about this second family. Although sestrins do not exhibit any sequence or structural similarity to SRX they appear to utilize a similar catalytic mechanism. Their enzymatic activity for sulfinic acid reduction requires a critical cysteine, ATP, magnesium and DTT. Human sestrinII Hi95 has been shown to specifically reduce overoxidized PrxII in HeLa cells, and knockdown of Hi95 using siRNA was found to increase cellular ROS levels. Overexpression of Hi95 decreases ROS levels (Budanov et al. 2004). Sestrins, in contrast to SRX are only present in multicellular organisms ranging from nematodes

to mammals, and it will be interesting to see whether SRX or sestrin have additional activities in addition to the repair of peroxiredoxins (Jonsson and Lowther 2007).

Taken together, typical 2-Cys PRX have been shown to protect cells from hydrogen peroxide. At low H_2O_2 concentrations PRX act as antioxidants. Under oxidative stress conditions, however, PRX switch from a peroxidase to a molecular chaperone due to structural changes initiated by overoxidation of the peroxidatic cysteine. The redox-induced chaperone activity of PRX might prevent aggregation of cytosolic proteins and inhibit ROS-induced cell death.

1.8 Outline

One of the most discussed potential mechanisms of aging is the accumulation of oxidative damage to cellular macromolecules (Imlay 2003). This free radical theory of aging is supported by excellent correlative evidence, but it is still unclear whether the accumulation of ROS is a cause or a consequence of the aging process. *C. elegans* is a commonly used model organism for aging studies and a variety of different longevity mutants are available. Many of the long-lived *C. elegans* mutants have an increased resistance towards oxidative stress, which supports the free radical theory of aging. The goal of this study was to investigate the influence of oxidative stress on the physiological process of aging in the model organism *C. elegans*. The prerequisite was to determine what behavioral processes are most sensitive to oxidative stress and to potentially correlate them with age-related changes. Following this identification, I set out to investigate the underlying cellular changes using proteomic techniques. These experiments revealed *C. elegans* proteins that are most sensitive to oxidative stress. These proteins could be novel redox-regulated proteins and be used as biomarkers for oxidative damage in *C. elegans.* Determining what

proteins are most susceptible to exogenous or endogenous oxidative stress will extend our understanding of the altered physiology of aging eukaryotic cells.

2 Theoretical Background

2.1 C. elegans as a model system for aging research

C. elegans is one of the major genetic model systems used in aging research. It has the advantage of being a small, well-characterized organism that is easy to maintain. *C. elegans* live on petri dishes, feed on *Escherichia coli* and can be stored frozen. It is convenient for aging research that *C. elegans* exhibit a fast life cycle. Development to the adult stage occurs in 2.5 days and the mean lifespan is 2-3 weeks (Altun Z.F. 2002-2006). *C. elegans* comes in two sexes, males and hermaphrodites that are able to self-reproduce. *C. elegans* are transparent making it easy to monitor obvious phenotypes of aging, such as tissue deterioration. In addition, their transparency allows the use of fluorescent probes for protein localization studies and transcriptional expression pattern analysis. An additional advantage of this model organism is the possible utilization of novel molecular biological and biochemical techniques, such as RNA interference, which can be used to reduce or eliminate the function of single genes. The significant homology between the human genome and the genome of *C. elegans* (35%), together with the discovery of largely conserved aging pathways, makes *C. elegans* one of the best model organisms for gerontological research.

2.1.1 Lifespan extensions in *C. elegans*

A milestone in aging research was the discovery of *C. elegans* mutants with extremely extended lifespans. Many of these long-lived mutants genetically downregulate the insulin/IGF-1 like signaling pathway (Kenyon 2001). This signaling pathway is regulated by insulin-related hormones that bind to DAF-2, an insulin-receptor like tyrosine kinase, and culminates in the constitutive repression of the transcription factor DAF-16. Mutations in *daf-2* or other members of this signaling cascade (*age-1, daf-23, daf-28, spe-26*), lead to the derepression of DAF-16 and

result in a lifespan extension of ~56% in mutant worms (Kenyon 2001). Importantly, these mutant animals are resistant to oxidative, heat and ultraviolet stress, which appears to be due to the DAF-16 mediated up-regulation of ROS-detoxifying enzymes (Honda and Honda 1999; Sampayo et al. 2003). The insulin/IGF-1 like signaling cascade appears to be a conserved longevity pathway in worms, fruit flies, rodents and humans (reviewed in (Hekimi and Guarente 2003; Cheng et al. 2005).

Another long-lived *C. elegans* mutant, *isp-1*, has a defect in an iron-sulfur protein of complex III of the electron transport chain and shows a significant decrease in oxygen consumption and ROS production. Because *daf-2, isp-1* double mutants do not live longer than the single mutants, the maximum lifespan appears therefore to benefit of either high ROS detoxification (*daf-2*) or low ROS production (*isp-1*) (Hekimi and Guarente 2003). This is in contrast to *daf-2, clk-1* double mutants, which live up to 5 times longer than the wild type (Taub et al. 1999; Taub et al. 2003). CLK-1 is involved in the biosynthesis of ubiquinone (UQ), an antioxidant in all cellular membranes and an important redox cofactor in the mitochondrial electron transport chain (Rodriguez-Aguilera et al. 2005). Long-lived *clk-1* mutants show a decreased accumulation of lipofuscin, a byproduct of oxidative damage. This phenotype could be due to the accumulation of the UQ precursor demethylubiquinone, whose redox cycle is known to produce less ROS. Thus, the *clk-1* mutant might have reduced extra-mitochondrial ROS formation.

Another mechanism of extending lifespan in *C. elegans* is caloric restriction. Caloric restriction experiments usually limit food intake to 30-40% of the regular diet, and have been found to extend lifespan in certain rodents, *C. elegans* and Drosophila. The mechanism by which the lifespan extension occurs is still subject to speculation. One hypothesis is that caloric restriction leads to a decrease in metabolism, which in turn, leads to reduction in ROS-production (Guarente and Kenyon 2000).

Interestingly, the mere sensing of food by *C. elegans'* sensory neurons has an effect on lifespan. When sensory perception is decreased due to ablation of specific sensory neurons or mutations that perturb the sensory cilia or signaling pathways, the mean lifespan of these worms can be extended up to 50% (Apfeld and Kenyon 1999). These animals feed normally, have the same developmental rates and reproductive output. It has been suggested, that this lifespan extension is caused by downregulation of the insulin/IGF-1 like signaling pathway. The possible explanation for this link is that sensing of food triggers the release of an insulin/IGF-1 like hormone that accelerates aging.

2.1.2 The effect of temperature on lifespan assays

The main determinant of lifespan in *C. elegans* is the temperature at which the nematodes are cultivated. Their lifespan can be increased by simply reducing the culture temperature. *C. elegans* are able to survive at temperatures from 6 to 26°C with a temperature optimum between 15 and 25°C. When cultivated outside the limits of this temperature optimum, the nematodes suffer from environmental stress, which is accompanied by a large decrease in fecundity (Van Voorhies and Ward 1999). Worms cultivated at 15°C can survive 2-3 times longer than worms reared at 25°C. This effect on longevity is thought to be caused by a difference in the metabolic rates at the different temperatures (for review (Van Voorhies 2002). At lower cultivation temperature, ectothermic animals can greatly reduce their metabolic rate and continue all necessary physiological functions at lower rates. This ability allows *C. elegans* to survive stressfull environmental conditions that would be lethal to endothermic organisms. Metabolic rate is thought to be linked to the aging process because a reduced metabolic rate would in turn lead to decrease in ROS generation.

2.1.3 Characterization of age-related changes in *C. elegans*

To understand the aging process, it is important to characterize the physiological changes that occur during *C. elegans* aging. These age-related changes have been measured and quantified, and some of these aging markers are now even predictors of lifespan (Gerstbrein et al. 2005). The best way to analyze age-related changes is by using longitudinal studies, in which a population of worms is analyzed at different timepoints in life. Longitudinal studies provide the most information about the relationship of the different measures of the aging process and lifespan. Here, I present an overview of the various age-related changes that occur and the methods of measuring these changes. In addition, I will present some of the data that I collected with aging wild type worms during the establishment of these techniques in the laboratory.

2.1.3.1 Survival and mortality rate

Lifespan measures in *C. elegans* are typically expressed in terms of survival or mortality rate. Survival curves are obtained by plotting the surviving fraction of a population over time in a longitudinal study, and are helpful for visualizing the minimal, maximal and mean lifespan (Figure 2.1A). The maximal lifespan can either be described as the age of the last survivor at death, or as the average age of the last 10% of surviving worms. The mean lifespan (MLS) and standard error (SE) can be calculated using the following equations (Wu et al. 2006):

$$MLS = \frac{1}{N} \sum_{j} \frac{x_j + x_{j+1}}{2} \cdot d_j$$

where d_j: number of worms that died from timepoint x_j to timepoint x_{j+1}

$x_j + x_{j+1}$: time interval (e.g. between day 3 and 5: $x_j + x_{j+1} = 3 + 5$)

N: total number of worms

$$SE = \sqrt{\frac{1}{N(N-1)} \sum_j \left(\frac{x_j + x_{j+1}}{2} - MLS\right)^2 \cdot d_j}$$

Mortality of most species increases exponentially with age. This relationship can be approximated with the Gompertz equation (Olshansky and Carnes 1997):

$$m(t) = Ae^{\alpha t}$$

where m(t): mortality rate at time t (fraction of worms that died in a specific time interval)

A: initial mortality rate (mortality rate at the beginning of adulthood)

e: Euler's number

α: exponential Gompertz component (acceleration of mortality over time)

t: time (chronological age)

This equation can be visually expressed by plotting mortality on a logarithmic scale as a function of chronological age (Figure 2.1B). The Gompertz curve is useful in elucidating whether differences in the mean lifespan of two *C. elegans* populations result from either a change in the initial mortality rate (A), reflected as the y-intercept of the regression line, or from a change in the acceleration of mortality (α), reflected as a different slope.

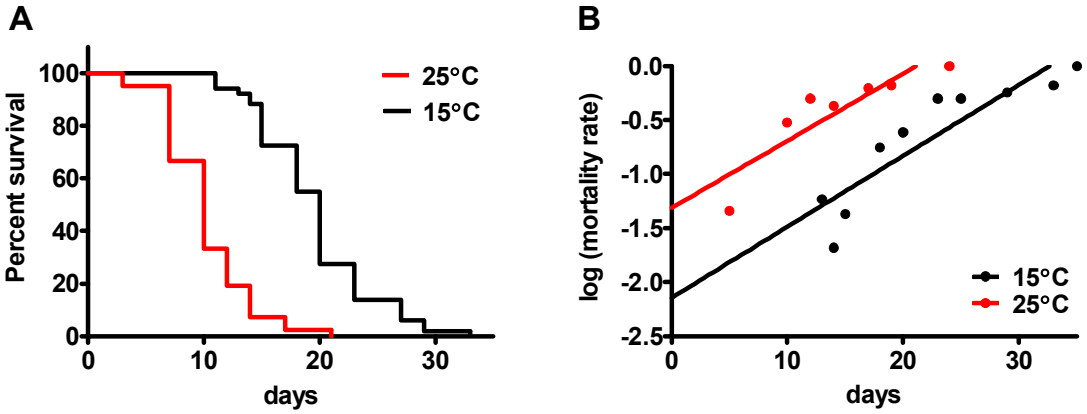

Figure 2.1: Survival and Gompertz curve of wild type worms at different temperatures

A) *The lifespan of a wild type* C. elegans *population, reared at 15°C and 25°C is plotted in a survival curve. The surviving fraction of the population is plotted against the days of the longitudinal study.* ***B)*** *The same lifespan data is plotted in a Gompertz curve that expresses mortality rate on a logarithmic scale as a function of the chronological age. The decreased mean lifespan at 25°C is due to a change in the initial mortality, and not due to an accelerated aging rate.*

2.1.3.2 Activity span

The aging process in *C. elegans* is accompanied by changes in activities, such as feeding, defecation and body movement. *C. elegans* eat bacteria that are suspended in liquid, which they take up with their pharynx. Feeding consists of two motions: pumping, which is the near-simultaneous contraction of both pharyngeal bulbs (trapping bacteria in the bulbs and subsequently pushing bacteria into the intestine), which is followed by the near-simultaneous relaxation (liquid will be regurgitated) (Altun Z.F. 2005b). The pharyngeal pumping rate increases from about a 100 pumps per minute at the L4 larval stage (day 0 of adulthood) to about 300 pumps per minute on day 2 of adulthood (Huang et al. 2004). After this maximum pumping rate on day 2 a gradual age-related decline in pharyngeal pumping sets in, which culminates in no

pumping on approximately day 10. The long-lived mutant *daf-2* has a prolonged pharyngeal pumping span, whereas the short-lived *daf-16* mutant has a significantly decreased pharyngeal pumping span (Huang et al. 2004).

Defecation rate is another measure that declines with age. Defecation is achieved through rhythmic muscle contractions and occurs at regular intervals (Altun Z.F. 2005a). It has been reported that the intervals between the muscle contractions increase with age (Bolanowski et al. 1981).

One of the easiest measures of activity is body movement. The body movement of a young adult worm is coordinated and sinusoidal. Typically, the worms display fast and coordinated movement for 60% of their lifespan. Similar to the decline of pharyngeal pumping, the decline in motility is correlated with age (Figure 2.2A). As the worms age, the motility becomes less and less coordinated. Instead of continually moving forward, the worms begin to often change direction. In addition, their ability of bending their body declines. This sluggish movement is easily detecable in the bacterial lawn where straight tracks replace the sinusoidal trails. When the worms get even older (on approximately day 8 at 20°C), body movement stops altogether. The flaccid worm is able to minimally move its head or tail and can contract upon stimulation (Herndon et al. 2002; Huang et al. 2004). The *C. elegans* body movement can be quantified in various ways. The classical way is to count the backward waves per minute on successive days during lifespan. Body bends and average speed can also be determined using an automated worm tracking system that records movement over a set timeframe in the range of 10-15 minutes (Hsu et al. 2008). These methods are time intensive and comparative studies of more than one population becomes difficult. An easier way is to classify worms according to their body movement. Fast and coordinated movement is classified as A- or type I movement, uncoordinated movement is classified as B- or type II movement, and

minimal movement is classified as C- or type III movement (Hosono et al. 1980; Huang et al. 2004).

2.1.3.3 Reproduction

Most individuals of a *C. elegans* population are hermaphrodites, and males make up only 0.5% of a naturally occurring population. Hermaphrodites are able to self-fertilize and produce about 300 offspring by selfing. The self-fertile reproductive span ceases early in life with only 35% of their lifespan spent producing progeny (Collins et al. 2008). The fertility span can be measured as the fraction of the population that is able to produce living offspring during adulthood (Figure 2.2A). Another measure of reproductive capability is the number of progeny produced over time. The number of progeny produced on each day declines as a function of age (Huang et al. 2004). The determining factor for progeny production seems to be the number of sperm that is generated by the hermaphrodites (Hodgkin and Barnes 1991). The sperm number of aging hermaphrodites can be determined and can also be used as a measure of age-related decline. Interestingly, it has been shown that even when hermaphrodites are mated and sperm is not limited, an age-related decline in progeny production will eventually occur. Progeny number, however, will increase 2-3 fold and the reproduction span will be prolonged, suggesting that the observed age-related decline is independent of sperm depletion (Hughes et al. 2007). Progeny production seems to be a very sensitive process, and a slight decrease in temperature above the optimum leads to a dramatic decrease in brood size (Van Voorhies and Ward 1999). A reduction in offspring is the easiest measure of physiological stress on *C. elegans*.

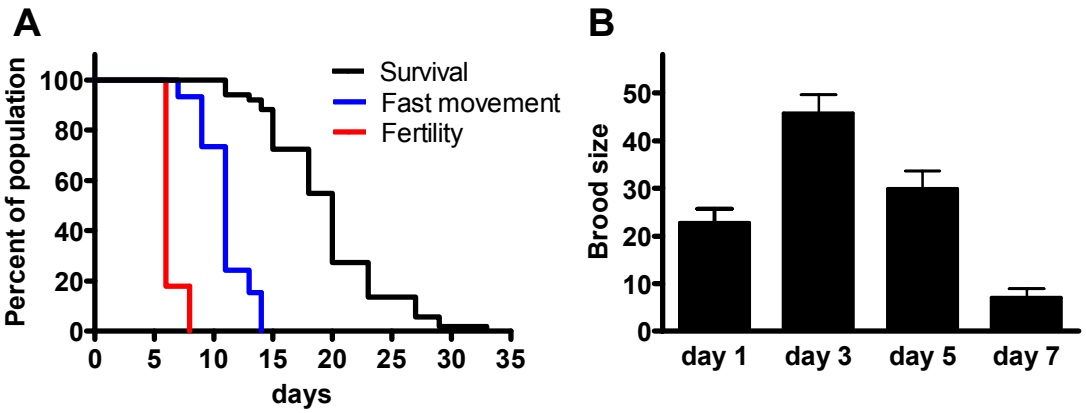

Figure 2.2: Age-related decline in activity and progeny production

An aging worm population can be characterized by the decay of several physiological functions. ***A)*** *Fertility decreases after ~35% of the lifespan and fast movement declines after ~60% of the lifespan.* ***B)*** *The decrease in fertility can also be described as the mean brood size on successive days (Mean and SE are shown).*

2.1.3.4 Appearance

Another age-related change is a change in appearance of the worms with increasing age. The best way of distinguishing a mother from her adult progeny is her size. There is a 70% increase in length from day 3 to 14 at 20°C and a more than 200% increase in volume (Collins et al. 2008). As the worms are losing agility, they also become more flaccid, limp and saggy. The other change in appearance is the accumulation of dark pigments in the intestine (Figure 2.3 A, B). Intestinal autofluorescence is caused by lysosomal deposits of the pigment lipofuscin. The accumulation occurs progressively as a result of the oxidative degradation and autophagocytosis of cellular components (Herndon et al. 2002). Lipofuscin accumulation can be quantified *in vivo* with fluorescence microscopy and *in vitro* using crude *C. elegans* extracts and measuring fluorescence in the spectrometer (Figure 2.3 C-E). It has been shown that lipofuscin accumulation is delayed in the long-lived *C. elegans* species *daf-2* and *lin-4*, and lipofuscin accumulation can be

used as a predictor of lifespan (Gerstbrein et al. 2005). Analysis of age-related changes in tissue integrity revealed that the pharynx and the body wall muscles are especially prone to deterioration. The pharynx shows necrotic cavities and loss of structural features. Whether this deterioration is the reason for the decline in pharyngeal pumping is still unclear (Garigan et al. 2002). With increasing age, *C. elegans* also suffers from sarcopenia, the loss of muscle structure and function. This loss in muscle intergrity is positively correlated with the movement decline during the aging process (Herndon et al. 2002). The nervous system on the other hand, does not seem to suffer from age-related deterioration. It is therefore unlikely that the decline of neuronal function is the reason for the decline in pharyngeal pumping and locomotion (Garigan et al. 2002).

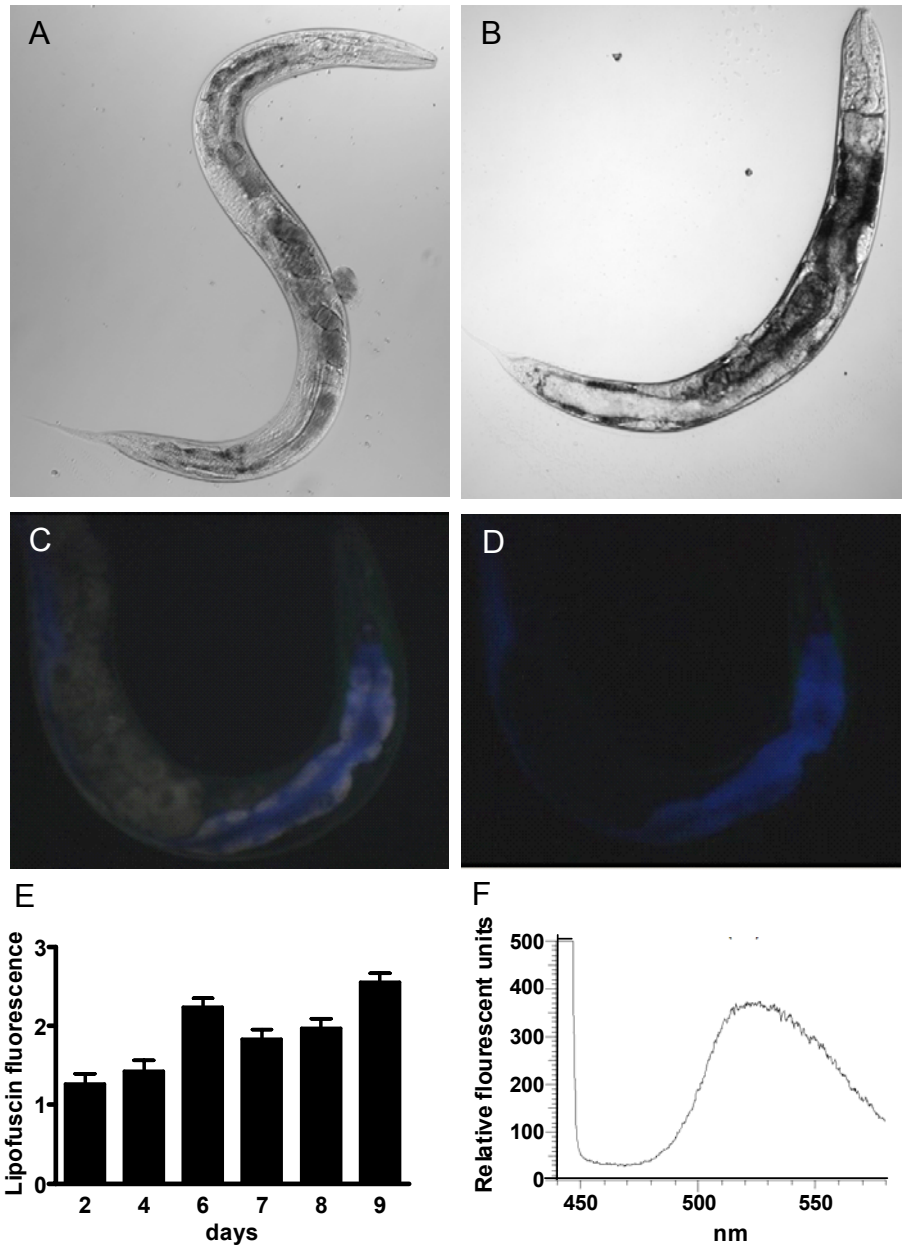

Figure 2.3: Age-related changes in appearance

A dramatic change in appearance accompanies the change in agility. ***A)*** *Wild type worm on day 2 of adulthood and* ***B)*** *on day 7 of adulthood at 25°C. Dark intestinal pigmentation accumulates and the worm appears more flaccid. The dark pigmentation is lipofuscin and can be visualized (****(C)*** *and* ***(D)****) by fluorescence microscopy with an excitation wavelength of 350/50 nm and an emission ≥ 420 nm. The fluorescence co-localizes with the intestine as shown in this overlay. Images acquired during CytoViva demo.* ***E)*** *Lipofuscin fluorescence can be quantified and increases during lifespan.* ***D)*** *Lipofuscin fluorescence in crude* C. elegans *protein extracts can be measured with the fluorescence spectrometer with an emission maximum at 530 nm, when excited at 430 nm.*

2.1.3.5 Biochemical changes

In contrast to the behavioral changed that accompany aging, which are well documented, not much is known about the biochemical changes upon aging. More than 20 years ago, Klass et al characterized DNA damage that occurrs in an aging worm population. DNA single-strand breaks are found to increase with age and so do the amount of 5-methylcytosine (Klass et al. 1983). Deamination of 5-methylcytosine in DNA can lead to base pairing mismatch. These changes indicate that DNA integrity or DNA repair mechanisms become compromised with increasing age in *C. elegans*. No other investigations on genome and chromosome stability have been performed since then.

Other biochemical measures involve the analysis of oxidative protein damage. This is the measurement of protein carbonylations. Protein carbonylations can increase up to 3-fold from the beginning of adulthood to the end of the lifespan. Short-lived strains, such as *mev-1* and *daf-16* mutants show an accelerated accumulation of protein carbonylations (Adachi et al. 1998). Oxidative modifications of proteins are, however, not limited to carbonylation. Peptide backbones, tryptophane residues and especially thiol containing aminoacids are easily oxidized. The development of novel techniques that allow the investigation and quantification of oxidative thiol modifications has the potential to elucidate age-related changes in protein oxidation. The application of these techniques to aging *C. elegans* populations will contribute to the understanding of age-related changes on a biochemical level.

2.2 Proteomic techniques to analyze oxidative protein modifications

Thiol groups of an increasing number of proteins have been discovered to be specifically modified by distinct reactive oxygen species (ROS). Based on the specific

reactivity of the individual oxidants, it appears that individual oxidative stress treatments differ in their protein targets and affect a very distinct set of proteins (Leichert and Jakob 2006). By knowing the pattern of proteins that are specifically affected by one or the other oxidative agent, and by comparing these to the pattern of affected proteins in the aging process, it will be possible to determine what type(s) of ROS are generated at what time during the eukaryotic aging process. The two methods that I will introduce in this section, allow us to globally monitor and quantify the thiol-disulfide status of cellular proteins. The application of these techniques in *C. elegans* will provide us with the identification of proteins that become targets for oxidative protein modifications. These proteins have the potential to serve as biomarkers for oxidative stress can then be potentially correlated with physiological changes that occur during aging.

2.2.1 Differential thiol trapping combined with 2D gel electrophoresis

The differential thiol-trapping technique is an innovative approach to monitor and identify redox sensitive proteins in cells and organisms in response to various oxidative stress treatments and aging. This technique was developed in our lab for *E. coli*. It is based on the sequential reaction of two variants of the thiol modifying reagent iodoacetamide (IAM) with accessible cysteines in proteins (Figure 2.4) (Leichert and Jakob 2004).

This method allows the examination and comparison of the thiol-disulfide status of all cellular proteins that can be resolved in 2-dimensional gels (>1000 proteins) and has been successfully applied to identify proteins sensitive to oxidative and nitrosative stress in *E. coli,* yeast and phagocytes (Leichert and Jakob 2004). The cells are exposed to the desired oxidative stress treatment, and then treated with trichloracetic acid (TCA). All accessible thiol groups are alkylated with cold, un-labeled IAM under denaturing conditions. In a next step, all reducible thiol modifications that have

developed during the oxidative stress treatment such as disulfide bonds, sulfenic acids, S-glutathionylation and S-nitrosylation are reduced and the newly accessible thiol groups are now modified with ^{14}C-labeled IAM. Therefore, radioactivity is specifically incorporated into proteins that contain thiol modifications. High ratios of ^{14}C/protein are present in proteins with thiol modifications while low ratios of ^{14}C/protein are present in proteins, whose thiol groups are not significantly modified. This technique generates chemically identical proteins, which migrate to the same spot in 2D gels but differ in their ^{14}C to protein ratio depending on their *in vivo* redox status. Any oxidative stress-mediated increase in the thiol oxidation status is reflected by an increase in the ^{14}C to protein ratio and represents proteins with redox-sensitive cysteines. Proteins of interest can be identified from gels using mass spectrometric techniques.

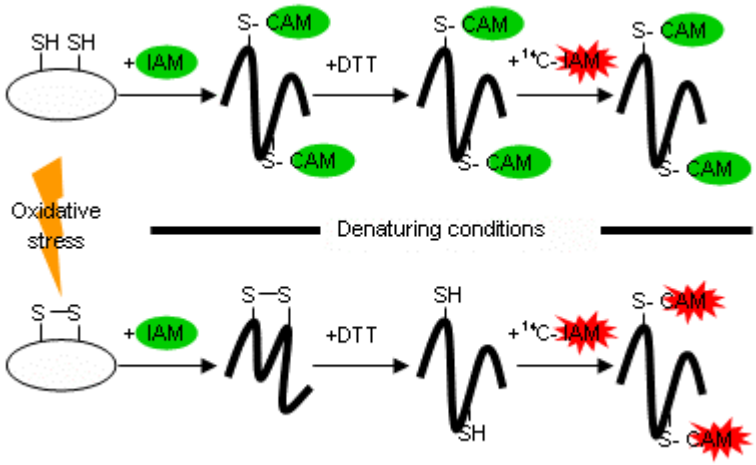

Figure 2.4: Schematic overview of the differential thiol trapping technique

In the first thiol trapping step, all freely accessible thiol groups are alkylated with iodoacetamide (IAM). Subsequently all reversible thiol groups are reduced with DTT, and all newly accessible thiol groups can now be alkylated with ^{14}C-labeled IAM. This figure was kindly provided by Dr. Lars Leichert (Leichert and Jakob 2004).

2.2.2 OxICAT

Although our 2D gel approach allows the separation and identification of more than 1000 proteins, a number of proteins are poorly resolved on 2D gels. These include membrane proteins, low abundance proteins and those with extreme isoelectric points. To further increase the number of proteins that we can analyze, a modified version of the differential thiol trapping technique has been established in the lab. This method no longer relies on 2D gels but uses the highly sensitive and quantitative proteomic method called Isotope-Coded Affinity Tag (ICAT) technique (Leichert et al. 2008). The ICAT reagent consists of 3 functional groups: a thiol reactive iodoacetamide group, a cleavable biotin affinity tag and a linker that exists in an isotopically light ^{12}C-form and an isotopically heavy ^{13}C-form. Similar to the differential thiol trapping technique, all *in vivo* reduced cysteines in a cell lysate are labeled with light ^{12}C-ICAT reagent and all *in vivo* oxidized cysteines in the very same sample are labeled with heavy ^{13}C-ICAT reagent. This labeled protein extract is then digested with trypsin and cysteine containing peptides are enriched using streptavidin affinity chromatography. After cleavage of the biotin tag, the ICAT samples are analyzed by liquid chromatography MS/MS analysis. Cysteine-containing peptides derived from a protein that was partially oxidized *in vivo* will co-elute from the HPLC column but yield distinct peaks in the mass spectrum (peak doublets) that are 9 Da apart and whose relative ion intensities represent the relative abundance of the oxidized and reduced protein species in the cell lysate (Figure 2.5). Oxidation-sensitive proteins can be identified *in vivo* by detecting changes in the ratio of heavy to light labeled peptides upon treatment of cells with different oxidative stressors.

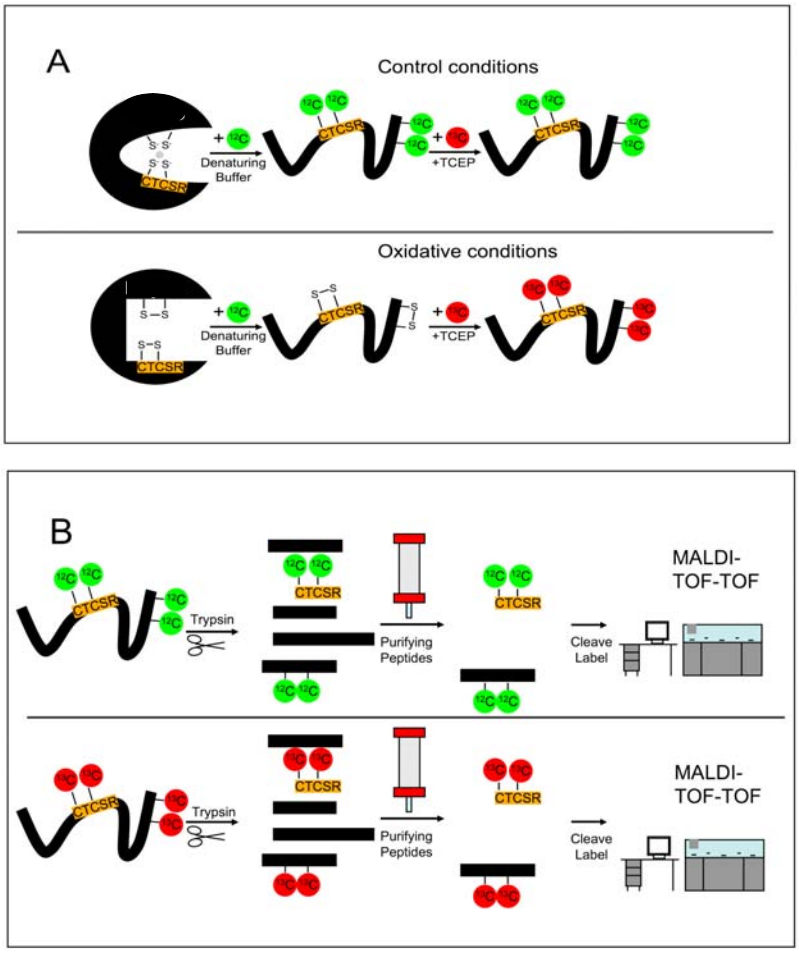

Figure 2.5: Schematic overview of the OxICAT technique

OxICAT is used to differentially label reduced cysteines with light ^{12}C-ICAT and oxidized cysteines with heavy ^{13}C-ICAT. ***A)*** *The redox center of a model protein is fully reduced under non-stress conditions (top) but oxidized upon oxidative stress conditions (bottom). In the first step, all free cysteines in the protein are modified with light ^{12}C-ICAT reagent. Reduction with a thiol specific reductant reduces thiols that are oxidized and therefore previously not accessible to the light ICAT reagent. These newly accessible cysteines are now modified with heavy ^{13}C-ICAT.* ***B)*** *Subsequent steps include digestion of the protein, purification of cysteine containing peptides via the affinity tag and mass spectrometric analysis which detects the mass difference between light labeled and heavy labeled peptides. Figure kindly provided by Dr. Lars Leichert.*

2.3 Methods

2.3.1 Cultivation and maintenance of *C. elegans* strains

C. elegans strains are generally maintained on nematode growth medium (NGM) and fed *E. coli* OP50 (Brenner 1974). NGM plates were allowed to dry overnight before a dense culture of OP50, grown in LB medium, was spotted on the plates. The plates were kept at room temperature for 24-48 h to allow the bacteria to form a lawn. General maintenance plates with growing *C. elegans* plates were grown at 15°C, experimental plates were kept at either 15 or 25°C, as indicated. To avoid starvation and crowding, worms were transfered to fresh NGM plates every 7-10 days by either transfering single worms using a platinum wire pick or by chunking. Chunking is the transfer of a piece of agar from the original to a fresh plate (Stiernagle).

2.3.1.1 Freezing of C. elegans *strains*

C. elegans can also be maintained as a cryogenic culture at -80°C or in a liquid nitrogen tank. Two 10 cm plates with worms that have just exhausted the bacterial lawn were used for the freezing procedure. The exhaustion of food will lead to abundance in L1 and L2 larvae, which are able to survive freezing. The worms were washed off with M9 media and collected in separate 15 ml centrifuge tubes. The worms were then sedimented by gentle centrifugation at 2,000g for 1 min. All excess M9 media is removed using an aspirator. The worms should be swimming in 1.5 ml M9, all excess M9 media was removed using an aspirator. The same volume (1.5 ml) of freezing solution (section 3.4.6) was added to each centrifugation tube. The total volume of 6 ml of worm solution was distributed into 7 cryogenic vials, placed into a small styrophor container and transferred into the -80°C freezer. The styrophor will facilitate gradual freezing in contrast to shock freezing. One of the vials was thawed after a few days of freezing to ensure the recovery of the worms. Thawing is best

performed at room temperature. The freezing solution was carefully removed and the frozen worms were placed on a fresh NGM agar plate with OP50 (Stiernagle).

2.3.1.2 Age-synchronization of C. elegans *cultures using hypochlorite treatment*

For age-synchronization of worms an egg preparation is performed. Eggs will be isolated from gravid adults by hypochlorite treatment. Worms were first cultivated on 10 cm NGM plates. The largest number of eggs can be extracted when the NGM plates are densly populated but not starved. The gravid animals were washed off with either M9 medium or water into a 15 ml centrifugation tube and gently centrifuged at 2,000g for 1 min. The worms were kept in 5 ml liquid, and then 5 ml of a freshly prepared hypochlorite lysis solution (section 3.4.6) was added. The tubes were vortexed and an aliquot was put onto a microscope slide to monitor the release of the eggs. The hypochlorite treatment will lead to the rupture of the worms and the discharge of the eggs. The eggs are protected from the hypochlorite treatment by their thick cuticle. It is important to stop the reaction once the adults rupture to avoid killing the eggs. The tubes were centrifuged at 2,500g for 30 sec and the hypochlorite solution is aspirated. The eggs were washed with 3 x 5 ml M9 medium to remove the remaining lysis solution. The eggs were then seeded onto fresh NGM plates with OP50 as food source for the hatching animals. Alternatively, the eggs were resuspended in liquid M9 medium and allowed to hatch overnight upon gentle shaking in a water bath at room temperature. This will lead to improved synchronization because lack of food will arrest the development in the L1-larval stage for a few weeks before dauer stage is entered. The L1 larvae were collected by centrifugation and seeded onto fresh NGM plates on the subsequent day (Hope 1999).

2.3.1.3 Large-scale C. elegans *cultivation*

For large-scale *C. elegans* cultivation, egg plates are used. Egg plates are typically 15 cm in diameter and consist of Super NGM media as base and egg custard, which is layered on top of the base. To prepare the egg custard, 6 chicken eggs were rinsed off with ethanol and the yolks were collected. The 6 yolks were mixed with 100 ml LB medium. Lysozyme, which is present in the yolks, was inactivated by incubating the custard for 1h in a 60°C waterbath. The custard was filtered through a sterilized piece of cheese cloth and combined with 25 ml of a dense overnight culture of *E. coli* HB101. 14 ml of this egg custard was then layered over each base of Super NGM medium. The plates were left to dry overnight at room temperature and on the subsequent day, a growing culture of *C. elegans* was chunked onto the egg plates. The egg plates were grown for 6 days at 20°C and periodically checked for moisture. If the plates appeared dry, 2-3 ml of M9 media was added. After 6 days of incubation, a dense lawn of gravid adults was visible in the egg custard. Worms were washed off with the custard using M9 medium and initially cleaned in several centrifugation steps. To further separate the worms from the remaining egg custard, a sucrose flotation was performed. Worms were kept in 20 ml M9 medium in a 50 ml centrifugation tube and combined with 20 ml ice-cold 60% sucrose solution. The worms were then centrifuged for 5 min at 4°C at 3000g with a slow brake. The worms will float on top and can be filtered over a nitex membrane to separate the gravid animals from the larvae. The gravid animals were then again collected in 37.5 ml M9 medium in a 50 ml centrifugation tube. For egg release, 10 ml of household bleach (Clorox) and 2.5 ml of 10 N NaOH were added to a final volume of 50 ml. The rupture of the animals is monitored under a stereo microscope as before. The hypochlorite solution was removed in 3 washing steps and eggs were allowed to hatch over night in liquid M9 medium during gentle shaking in a 25°C waterbath (McGhee 1999).

2.3.1.4 Generating males by heat shock

C. elegans males make up 0.5% of a *C. elegans* population and arise spontaneously by chromosomal nondisjunction. Chromosomal nondisjunction can be promoted by heat shock treatment of L4 larvae. About 6 plates with five L4 larvae each were incubated for 5 h at 30°C. The plates were then returned to 15°C and the resulting offspring should contain a few males that can be maintained by mating to N2 hermaphrodites (Hope 1999).

2.3.1.5 Mating and outcrossing

A typical mating is set up by combining three young adult hermaphrodites with about 10 males. The mating plates are kept at 15°C and moved every day for 3 days onto fresh plates. The eggs on the mating plates are allowed to hatch and the resulting males can be maintained by repeated matings.

The *C. elegans* mutant strains *prdx-2* and *sesn-1*, used in this study, have been obtained from the Caenorhabditis Genomic Center (CGC) and the Japanese Knockout consortium, respectively. Both strains were created by UV/TMP mutagenesis and may carry additional mutations (WormBase, http://www.wormbase.org, release WS193, August 21st 2008). To exclude that potential background mutations contribute to the observed phenotype, we conducted three repeated outcrossings against wild type animals. In the first mating, three mutant hermaphrodites were crossed with 10 wild type males. The mating was moved to fresh plates on three consecutive days. The progeny from day 2 of the mating (F1 generation) was singled. After they produced offspring by selfing (F2 generation), the F1 generation was genotyped at the locus of the mutation (see 2.3.1.6 for genotyping). If mating occurred, the F1 generation will be heterozygous and only progeny from these animals was used in the subsequent mating. The F2

generation produced by selfing will be either heterozygous, homozygous wild type or homozygous mutant (Figure 2.6). The homozygous F2 animal is now outcrossed once. This animal can be propagated and then frozen. Alternatively, the F2 animals from the first cross can be used for the next cross, without immediate genotyping. Therefore, about 20 hermaphrodites of the F2 generation were mated with 3 wild type males each, and the mating was again moved to fresh plates on three consecutive days. After the third day, the mated hermaphrodite of the F2 generation was genotyped and only the progeny of the homozygous mutant was kept. This homozygous mutant strain is now outcrossed twice and can be frozen and/or used for the next crossing.

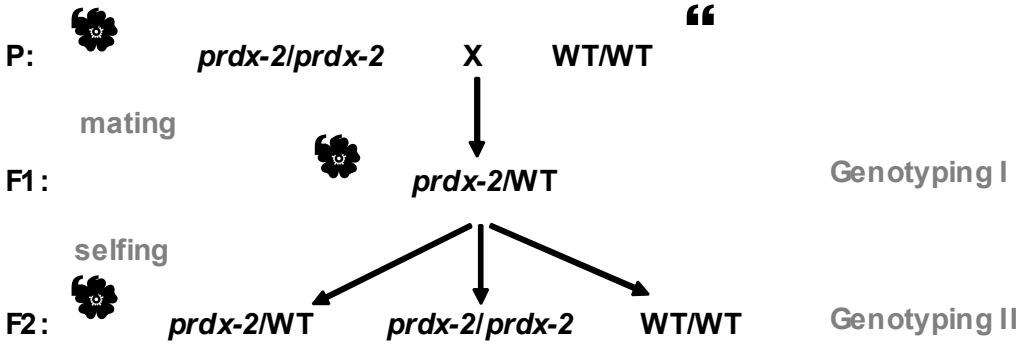

Figure 2.6: Schematic overview of the first mating during the outcrossing of strain *prdx-2*

The parental generation (P) consisting of homozygous prdx-2 *hermaphrodites and wild type (WT) males are allowed to mate. The filial generation 1 (F1) is heterozygous wild type and* prdx-2*. The F1 generation is allowed to produce progeny by self-fertilization before they are genotyped. The possible genotypes of the F2 generation are heterozygous, homozygous* prdx-2 *and homozygous wild type, which will be determined by genotyping.*

2.3.1.6 Genotyping individual worms by PCR

To genotype, worms were lysed using 1x PCR reaction buffer containing 1 µg/µl Proteinase K (final concentration). 10 µl of this PCR lysis buffer was placed into the

lid of a PCR tube. A single worm was placed into the lysis buffer. The lid was closed and the reaction was briefly centrifuged and shock frozen at -80°C for 10 min. Subsequently the reaction tubes were placed into the PCR cycler and the lysis and genotyping program was started (Table 2.1). After the lysis step, the PCR reaction mix was added to each tube. The result of the PCR reaction was then visualized on an agarose gel. For genotyping of mutants, primers were used that flank the deletion in the gene of interest. Two different sized PCR products were obtained for wild type and mutant gene as illustrated in Figure 2.7.

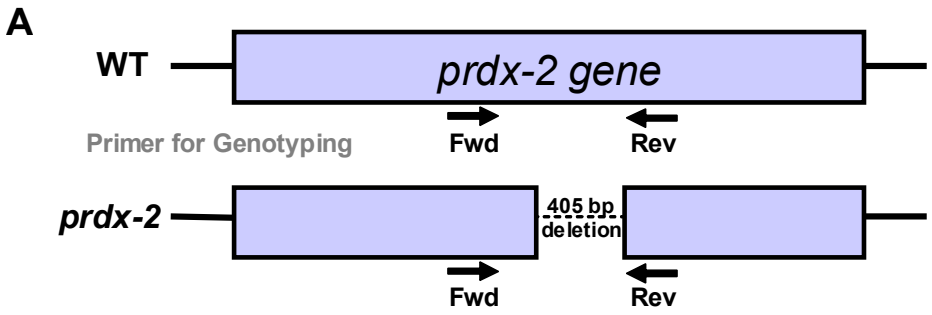

B

Genotyping

prdx-2/*prdx-2*	*prdx-2*/WT	WT/WT
376 bp	781 bp 376 bp	781 bp

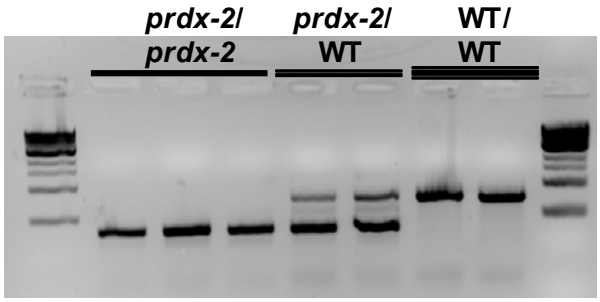

Figure 2.7: Principles of PCR-genotyping illustrated with the *prdx-2* mutant

The prdx-2 *mutant was made by UV/TMP mutagenesis, which created a 405 bp deletion in the* prdx-2 *gene (WormBase, http://www.wormbase.org, WS193, August 21, 2008).* ***A)*** *For genotyping, primers were designed that flank this deletion.* ***B)*** *PCR with these primers lead to two different amplification products that were easily distuinguished on an agarose gel. Heterozygous worms will display both sized PCR products.*

Table 2.1: PCR reaction for lysis and genotyping

Step	Temperature	Duration	Cycles
Lysis	60°C	60 min	
Inactivation of Proteinase K	95°C	15 min	
Addition of PCR reaction mix	65°C	15 min	
Initial Denaturation	95°C	5.0 min	
Denaturation	95°C	0.5 min	35
Primer Annealing	58°C	0.5 min	
Elongation	72°C	1.0 min	
Final Elongation	72°C	8.0 min	
Storage	4°C	∞	

2.3.2 Behavioral *C. elegans* experiments

2.3.2.1 Lifespan, movement and brood size analysis

Lifespan analyses were performed at either 15°C or 25°C as indicated. Synchronized L4 larvae (day 0 of adulthood) were singled and transferred onto fresh NGM plates with OP50 every other day until egg production ceased. After this period, animals were transferred every 4-7 days. Animals were scored as dead when they failed to respond to repeated tapping with a platinum wire pick. Animals that desiccated at the edge of the plate, escaped or died due to internal hatching were excluded from the lifespan analysis. At least 50 worms were tested in each experiment. Animals were scored for their movement behavior as described in 2.1.3.2 and in (Herndon et al. 2002; Huang et al. 2004). Fast and coordinated movement is classified as A-movement, uncoordinated movement is classified as B-movement, and minimal movement is classified as C-movement. Animals that were affected in their movement due to internal hatching or protruding gonads were excluded from the analysis. Animals were scored as self-fertile when progeny is present on the plate on the day of transfer. For brood size evaluation, the number of eggs and larvae was

counted as described in 2.1.3.3. Animals that suffered from internal hatching were excluded from fertility and brood size measurements.

2.3.2.2 Statistical analysis of lifespan and behavior

Statistical analyses were performed using GraphPad Prism4 software. The mean lifespan (MLS) and Standard Error (SE) were calculated as described in 2.1.3.1 and (Wu et al. 2006). The same equations were used to calculate the Mean Fast Movement Span. To compare lifespan and behavior of two populations the Mann-Whitney test was performed. To compare more than two populations, the Kruskal-Wallis test and the Dunn's post hoc test were performed. To compare survival after oxidative stress treatment the non-parametric log-rank test was used (Glantz 2005).

2.3.2.3 Microscopy and imaging

Microscopy and imaging analysis was used to assess *C. elegans* appearence, growth rate and tissue integrity (Stiernagle). For these analyses, single were picked, placed onto a microscope slide with a 3% agarose pad in 10 µl M9 supplemented with 10 mM Levamisole for paralysis. DIC-imaging was performed on a Leica SP5 Confocal microscope (DM6000B) and images were analyzed with LAS AF software (Yochem). Analyses of movement behavior were performed on small NGM plates under a Nikon Eclipse E600 stereoscope. Pictures were taken every 2 seconds for 30 seconds with a Spot-2 (Diagnostic Instruments Inc.) camera. Movies were made with Adobe ImageReady software and Open Video Converter (DigitByte Studio).

2.3.2.4 Worm tracker

Movement behavior can also be analyzed using an automated worm tracking system. The tracking system consists of a steroscope (Zeiss Stemi 2000C), a digital camera (Cohu 7800) and a digital moving stage (Parker Automatic). The digital moving stage

holds the NGM plate. The NGM plate was freshly spread with a thin layer of OP50 before the worm, at day 1 of adulthood, was placed onto the plate. Recording was continuous for 10-16 min, and the velocity of the animal was calculated (Feng et al. 2006).

2.3.2.5 Oxidative stress treatment

Oxidative stress treatment was performed with synchronized L4 larvae. Synchronized L4 larvae were collected by centrifugation in M9 medium and separated from the feeding bacteria in three washing steps. For the oxidative stress treatment, 100 µl of worms (~30,000 worms) were incubated in a total volume of 2 ml M9 with the indicated concentration of hydrogen peroxide at room temperature in a rotating roller drum for 30 minutes. To compare the H_2O_2 sensitivity of wild type and mutant strains, 50 µl of fluorescent unc54::YFP worms were mixed with 50 µl of the respective mutant and treated with H_2O_2. The worms were collected by centrifugation and the oxidant was washed away with M9 medium. For lifespan and behavior assays, the animals were seeded onto fresh NGM plates and immediately singled. Singling and scoring was performed blinded at least for the day 0 evaluation. To prepare protein extracts for proteomic analyses, 50-100 µl worms were harvested onto 10% (w/v) trichloracetic acid (TCA), shock frozen in liquid nitrogen and homogenized with mortar and pestle.

For the recovery studies, the animals were seeded on fresh NGM plates and allowed to feed on *E. coli* OP50 before they were harvested.

2.3.3 Biochemical techniques

2.3.3.1 C. elegans *protein extracts*

Staged or mixed populations can be used to obtain protein extracts from *C. elegans*. When using a mixed population, filtration through a nitex membrane (37 μm) was used to remove eggs, because eggs are difficult to lyse. 50-200 μl of worms were harvested in a 15 ml centrifugation tube and washed twice with M9 medium to remove the feeding bacteria. For complete buffer exchange, the worms were washed an additional two times in starting buffer. Subsequently, 426.5 μl of the worm suspension were transferred into a 1.5 ml tube, and 71.5 μl of 7x Proteinase Inhibitor Cocktail and 2 μl of PMSF (0.25 M) was added. The worms were shock frozen in liquid nitrogen and thawed at room temperature. The freeze thaw cycle was repeated 3 times. The suspension was then pipetted into an ice-cold mortar and homogenized while frozen. The frozen worm lysates were transferred into a fresh 1.5 ml tube and the protein concentration of the lysate was determined by Bradford assay. The protein yield depends largely on the starting material and the density of the worm suspension (Table 2.2). In Bradford assays, Coomassie Brilliant Blue G-250 binds to positively charged and hydrophobic amino acids. This binding leads to absorbance a 595 nm, which is linearly related to the protein concentration. A standard curve can be established with defined BSA concentrations.

Table 2.2: Typical protein yield for worm lysis

Volume of worms for lysis	Protein yield
50 μl	75-200 μg
100 μl	~300 μg
200 μl	420-600 μg

2.3.3.2 SDS-PAGE and staining of protein gels

Proteins were separated and visualized by SDS polyacrylamide gel electrophoresis (PAGE). For SDS-PAGE, protein samples were supplemented with 5x Laemmli buffer and incubated at 95°C for 5 min. Alternatively, 50 single worms or 10 µl of a dense worm population were directly picked or pipetted into 5x Laemmli buffer and boiled for 30 min at 95°C. The samples were then applied onto pre-cast 14% Tris-glycine polyacrylamide gels and separated in an electrical field with a maximum voltage of 200 mV and 35 mA per gel for one hour. SDS polyacrylamide gels were stained according to the efficient Coomassie staining method developed by (Fairbanks et al. 1971) and modified by (Wong et al. 2000).

2.3.3.3 Immunoblotting (Western Blot) and Stripping

Immunoblotting is used to detect and quantify a particular protein in a complex protein mixture with high specificity and selectivity. Proteins, that are either separated with SDS-PAGE or 2D-gels can be transferred onto a nitrocellulose membrane by the application of an electric field (Towbin et al. 1979). The protein of choice is detected by a specific primary antibody and an enzyme-linked secondary antibody, whose binding can be visualized on film via a chemiluminescence reaction. Western blotting of small SDS polyacrylamide gels was performed using a semi dry blotting unit at 50 mA per blot for 90 min. The larger 2D gels were blotted at 150 mA for 2 h. Antibodies used for immunoblotting are described in section 2.4.4. To detect different proteins on the same gel, the western blots were stripped by incubating the nitrocellulose membrane for 30 min in stripping buffer (section 2.4.6) and three subsequent washing steps with TBS-T.

2.3.3.4 Sample preparation for 2D Gel electrophoresis and differential thiol trapping

To prepare *C. elegans* protein extracts for proteomic analyses, such as 2D gel electrophoresis and differential thiol trapping, 50-100 µl worms were harvested onto 10% (w/v) trichloracetic acid (TCA), shock frozen in liquid nitrogen and homogenized with mortar and pestle. The TCA-treated protein extracts from *C. elegans* were centrifuged (13,000g, 4°C, 30 min) and the resulting pellet was consecutively washed with 500 µl 10% (w/v) TCA and 200 µl 5% (w/v) TCA and the supernatant removed completely.

For 2D Gel electrophoresis, the pellet was resolved in 100 µl denaturing alkylating buffer (DAB) (section 2.4.6.) supplemented with 10 mM DTT. The protein extract was incubated for 1h at 23°C, 1320 rpm. Then, 20 µl DAB with 100 mM iodacetamide (IAM) was added to the mixture to alkylate all free thiols, which was further incubated for 10 min under the same conditions. The lysate was centrifuged (13,000g, 4°C, 30 min) to remove worm debris and insoluble protein. The supernatant was separated from the pellet and proteins were precipitated by the addition of 120 µl 20% (w/v) TCA and incubated on ice for at least 20 min. The TCA-treated protein pellet was centrifuged (13,000g, 4°C, 30 min) and the resulting pellet consecutively washed with 500 µl 10% (w/v) TCA, 200 µl 5% (w/v) TCA and three times with 500 µl ice-cold ethanol. The supernatant was removed completely and the pellet was allowed to air-dry. The pellet was resolved in 500 µl 2D Urea Buffer (section 2.4.6) and ready for 2D gelelectrophoresis (section 2.3.3.5).

For differential thiol trapping the original TCA-pellet was resolved in 40 µl DAB supplemented with 100 mM IAM and incubated for 10 min at 23°C (1320 rpm) to alkylate all free thiols. The lysate was centrifuged (13,000g, 4°C, 30 min) to remove

worm debris and insoluble protein. The supernatant was separated from the pellet and proteins were precipitated by the addition of 40 µl 20% (w/v) TCA and incubated on ice for at least 20 min. The TCA-treated protein pellet was centrifuged (13,000g, 4°C, 30 min) and the resulting pellet consecutively washed with 500 µl 10% (w/v) TCA and 200 µl 5% (w/v) TCA. The air-dried pellet was resolved in 20 µl DAB supplemented with 10 mM DTT to reduce all reversible thiol modifications and incubated for 1 h at 23°C, 1320 rpm. Then, 20 µl of DAB buffer supplemented with ^{14}C labeled IAM was added to the solution to alkylate all newly accessible thiol groups. The 40 µl reaction was stopped after 10 min by precipitation with 40 µl ice-cold 20% TCA. To precipitate the proteins, the solution was incubated on ice for at least 20 min. The TCA-treated protein pellet was centrifuged (13,000g, 4°C, 30 min) and the resulting pellet consecutively washed with 500 µl 10% (w/v) TCA, 200 µl 5% (w/v) TCA and three times with 500 µl ice-cold ethanol. The supernatant was removed completely and the pellet was allowed to air-dry. The pellet was resolved in 500 µl 2D Urea Buffer and ready for 2D gel electrophoresis as described in section 2.3.3.5 and in (Leichert and Jakob 2006).

2.3.3.5 Two-dimensional SDS-PAGE and protein visualization

Two-dimensional gelelectrophoresis is a widely used method for the analysis of complex protein mixtures, such as cell lysates. The separation is based on the distinct isoelectric point (pI) and the specific molecular weight of proteins. In the first isoelectric focusing (IEF) step, proteins separate on an immobilized pH gradient, where the proteins migrate in an electric field according to their internal net charge until they reach a location, where the pH equals their pI. The second step is SDS-PAGE (section 2.3.3.2), which separates the proteins according to their molecular weight. Each spot on the resulting two-dimensional gel corresponds to a single

protein species in the sample. In this study, 2D gels were used to analyze changes in the *C. elegans* proteome upon H_2O_2 stress and for analysis of the redox proteome using differential thiol trapping. Commercially available IPG strips with a pH gradient from 3-10 and an IPGphor unit were used for isoelectric focusing. The IPG strips were loaded with 450 µl protein samples in 2D gel buffer and layered over with 1.5 ml mineral oil. Strips were focused according to the manufacturer's protocol. After the focusing, the IEF strips were equilibrated and then loaded onto 13% 2D gels from Ettan Dalt and run in the accompanying separation unit at 20°C at 50 mA for 1 hour and, subsequently, at 100 mA for 16 hours. The proteins were visualized by colloidal coomassie blue staining. The colloidal coomassie staining solution was prepared by dissolving Coomassie Brilliant Blue G-250 in a minimum amount of methanol and the subsequent addition of phosphoric acid. In a separate flask ammonium sulfate was dissolved in water and methanol was slowly added under stirring, which caused the formation of a precipitate. Next, the methanol/coomassie blue solution was carefully added to the methanolic ammonium sulfate solution. The 2D gels were placed directly into the staining solution and incubated overnight on a rotating platform. A 10% (v/v) acetic acid solution was used for destaining the gels. The gels were scanned using an Expression 1680 scanner with transparency unit at 200 dpi resolution / 16 bit grayscale. Gels were dried and phosphorimages are obtained by exposing LE Storage Phosphor Screens to the dried gels for 10 days. The phosphor image screens were scanned with the Personal Molecular Imager FX at a resolution of 100 µm. The original image size of the phosphor image was changed to a resolution of 200 dpi with PhotoShop software. The images of the colloidal Coomassie blue-stained proteins and the phosphor images were analyzed using Delta 2D Software.

2.3.3.6 Data analysis of 2D gels and differential thiol trapping

To quantify abundance of proteins on 2D gels for comparative studies, data analysis was performed with Delta 2D Software. To quantify the abundance of PRDX-2 and PRDX-2-SO_2H the following normalization technique was used. The Delta 2D Software normalizes spot intensities over the overall darkness detected on one gel. This allows the comparison of proteins whose protein amount does not change, even though the loaded protein amount may vary. Typically, more than 50 non-changing spots were used for protein normalization of candidate spots, such as PRDX-2. The absolute spot intensity of the candidate proteins was normalized over the absolute spot intensites of the normalization spots.

A similar approach was used to quantify the differential thiol trapping experiments. For each experiment, the phosphor image with the highest overall ^{14}C-activity was selected for spot detection. The 100 most abundant spots were chosen from the detected set of spots and the boundaries transferred to all other phosphor images and protein gel images. The absolute intensity for each of these 100 spots on the protein gel and the phosphor image was determined to quantitatively describe the ratio of ^{14}C-activity/protein for each protein spot. The ratio of ^{14}C-activity/protein was calculated by dividing the normalized intensity of the protein spot on the phosphor image by the corresponding intensity of the Coomassie stained protein spot. For a protein to be considered significantly thiol modified, the average of ^{14}C-activity/protein ratio for a given protein spot had to be at least 1.5 fold above the average of ^{14}C-activity/protein ratio under control condtions. Proteins of interest were excised and identified by Peptide Mass Fingerprinting at the Michigan Proteome Consortium.

2.3.3.7 Sample preparation for OxICAT analysis

To prepare *C. elegans* protein extracts for OxICAT analysis, 50-100 µl worms were harvested onto 10% (w/v) trichloracetic acid (TCA), shock frozen in liquid nitrogen and homogenized with mortar and pestle. The TCA-treated protein extracts from *C. elegans* were centrifuged (13,000g, 4°C, 30 min) and the resulting pellet was washed with 500 µl 10% (w/v) TCA and 200 µl 5% (w/v) TCA and the supernatant removed completely. For OxICAT analysis, the first alkylation step was performed in the anaerobic chamber. The pellet was dissolved in 80 µl of DAB supplemented with the contents of one vial of cleavable light ICAT reagent that was dissolved in 20 µl of acetonitrile (ACN). To alkylate all free thiols, the sample was incubated at 37°C for 2 h at 1300 rpm. After the incubation 500 µl of acetone, kept at -20°C, was added and the reaction was stored at -20°C for at least 2 h. Then, the samples were centrifuged (13,000g, 4°C, 30 min) and the pellet was washed twice with 500 µl acetone (-20°C). The pellet was allowed to air-dry and subsequently dissolved in 80 µl DAB and 2 µl of reducing reagent (TCEP) provided in the ICAT kit. The sample was then transferred to the heavy ICAT vial, which was previously dissolved in 20 µl ACN. In this second alkylation step, the sample was incubated at 37°C for 2h at 1300 rpm. After the sample was transferred into a fresh tube with 500 µl of acetone (-20°C) and the reaction was stored at -20°C for at least 2 h. Then, the samples were centrifuged (13,000g, 4°C, 30 min) and the pellet was washed twice with 500 µl acetone (-20°C). The pellet was allowed to air-dry and subsequently dissolved in 80 µl denaturing buffer from the ICAT kit and 20 µl ACN. 100 µl of one vial of trypsin, which was dissolved in 200 µl ddH_2O and provided in the ICAT kit was added to the sample and incubated for 12 -16 h at 37°C. The tryptic digest of the protein samples were then purified via a small cation exchange column. The sample was briefly

centrifuged and transferred into a 15 ml centrifugation tube. Then 4 ml cation exchange buffer load were added. After equilibration of the cation exchange column, the labeled protein extract was loaded onto the column. After washing with 1 ml of the loading buffer, the peptides were eluted with 500 µl of the cation exchange buffer elute. The peptides were further purified with a small affinity chromatography column also supplied with the ICAT kit. After the column was equilibrated, the sample was loaded and then washed with 500 µl affinity buffer load, 1 ml affinity buffer wash 1, 1 ml affinity buffer wash 2 and lastly with 1 ml ddH_2O. The peptides were eluted with 800 µl affinity buffer elute. The peptides were dried using a speedvac for about 6 h. Subsequently the ICAT affinity tag was cleaved off by incubating the peptides in 90 µl of a 95:5 mxture of Cleavage reagent A : Cleavage reagent B for 2 h at 37°C. Before the sample can be submitted for LC-MSMS, the peptides again had to be dried in a speedvac. Mass spectrometery was performed at the Michigan Proteome Consortium (Leichert et al. 2008).

2.3.3.8 Data analysis of OxICAT experiment

The OxICAT data was analyzed using a modified version of the open source program *msinspect.* Data analysis is described in great detail in (Leichert et al. 2008). In short, ICAT pairs were defined as mass signals that differ by multiples of 9 Da and elute in the same fraction of the HPLC. The oxidation state of these ICAT pairs was then calculated by the *msinspect* software. To be considered redox-sensitive peptides, the cysteines had to be on average at least 1.5 fold more oxidized under the chosen experimental conditions as compared to control conditions, and the largest mass peak had to be at least 4-fold above background under all conditions. These calculations were performed in Excel. Importantly, all of the peptides that were found

to show an increase in oxidation state were then handcurated using the visualization tools in *msInspect*.

2.3.3.9 PRDX-2 purification, reduction and overoxidation.

The plasmid pJC45 containing the His-tagged variant of *C. elegans* PRDX-2 was transformed into *E. coli* BL21 (DE3)(pAPlacIQ). After IPTG induction and overexpression of PRDX-2, the cells were harvested and lysed by two cycles of french press. PRDX-2-His was purified with a Ni-NTA column as described by the manufacturer. The cell lysate was loaded onto the equilibrated Ni-NTA column, then first washed with 5 mM imidazole, 20 mM Tris, 0.5 M KCl (pH 7.5) and then with the same buffer containing 100 mM imidazole. Elution of the protein was achieved by running an imidazole gradient from 100 mM to 1 M in 360 ml. The purity of the recombinant PRDX-2 was verified with SDS-PAGE. *In vitro* reduction of purified PRDX-2 was achieved by incubating PRDX-2 with 5 mM DTT for 15 min at room temperature. To overoxidize 100 µM PRDX-2, purified PRDX-2 was incubated with 2.5 µM *E. coli* thioredoxin (Trx), 0.08 µM *E. coli* thioredoxin reductase (TrxR) and 10 mM H_2O_2 for 1h at RT (Chang et al. 2004).

2.3.3.10 Peroxidase assay

To determine the peroxidase activity of PRDX-2 and PRDX-2-SO_2H the classical NADPH oxidation assay was used. NADPH oxidation is coupled via thioredoxin reductase (TrxR) and thioredoxin (Trx) to H_2O_2 reduction by PRDX-2 (Figure 2.8).
NADPH oxidation was monitored as a decrease in absorbance at 340 nm at room temperature in a reaction mixture containing 50 mM Hepes (pH 7.0), 200 µM NADPH, 2.5 µM Trx, 0.08 µM TrxR, 2.5 PRDX-2, 500 µM H_2O_2.

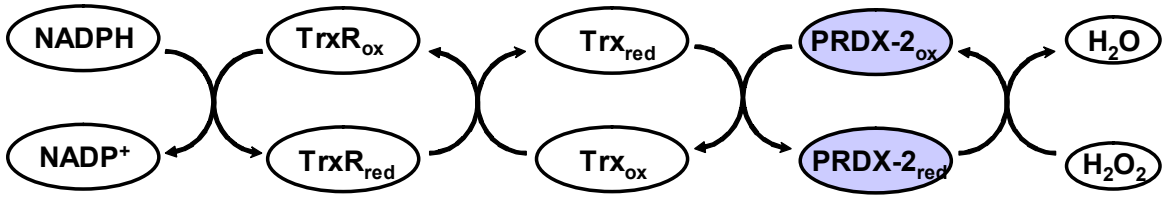

Figure 2.8: Peroxiredoxin's peroxidase activity can be measured by NADPH oxidation

Peroxiredoxin-2 (PRDX-2) is able to reduce H_2O_2 to H_2O. This reaction leads to the formation of an intermolecular disulfide bond. Reduction of PRDX-2 is achieved via the thioredoxin system. The disulfide bond of PRDX-2 is reduced by thioredoxin (Trx), which in turn is oxidized. The reduction of Trx is then achieved by the oxidation of thioredoxin reductase (TrxR). TrxR contains NADPH as a cofactor, which is the final electron donor in the reduction of TrxR.

2.3.3.11 Chaperone Assay

The chaperone activity of PRDX-2 was analyzed by testing its influence on the thermal aggregation pattern of citrate synthase (CS) at 43°C (Jakob et al. 1999). Aggregation of CS was analyzed by separating the insoluble aggregated fraction from the soluble fraction and subsequent visualization of CS on SDS-PAGE. 100 µM $PRDX_{red}$, PRDX-SO_2H or lysozyme was diluted 1:10 into 40 mM Hepes, pH 7.5 at 43°C. Then, 0.5 µM citrate synthase was added and the samples were incubated for 20 min at 43°C. After the incubation, the samples were centrifuged (5,000 rpm, for 30 min at 4°C) and the soluble supernatant was loaded onto a 14% SDS-PAGE.

2.4 Materials

2.4.1 Strains

2.4.1.1 C. elegans *strains*

Table 2.3: ***C. elegans*** **strains used in this study**

Description	Strain name	Allele and transgene	Source
wild type	N2 (Bristol)		CGC
wild type, fluorescent body wall muscle	AM134	*rmIs126*[P(unc-54)Q0::YFP)]	CGC
prdx-2 knock-out	VC289	*prdx-2*(gk169)II	CGC
sesn-1 knock-out	n.a.	Y74C9A.5(tm2872)	Mitani Lab, (Japanese knockout Consortium)

For the oxidative stress treatment strain AM134 *rmIs126*[P(unc-54)Q0::YFP)] was used as wild type. I analyzed the behavior and lifespan of the unc54::YFP strain and found it to be indistinguishable from the N2 strain.

2.4.1.2 E. coli strains

Table 2.4: ***E. coli*** **strains used in this study**

Name	Strain and plasmid	Genotype	Source
CK 56	OP50	*E. coli* B, Uracil auxotroph	CGC
CK 91	HB101	*supE*44, *hsdS*20(r_B^- m_B^-), *recA*13, *ara*-14, *proA*2, *lacY*1, *galK*2, *rpsL*20, *xyl*-5, *mtl*-1, *leuB*6, *thi*-1	Cszankovski lab
CK 84	DH5α pJC45-Ceprx2(Amp)	F^- 80d*lacZ* M15 (*lac*ZYA-*arg*F) U169 *rec*A1 *end*A1 *hsd*R17(r_k^-, m_k^+) *pho*A *sup*E44 $^-$ *thi*-1 *gyr*A96 *rel*A1	Iris Bruchhaus
CK 85	BL21(DE3) pAPlacIQ (KanR)	F^- *ompT gal [dcm] [lon] hsdS*$_B$ (r_B^- m_B^-; an *E. coli* B strain) with DE3, a λ prophage carrying the T7 RNA polymerase gene	Iris Bruchhaus

2.4.2 Primers

Primers were used for genotyping of *prdx-2* and *sesn-1* strains. All primers were purchased from Invitrogen (Carlsbad, CA).

Table 2.5: Primer used for genotyping

Primer Name	Sequence
PRDX2-FLANK-FWD	5'-GTTCTCATTTCGTCCTCCG-3'
PRDX2-FLANK-REV	5'-GGCCTGAACAAGACGAAGAG-3'
SESN1-FLANK-FWD	5'-CGTATAACAACGATGTTAGG-3'
SESN1-FLANK-REV	5'-CTCCGTCTCCAGATGCATG-3'

2.4.3 Proteins

BSA (bovine serum albumin)	Roche, Mannheim, Germany
Citrate Synthase	Roche, Mannheim, Germany
Lysozyme	MP Biomedicals, Irvine, CA
PfuTurbo DNA polymerase	Stratagene, La Jolla, CA
Proteinase K	MP Biomedicals, Irvine, CA
Taq DNA Polymerase	Fisher Chemical, Fair Lawn, NJ
Thioredoxin	Promega, Madison, WI

Purified thioredoxin reductase was kindly provided by Dr. Guoping Ren (Universiy of Michigan). All restriction enzymes were obtained from Promega (Madison, WI) or New England Biolabs.

2.4.4 Antibiotics, antibodies, dyes and markers and inhibitors

The following antibiotic concentrations were used:

Ampicillin	200 µg/ml
Kanamycin	100 µg/ml

Goat α-rabbit IgG HRP conjugated, from goat	Pierce, Rockford, IL
Rabbit α-PRDX-2	lab collection (Alpha Diagnostics International, San Antonio, TX)
Rabbit polyclonal α-Peroxiredoxin-SO3	Abcam Inc, Cambridge, MA
1 kb DNA Ladder PR-G5711	New England Biolabs Inc., MD
Ampicillin	MP Biomedicals, Irvine, CA
Bromophenolblue	MP Biomedicals, Irvine, CA
Coomassie brilliant blue G-250	MP Biomedicals, Irvine, CA

Coomassie brilliant blue R-250	MP Biomedicals, Irvine, CA
Ethidium bromide	Gibco, Rockville, MD
Kanamycin	MP Biomedicals, Irvine, CA
Mark 12, protein molecular weight marker	Invitrogen, Carlsbad, CA
Proteinase Inhibitor Cocktail	Roche, Germany
SuperSignalWestPico	Pierce, Rockford, IL
Xylene cyanol FF	MP Biomedicals, Irvine, CA

2.4.5 Chemicals

A	
Acetic acid, glacial	Mallinckrodt Baker, MO
Acetone	ICN, Aurora, OH
Acrylamide, ultra pure	MP Biomedicals, Irvine, CA
Agarose	MP Biomedicals, Irvine, CA
S-Adenosyl-L-Methionine, AdoMet	Sigma, St.Louis, MO
Ammonium Chloride, $(NH_4)Cl$	MP Biomedicals, Irvine, CA
Ammonium Sulfate, $(NH_4)SO_4$	MP Biomedicals, Irvine, CA
B	
Bacto-Agar	Difco, Detroit, MI
Bacto-Tryptone	Fisher chemicals, Fair Lane, NJ
Bacto-Yeast Extract	Fisher chemicals, Fair Lane, NJ
C	
Calcium chloride, $CaCl_2$	Fisher chemicals, Fair Lawn, NJ
Chaps	Pierce, Rockford, IL
Cholesterol	MP Biomedicals, Irvine, CA
Clorox household bleach	Clorox
Count-off	MP Biomedicals, Irvine, CA
D	
Dimethyl sulfoxide, DMSO	Sigma, St.Louis, MO
1,2-dithiothreitol, DTT	Sigma, St.Louis, MO
E	
Ethanol	Mallinckrodt Baker, MO
Ethylenediamine tetra acetic acid, EDTA	Sigma, St.Louis, MO
G	
Glycerol, ACS	Fisher, Pittsburgh, PA
Glycine	Sigma, St.Louis, MO
H	
Hydrochlorid acid, HCl	Fisher, Pittsburgh, PA
Hydrogen peroxide, H_2O_2	Fisher Chemical, Fair Lawn, NJ
N-(2-hydroxyethyl)-piperazine-N'-2-ethan sulfonic acid, Hepes	MP Biomedicals, Irvine, CA
I	
Iodo Acetamide	MP Biomedicals, Irvine, CA
Iodo[1-^{14}C]Acetamide	Amersham Biosciences, NJ
Imidazole	MP Biomedicals, Irvine, CA
IPTG	Research Products International
L	
Levamisole	Fisher Chemical, Fair Lawn, NJ

M	
MacConkey agar base	Difco, Detroit, MI
Magnesium sulfate, $MgSO_4$	Mallinckrodt Baker, Hazelwood, MO
Magnesium chloride, $MgCl_2$	Sigma, St.Louis, MO
β-Mercaptoethanol	MP Biomedicals, Irvine, CA
Methanol	EM Science, Gibbstown, NJ
N	
Nitrogen	Cryogenics, Detroit, MI
Nonfat dry milk	Hunt-Wesson, Fullerton, CA
P	
Pharmalytes 3-10	Amersham Biosciences, NJ
Phenol	MP Biomedicals, Irvine, CA
Phosphoric acid	Fisher Chemical, Fair Lawn, NJ
PMSF	MP Biomedicals, Irvine, CA
Potassium chloride, KCl	Sigma, St.Louis, MO
Potassium hydroxide, KOH	Merck, Whitehouse Station, NJ
2-propanole	Fisher chemicals, Fair Lawn, NJ
S	
Serdolit MB-1	Serva, Heidelberg, Germany
Sodium acetate	J.T. Baker, NJ
Sodium azide	MP Biomedicals, Irvine, CA
Sodium chloride, NaCl	Fisher, Pittsburgh, PA
Sodium citrate	Sigma, St.Louis, MO
Sodium dodecyl sulfate, SDS	Gibco, Rockville, MD
Sodium hydroxide, NaOH	Sigma, St.Louis, MO
Sucrose	Fisher chemicals, Fair Lawn, NJ
T	
Thiourea	Fluka, Milwaukee, WI
Trichloroacetic acid, TCA	Merck, Whitehouse Station, NJ
Tris-(hydroxymethyl)-aminomethan, Tris	MP Biomedicals, Irvine, CA
Tryptone	Fisher Chemical, Fair Lawn, NJ
Tween 20	MP Biomedicals, Irvine, CA
U	
Urea, ultra pure	MP Biomedicals, Irvine, CA

All other chemicals were either purchased from Fisher, MP Biomedicals, Fluka (Switzerland), Merck (Germany), Roth (Germany), Sigma or Sigma-Aldrich.

2.4.6 Buffers and solutions

Denaturing alkylating buffer (DAB)	Urea	6 g
	1M Tris-HCl (pH 8.5)	2 ml
	EDTA	0.2 ml
	10% SDS	0.5 ml
	ddH_2O	ad 10ml

LB medium	Tryptone	10 g
	Yeast Extract	5 g
	NaCl	5 g
	ddH_2O	ad 1 l
Freezing solution	NaCl	5.8 g
	1M KH_2PO_4 (pH 6)	50 ml
	Glycerol	240 ml
	ddH_2O	ad 1 l
	autoclave	
	1M $MgSO_4$	300 ml
Hypochlorite lysis solution:	Clorox Bleach	2 ml
	10N NaOH	0.25 ml
	ddH_2O	ad 5 ml
M9 medium	Na_2HPO_4	6 g
	KH_2PO_4	3 g
	NaCl	5 g
	1M $MgSO_4$•7 H_2O	0.25 g
	ddH_2O	ad 1 l
	autoclave	
NGM agar	NaCl	3 g
	Bacto-Peptode	2.5 g
	LB agar	19 g
	ddH_2O	ad 1 l
	autoclave	
	5 mg/ml Cholesterol	1 ml
	1M $CaCl_2$	1 ml
	1M $MgSO_4$	1 ml
	1M KH_2PO_4 (pH 6)	25 ml
SDS sample buffer (5x) (Laemmli buffer)	SDS	5 g
	Glycerol	30.5 g
	1 M Tris, pH 7.0	15 ml
	Bromophenolblue	0.025 g
	β-Mercaptoethanol	2.5 ml
	ddH_2O	ad 50 ml
SDS running buffer	Glycine	288 g
	Tris	58 g
	SDS	20 g
	ddH_2O	ad 20 l
Starting buffer	0.5M Hepes	50 ml
	5M NaCl	50 ml
	1M $MgCl_2$	0.5 ml
	NaN_3 (0.01% w/v)	0.05 g
	ddH_2O	ad 500 ml

Super NGM medium	NaCl	3 g
	Bacto Agar	18.75 g
	Bacto peptone	20 g
	ddH_2O	ad 1 l
	Autoclave	
	Cholesterol (5 mg/ml in Ethanol)	3 ml
	1M $MgSO_4$	1 ml
	1M $CaCl_2$	1 ml
	1M KH_2PO_4 (pH 6)	25 ml
TAE buffer	Tris	242 g
	Acetic Acid	57 ml
	0.5 mM EDTA, pH 7.5	100 ml
	ddH_2O	ad 10 l
TBS buffer	NaCl	160 g
	KCl	4 g
	Tris	60 g
	ddH_2O	ad 1 l
	adjust pH to 7.4 with HCl	
TBS-T buffer	NaCl	160 g
	KCl	4 g
	Tris	60 g
	Tween 20	20 ml
	ddH_2O	ad 1 l
	adjust pH to 7.4 with HCl	
Western blot transfer buffer	Methanol	200 ml
	Tris	5.8 g
	SDS	0.37 g
	Glycine	2.93 g
	ddH_2O	ad 1 l
Western blot stripping buffer	Glycine, pH 2	50 mM
	SDS 15 Tween 20	0.1% (w/v)
	adjust to pH 2.4 with HCl	
2D running buffer	Tris	29 g
	Glycine	149.8 g
	SDS	10 g
	ddH_2O	ad 10 l
2D resolving buffer	Tris	18.2 g
	SDS	0.4 g
	Sodium azide	10 mg
	ddH_2O	ad 100 ml
	adjust pH to 8.8 with HCl, filtrate	

2D sample buffer	Urea	42 g
	Thiourea	15.2 g
	Serdolit MB-1	1.0 g
	ddH_2O	to 50 ml; filtrate
	DTT	1.0 g
	Chaps	2.0 g
	Pharmalytes 3-10	500 µl
	aliquot and store at -20°C	
2D equilibration buffer	Urea	36 g
	Glycerol	30 g
	SDS	2 g
	2D resolving buffer	3.34 ml
	ddH_2O	bring to 100 ml
2D gel buffer	Tris	181.7 g
	SDS	4 g
	ddH_2O	ad 1 l
	Sodium azide	50 mg
	adjust pH to 8.6 with HCl, then filter	
2D agarose solution	Agarose	0.5 g
	Bromophenolblue	0.25 mg
	2D running buffer	ad 100 ml
2D 'heavy solution'	Glycerol	600 ml
	ddH_2O	400 ml
	Bromophenolblue	100 mg
2D colloidal coomassie	Ammonium sulfate	17% (v/v)
	Staining solution methanol	17% (v/v)
	Phosphoric acid	34% (v/v)
	Coomassie G-250	3% (v/v)
	ddH_2O	ad 3 l

2.4.7 Kits

Iodacetamide coated affinty tag (ICAT) Kit	Applied Biosystems, CA
Super Signal West Pico Chemiluminescent Substrate	Pierce Perbio, Rockford, IL
Wizard Plus SV Miniprep	Promega

2.4.8 Other material

Alcohol lamps	Homescience Tools, Billings, MT
Cellulose foil for gel drying	Pharmacia, Piscataway, NJ
Cheese cloth	Fisher, Pittsburg, PA
Conical PP tubes, 15 ml	Sarstedt, Newton, NC
Disposable plastic cuvettes, 1 ml	Fisher Lab Equipment, PA
ECL Western blot detection system	Pharmacia, Piscataway, NJ

Eggs	White Market, Ann Arbor, MI
Electrode Buffer Solutions pH 4.0, 7.0, 10.0	Fisher Lab Equipment, PA
Eppendorf LidBac, 2.0 ml Safe-Lock tubes	Brinkmann Instruments, NY
Gene pulser cuvettes	BioRad, Hercules, CA
Greiner Tubes, 50 ml	Bellco, Vineland, NJ
HiTrap Chelating HP Column	Amersham Biosciences, NJ
Immobiline DryStrips, misc	Amersham Biosciences, NJ
Liquid scintillation cocktail	MP Biomedicals, Irvine, CA
Microscope Slides and Coverslips	Fisher, Pittsburg, PA
Nitex Membrane 37 μm	Fisher, Pittsburg, PA
Nitrocellulose Membranes BA 58	Millipore, Bedford, MA
Petri dishes	Fisher, Pittsburg, PA
Pipet tips, misc	Molecular Bio Products, CA
Platinum Wire	Surepure Chemetals, NJ
Polyallomer centrifuge tubes, misc	Beckman, Fullerton, CA
Quartz cuvettes	Hellma Plainview, NY
Reaction tubes, 0.5, 1.5, 2.0 ml	Fisher, Pittsburgh, PA
SafeSkin, blue nitrile, Exam Gloves	Kimberly-Clark, WI
Scintillation Vials, 20 ml	Fisher Lab Equipment, PA
Syringe filters, 0.45 µM, sterile	Millipore, MA
Sterile syringes, misc.	Becton Dickinson, Franklin, NJ
Tissue Grind Pestle and Mortar	Kontes, Vineland, NJ
TBE-polyacrylamide gels, misc.	Novex, San Diego, CA
Tris-Glycine polyacrylamide gels, misc.	Novex, San Diego, CA
UltraOne, powder-free Latex Gloves	Microflex, Reno, NV
Whatman Chromatography Paper	Whatman, Clifton, NJ
X-ray film, Kodak X-OMAT AR-5 24x30	Kodak, Rochester, NY

All other consumables were purchased from Fisher Scientific.

2.4.9 Technical equipment

Äkta FPLC	Amersham Biosciences, NJ
Autoclave 3021 Gravity	Amsco
Blotting Unit	Owl
Centrifuge J2-HS	Beckman Fullerton, CA
Cooling unit	Revco Asheville, NC
Digital camera (Cohu 7800)	Cohu Camera, CA
Digital moving stage	Parker Automatic
Eppendorf Centrifuge 5415R	Eppendorf, Hamburg, Germany
Eppendorf Centrifuge 5804R	Eppendorf, Hamburg, Germany
Eppendorf Thermoblock, 24x2ml	Eppendorf, Hamburg, Germany
Eppendorf Thermomixer	Eppendorf, Hamburg, Germany
Ettan Dalt II glass plates 26x20 cm incl. Spacers	Amersham Biosciences, NJ
Ettan Dalt II Separation Unit and Power Supply/Control Unit	Amersham Biosciences, NJ
Film Developer SRX-101°	Konica, Mahwah, NJ

Fluor-S MAX MultiImager	BioRad, Hercules, CA
Fluorometer F-4500	Hitachi, Ontario, Canada
Fluorescence Stereoscope SZX16, SZX2-ILLT	Olympus, Center Valley, PA
Fraction Collector FPLC Frac-900	Amersham Biosciences, NJ
Freezer -80°C Ultima II	Revco, Asheville, NC
French Pressure Cell Press	American Instrument Company
Fridge-Freezer	Whirlpool
Gel Dryer Hoefer SE 1200 Easy Breeze™	Amersham Biosciences, NJ
Gel Electrophoresis chambers Xcell Surelock™	Invitrogen, Carlsbad, CA
GeneAmp PCR System 9600	Perkin Elmer Cetus
Gene pulser™	BioRad, Hercules, CA
Ice machine	Crystal Tips
Incubator 37°C Model 2015	VWR Scientific, IL
Incubator 43°C	National, a Heinecke Company
IPGphor Isoelectric Focussing System	Amersham Biosciences, NJ
Leica SP5 Confocal microscope (DM6000B)	Leica, Wetzlar, Germany
Liquid scintillation counter LS6800	Beckman, Fullerton, CA
Low Temperature Incubator 146E	Fisher Scientific, Pittsburg, PA
M 555 pH/Ion Meter w/ Arm, 120V	Corning Acton, MA
Magnet Stirrer nuova II	Sybron / Thermolyne
Microplate Reader ELx808	Bio-Tek Instruments, Winooski, VT
Microwave	Kenmore
Nikon Eclipse E600 stereoscope	Nikon, Melville, NY
Peristaltic Pump (Unispense)	Wheaton, Milville, NJ
Pipetman, misc.	Eppendorf, Hamburg, Germany
Power supply ECPS 3000/150	Pharmacia Fine Chemicals
Rotator for gels	Lab Line Inc.
Roller drum TC-7	NewBrunswick Scientific, NJ
Scale TL-2102	Denver Instrument Company
Scale, fine AB54-S	Mettler Toledo, OH
Scanner, EPSON Expression 1680	EPSON
Shaking Water Bath	Lab-Line, Melrose Park, IL
Spectrophotometer DU530	Beckman, Fullerton, CA
Spectrophotometer Jasco-550	Jasco, Easton, MD
SavantSpeedVac	GMI Inc., MN
Spot-2 camera	Diagnostic Instruments Inc., MI
Stereo 20/40x microscope	Homescience Tools, Billings, MT
Stereoscope (Zeiss Stemi 2000C)	Zeiss, Germany
Strip holder, 24 cm	Amersham Biosciences, NJ
Thermoblock, metal	VWR Scientific, IL
Vortex Mixer	VWR Scientific, IL
Water bath M6	mgw Lauda
White Light Transilluminator FB-WLT-1417	Fisher Lab Equipment, PA

2.4.10 Software and databases

Chromas 1.45	Conor McCarthy, Southport, Australia
Colibri Web Server	http://genolist.pasteur.fr/Colibri/
Delta2D	Decodon, Greifswald, Germany
Endnote 3.1.2.	ISI Research Soft, Berkeley, CA

EntrezPubMed	http://www3.ncbi.nlm.nih.gov/entrez/query.fcgi
FL Solutions	Hitachi, Ontario, Canada
Prism 4	GraphPad
Gene Runner 3.05	Hastings Software Inc.
ImageReady software	Adobe
KC3 data reduction software	Bio-Tek Instruments, Winooski, VT
Lalign Server	http://www.ch.embnet.org/software/LALIGN_form.html
LAS AF	Leica, Wetzlar, Germany
Microsoft Office XP Professional	Microsoft Corporation
Open Video Converter	DigitByte Studio
Moverz	Proteometrics
msinspect	open source
Photoshop	Adobe
Sigma Plot 8.0 for Windows	SPSS Scientific
Spectra Manager	Jasco, Easton, MD
WormAtlas	http://www.wormatlas.org
WormBase	http://www.wormbase.org
WormBook	http://www.wormbook.org

3 Results and Discussion

3.1 Oxidative stress in C. elegans

In the last 15-20 years, the aging field has made tremendous progress in identifying important longevity pathways and genes involved in lifespan determination (Guarente and Kenyon 2000). Still, very little is known about the underlying cause of aging and the biochemical effects of the mutations that result in lifespan expansion. One potential cause of aging is the accumulation of oxidative damage to biomolecules (Johnson, Sinclair et al. 1999). My goal was to monitor the effects of oxidative stress on physiological processes and on the proteome of *C. elegans*. Identification and characterization of oxidation sensitive proteins will be helpful as biomarkers for the aging process. In addition, analysis of the redox status of structurally or functionally important cysteine residues will enable us to use them as sensitive read-outs for the presence of ROS in cells and organisms (Leichert and Jakob 2006). The identification of redox-regulated proteins will increase our understanding of redox-regulated responses and help us develop strategies to counteract oxidative stress conditions.

3.1.1 Oxidative stress leads to reversible behavioral changes in *C. elegans*

To identify H_2O_2 concentrations that are high enough to induce physiologically relevant oxidative protein modifications without causing cell-death-mediated oxidative stress, synchronized wild type L4 larvae were exposed to a short-term treatment of H_2O_2 at various concentrations. I found that H_2O_2 concentrations in the low millimolar range fulfilled the criteria; short-term exposure of *C. elegans* to 6 to 10 mM H_2O_2 was non-lethal (survival rate >95% as compared to the untreated control group) and did not affect the mean lifespan of the organism (Figure 3.1A,B and Table 3.4). The survival data plotted as the logarithm of mortality rate (i.e. a Gompertz curve), shows that the oxidative stress treatment did not lead to an accelerated aging rate or to an

increase in the initial mortality rate. However, the oxidative insult resulted in an earlier onset of mortality; worms treated with H_2O_2 began to die at a younger age compared to untreated controls (Figure 3.1B). It caused very distinct behavioral defects, suggesting that the animals suffer from oxidative stress conditions (Figure 3.1). The most obvious effect was decreased thrashing of the worms after the H_2O_2 treatment and during the washing procedure, an experimental step which is important to facilitate recovery of the animals. The movement defect further intensified within the first hour of seeding the worms onto fresh plates containing OP50 as a food source. Almost 20% of the singled worms that were treated with 6 mM H_2O_2 and about 60% of the nematodes treated with 10 mM H_2O_2 showed highly impaired movement that ranged from no movement to slow and uncoordinated motility (Figure 3.1C). Importantly, within 72 hours after treatment, the vast majority of worms regained their fast, sinusoidal body movement, which they maintained until the typical age-related motility decline set in (Figure 3.1C). This result suggested that young worms have effective antioxidant systems that reverse the effects of oxidative stress and promote their recovery.

Another consequence of exposing *C. elegans* larvae to H_2O_2 was a statistically significant reduction in progeny production (Figure 3.1F and Table 3.4). While the non-treated control group produced the typical number of progeny during the self-fertile reproduction span (209 $\pm$ 13), animals that were treated with either 6 or 10 mM H_2O_2 had about 30% less progeny with a brood-size of 136 $\pm$ 13 and 139 $\pm$ 13, respectively. This reduction in brood size appeared not to be due to differences in the fertility span (Figure 3.1E) but due to a severe decline in egg production in the first three days after the oxidative stress treatment (Figure 3.1F). As observed before, the animals recovered within 72 hours of the treatment and showed a progeny production very similar to the progeny production of the control group (Figure 3.1F).

Table 3.1: Physiological processes after H_2O_2 treatment of *C. elegans*

H_2O_2 - Treatment	Life span [days] MLS ± SE	Max. LS ± SE	n	Progeny ± SE	n
0 mM	8.3 ± 0.4	14.0 ± 1.0	40	209 ± 12.9	40
6 mM	7.5 ± 0.4	12.3 ± 1.0	45	136 ± 12.5	42
10 mM	7.6 ± 0.5	12.9 ± 0.9	38	139 ± 12.9	35

Feeding behavior, measured as pharyngeal pumping, was also found to be impaired after the oxidative stress treatment. On day 1 after the stress treatment, the pumping rate was measured by counting the number of pumps during a 10 second period. For every worm, this measurement was repeated 3 times. The pumping rate of the oxidatively treated worms was decreased by almost 50% (Figure 3.1D). Moreover, I found that oxidatively treated wild type worms have significantly reduced body length after the oxidative stress treatment, which might be attributed to oxidant induced muscle contraction (Figure 3.1G and Figure 3.1A). Comparison of the size of the worms on day 1 after the stress treatment revealed an even greater difference between non-treated and oxidatively stressed worms. The H_2O_2 treatment therefore also inhibited growth of the adult worms (Figure 3.1G and Figure 3.1A). The observation that oxidative stress causes multiple behavioral defects might either reflect independent effects of ROS on distinct processes in *C. elegans* or might be due to the oxidative inactivation of one or more common effector proteins. For instance, ROS-mediated inactivation of muscle-specific proteins in body wall muscle cells and the pharynx would reduce motility and feeding, thereby affecting growth rate.

A Survival after H_2O_2 treatment

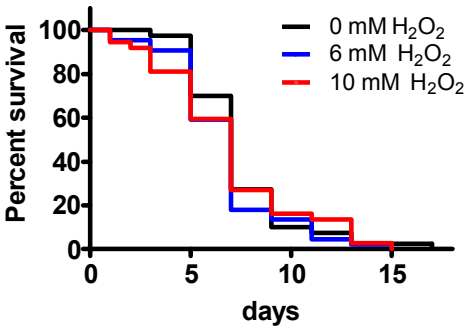

B Mortality rate after H_2O_2 treatment

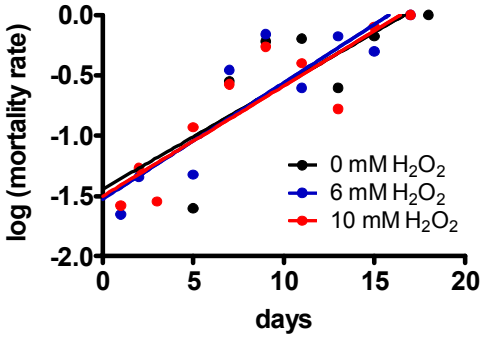

C Peroxide-induced movement defects

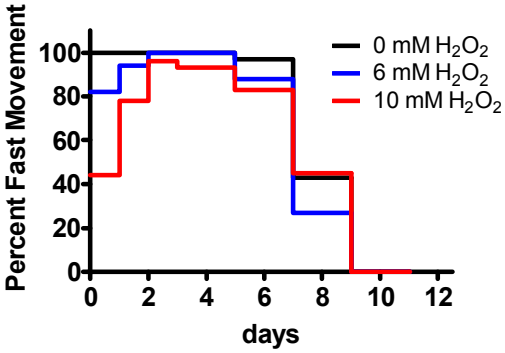

D Peroxide-induced defects in pharyngeal pumping

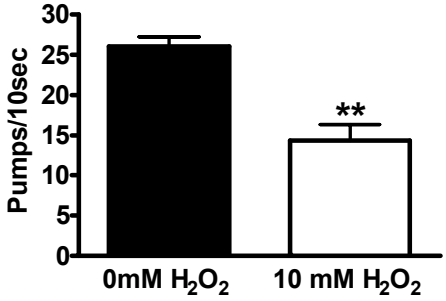

E Fertility span after H_2O_2 treatment

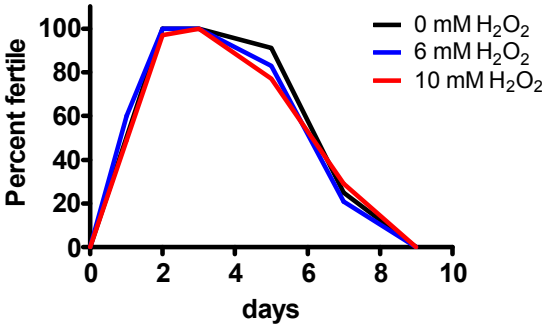

F Peroxide-induced defects in progeny production

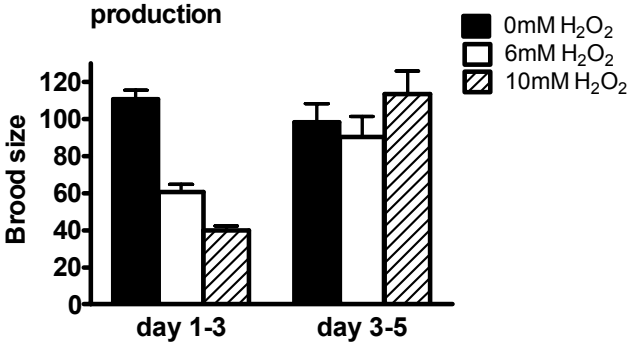

G Peroxide-induced defects in body length

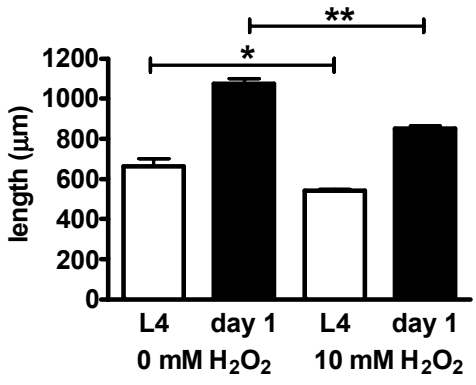

Figure 3.1: Short term H_2O_2 treatment causes reversible behavioral defects in *C. elegans*

Synchronized L4 larvae of wild type C. elegans *(day 0 of adulthood) were incubated with 0, 6, and 10 mM H_2O_2 for 30 min in liquid M9 media. The oxidant was washed away and the animals were seeded on fresh NGM plates with OP50 as food source and reared at 25°C. 50 worms were singled and scored for **A)** survival, **B)** mortality rate, **C)** fast movement, **D)** pharyngeal pumping rate (day 1 only), **E)** and fertility span, **F)** progeny production (day 5-9 not shown) and **G)** growth rate from L4 stage to day 1 of adulthood. No significant difference in the mean lifespan of oxidatively stress treated worms was observed (p-value 0.748, χ^2 0.580, non-parametric log rank test).*

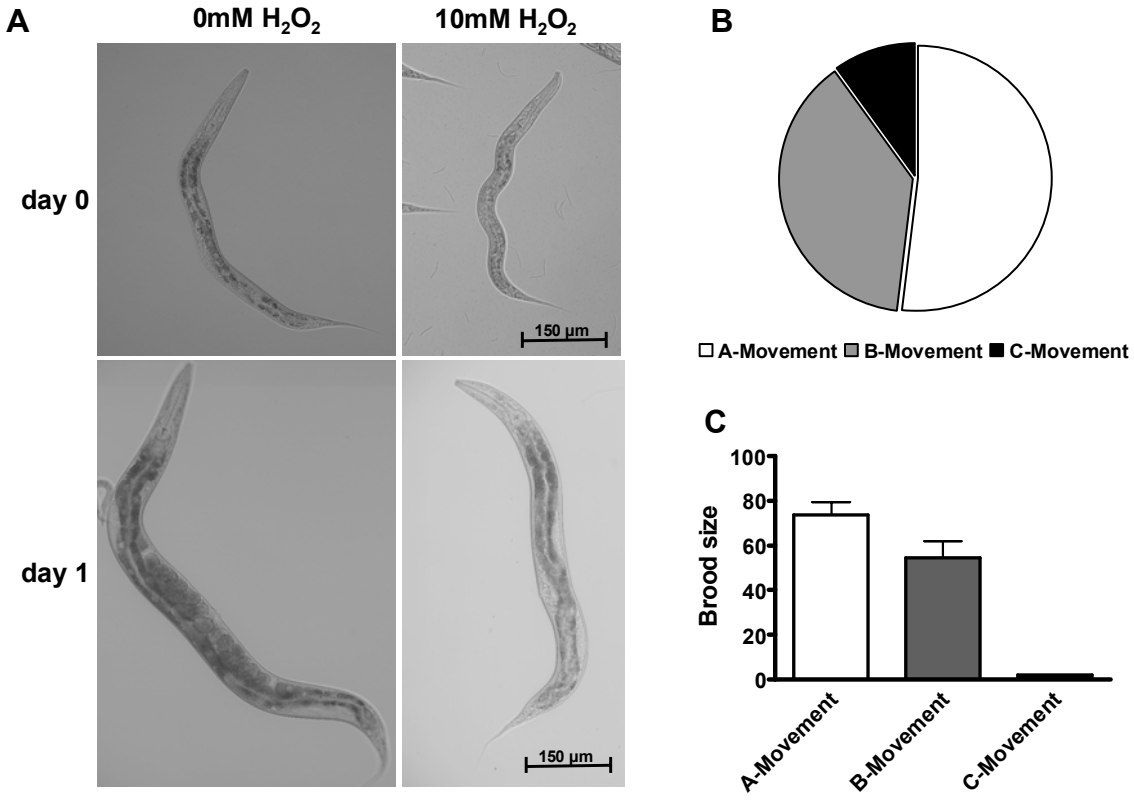

Figure 3.2: H_2O_2-induced movement defects associate with reduced brood size in wild type *C. elegans*

Synchronized wild type L4 larvae were subjected to short-term 10 mM H_2O_2 treatment. ***A)*** *Worms were imaged on day 0 and on day 1 after oxidative stress treatment to assess body length and growth rate from L4 stage to day 1 of adulthood* ***B)*** *Animals were scored according to their movement. 52% of oxidative stress treated animals revealed fast and coordinated A-movement, 37% of animals showed uncoordinated B-movement, and 11% of animals showed minimal C-movement.* ***C)*** *Correlation of movement behavior at day 0 and total brood size is shown.*

An excellent correlation between worms exerting H_2O_2-induced motility defects and having brood size defects while worms, whose motility seemed unaffected by the H_2O_2-treatment showed normal brood size and behavior (Figure 3.2C). This suggests that some worms are intrinsically more resistant than others, a notion that agrees well with lifespan studies, which reproducibly show that some animals are intrinsically fitter than others (Wu et al. 2006).

In summary, I show that exogenous oxidative stress treatment leads to defects in motility, egg production, growth rate reduction and size in *C. elegans*. Noteworthy, these phenotypes are reminiscent of age-related phenotypes, which also include changes in neuromuscular behavior (*e.g.,* decrease in rate of pharyngeal pumping and body movement), reproduction, morphology and metabolic activity (Collins et al. 2008). My results therefore suggest that increased intracellular oxidative stress might contribute to the age-related decline in fertility and mobility in *C. elegans*. In contrast to aging worms, however, young worms appear to possess potent antioxidant and repair systems, which clear the damaging effects of H_2O_2 and potentially other ROS and allow the worms to recover from the oxidative damage.

3.1.2 Oxidative stress leads to significant changes in the *C. elegans* redox proteome

Treatment of worms with 10 mM H_2O_2 caused severe yet reversible phenotypes suggesting that cellular proteins might be exposed to reversible oxidative stress conditions. To investigate what proteins harbor redox-sensitive cysteines that are affected by oxidative stress, I visualized the redox status of *C. elegans* proteins upon exposure to 10 mM H_2O_2 using our differential thiol trapping method combined with 2D gel electrophoresis (Leichert and Jakob 2004). For this experimental approach, I exposed synchronized L4 larvae to a 30 min oxidative stress treatment. After the removal of the oxidant, I collected ~30,000 worms, treated them with TCA to stop all thiol-disulfide exchange reactions and subsequently lysed the worms. Then, I irreversibly labeled all reduced cysteines in *C. elegans* proteins with the thiol-specific reagent iodoacetamide (IAM) under protein denaturing conditions. To visualize the oxidized cysteines, all existing oxidative thiol modifications were subsequently reduced with the thiol reductant DTT and labeled with a radioactive version of IAM (^{14}C-IAM). This technique generates chemically identical proteins, which migrate to

the same spot in 2D gels but differ in their ^{14}C to protein ratio depending on their *in vivo* redox status (Figure 3.3A). While low ratios of ^{14}C to protein (Figure 3.3A, green spots) represent proteins with predominantly reduced cysteines, high ratios of ^{14}C to protein (Figure 3.3A, red spots) indicate proteins with oxidized cysteines (Table 3.2). Any oxidative stress-mediated increase in the thiol oxidation status is reflected by an increase in the ^{14}C to protein ratio and represents proteins with redox-sensitive cysteines (Figure 3.3B).

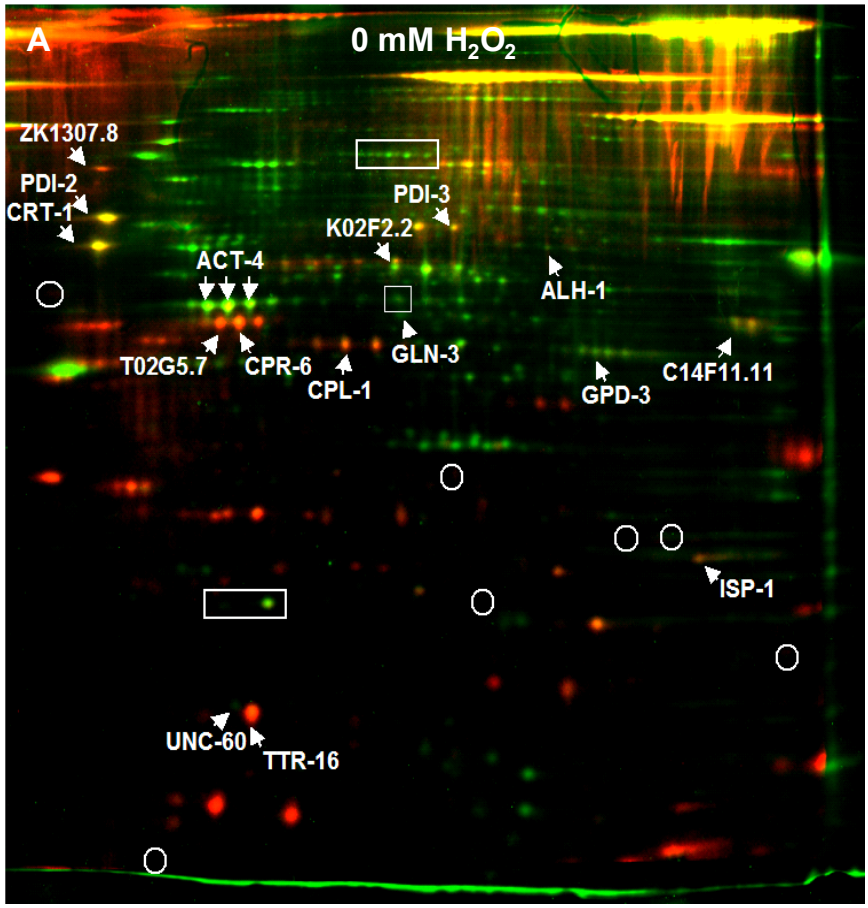
A
0 mM H_2O_2
ZK1307.8
PDI-2
CRT-1
PDI-3
K02F2.2
ACT-4
ALH-1
T02G5.7
CPR-6
CPL-1
GLN-3
GPD-3
C14F11.11
ISP-1
UNC-60
TTR-16

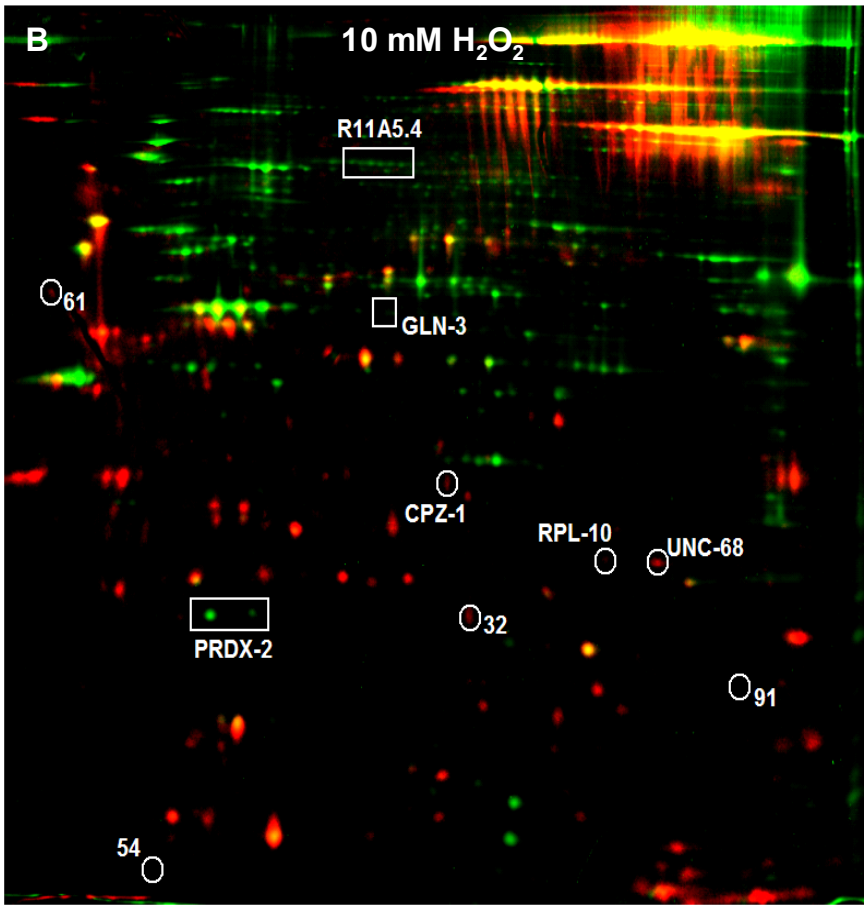
B
10 mM H_2O_2
R11A5.4
61
GLN-3
CPZ-1
RPL-10
UNC-68
32
PRDX-2
91
54

Figure 3.3: Identification of oxidative stress sensitive proteins in *C. elegans*

Synchronized L4 larvae of wild type C. elegans *were incubated with 0 (control) or 10 mM H_2O_2 for 30 min. After the oxidant was washed away, the animals were processed for differential thiol trapping in combination with 2D gel analysis. Colored overlay of the Coomassie blue-stained 2D gel (shown in green) and phosphor image (shown in red) of a differentially trapped protein extract from* C. elegans *treated with **A)** 0 mM H_2O_2 or **B)** 10 mM H_2O_2. Proteins with low ratios of ^{14}C-activity/protein ("reduced") appear green, while proteins with high ratios of ^{14}C-activity/protein ("oxidized") appear red. Proteins that show a significantly higher ^{14}C-activity/protein ratio (>1.5 fold) after 30 min H_2O_2 treatment than in untreated worms are circled and labeled in B). Selected proteins that undergo oxidative stress-mediated changes in protein amount (phosphoenolpyruvate carboxykinase isoforms, R11A5.4; glutamine synthetase, GLN-3) or mobility (Peroxiredoxin-2; PRDX-2) are surrounded by squares and labeled in B). All labeled proteins were identified by tryptic digest and mass spectrometry.*

The differential thiol trapping experiment revealed that of the 100 most oxidized proteins in L4 larvae exposed to 10 mM H_2O_2, the redox status of at least seven proteins changes substantially (>1.5 fold) upon the oxidative stress treatment (Figure 3.4). Four of these potentially redox-sensitive proteins are of low abundance and could not be identified by conventional mass spectrometry. Alternative approaches might be necessary to obtain their identity. Nevertheless, these four proteins might serve as excellent marker proteins to monitor if and at what point in the life span of *C. elegans*, peroxide stress conditions might affect the thiol status of proteins.

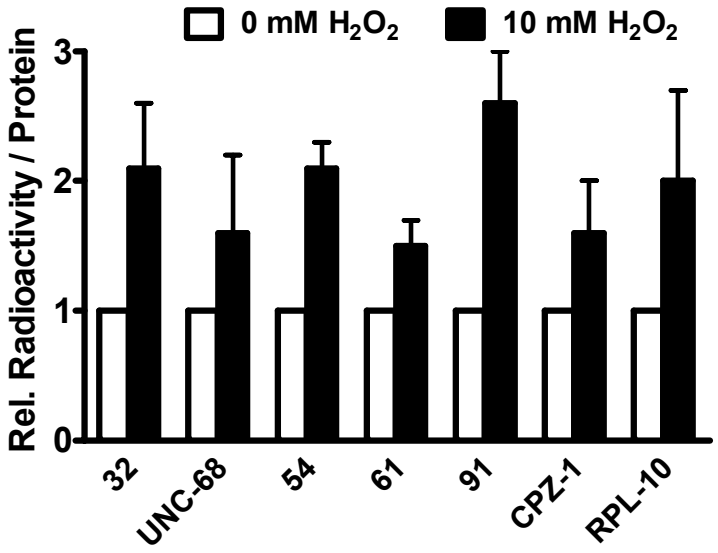

Figure 3.4: Quantification of oxidative stress sensitive proteins in *C. elegans*

The oxidation-dependent changes in the ^{14}C-activity/protein ratio of proteins that show a significantly higher ^{14}C-activity/protein ratio (>1.5 fold) after 30 min H_2O_2 treatment than in untreated worms are presented as bar chart.

The three redox-sensitive proteins, whose ID we obtained by mass spectrometry (ion score >95%), are the cysteine protease cathepsin Z (CPZ-1), the large ribosomal protein RPL-10, and a fragment of the ryanodine receptor UNC-68 (Figure 3.3). Cathepsin Z, which is widely expressed in hypodermal and intestinal cells of L4 larvae and should therefore be rapidly exposed to exogenous H_2O_2 treatment harbors two absolutely conserved C-X-Y-C motifs, one of which contains the active site cysteine. Because C-X-Y-C motifs are the hallmark of most thiol oxidoreductases and many redox-regulated proteins (Fomenko and Gladyshev 2003), it is likely that one or more of these cysteines are redox-sensitive. Recent *in vitro* studies showed that cathepsins are highly prone to oxidative inactivation by reversible thiol modifications (Headlam et al. 2006). These results are in excellent agreement with our studies and suggest that cathepsin Z is a redox-sensitive *C. elegans* protein, which is rapidly oxidized and potentially inactivated upon exposure of *C. elegans* to peroxide stress.

The second redox-sensitive protein that we identified is the ribosomal protein RPL-10. RPL-10 harbors 6 cysteines and its activity has been shown to regulate the translating ribosome population (Pachler et al. 2004). Importantly, redox proteomic analysis of chronologically aging yeast cells in our lab identified yeast Rpl-10 as a protein that becomes increasingly thiol-modified as yeast ages (Brandes and Jakob, ms in preparation). Because heterozygous deletion of *rpl-10* has been shown to also impact replicative lifespan in yeast (Chiocchetti et al. 2007), it is tempting to speculate that oxidative thiol modification of Rpl-10 might be involved in regulating translational efficiency during the lifespan of organisms.

The third protein with redox-sensitive cysteines is the ~550 kDa Ca^{2+} release channel receptor UNC-68, a ryanodine receptor RyR homologue expressed in the body wall muscle cells and pharynx of *C. elegans.* Striated muscle contraction is triggered by voltage-gated Ca^{2+}-channels, whose relatively small Ca^{2+}-influx subsequently activates the Ca^{2+} release channels, which cause the release of large amounts of stored Ca^{2+} from the sarcoplasmic reticulum (Maryon et al. 1998). It is well-established that the mammalian RyR homologues are redox-sensitive proteins. Oxidative modification of one or more of so-called hyper-reactive cysteines, which are highly conserved among Ryr-homologues, by low concentrations of either H_2O_2 or other cysteine-oxidizing agents have been shown to cause channel opening (Aracena-Parks et al. 2006). High concentrations of ROS or prolonged exposure of RyR homologues to ROS, on the other hand, cause the inactivation of RyR (Zima and Blatter 2006). Interestingly, *unc-68* mutants in *C. elegans* were originally identified as being defective in locomotion (*i.e.,* incomplete paralysis) and pharyngeal pumping (Maryon et al. 1998). In addition to these visible defects, *unc-68* mutants were shown to grow more slowly and have about 50% fewer offspring (Maryon et al. 1998). Noteworthy, these phenotypes are very similar to our H_2O_2-mediated

phenotypes suggesting that oxidation and inactivation of *C. elegans* UNC-68 might contribute to our observed oxidative stress phenotypes. Apart from this small group of redox-sensitive proteins, the majority of *C. elegans* proteins remained either largely reduced (*e.g.,* ALH-1, ACT-4, R11A5.4) (Table 3.1b) or oxidized (*e.g.,* TTR-16, CPR-6, CPL-1*)* in the presence of H_2O_2-induced oxidative stress (Table 3.1c). Although we were able to identify only few proteins that harbor cysteines, which are sensitive to exogenous H_2O_2 treatment, our findings agree with redox proteomic analyses in other organisms (Leichert and Jakob 2004; McDonagh and Sheehan 2008; Wan and Liu 2008). However, it is likely that our number is an underestimation. Non-abundant redox-sensitive proteins or redox-sensitive proteins with extreme isoelectric points, for instance, will escape our detection. More importantly, however, is the fact that our analysis involves the whole worm population, of which roughly 40% do not reveal any obvious phenotype and might not suffer from severe oxidative stress. Therefore, our threshold of significance (> 1.5 fold increase in ^{14}C/proteins ratio), which works well for redox proteomic studies in unicellular organisms (Leichert and Jakob 2004) and same-cell type tissue might be at the high end for these studies. The very same considerations make us confident, that the proteins that we did identify with this approach and threshold are indeed redox-regulated *C. elegans* proteins, which are likely to be involved in the physiology and oxidative stress response of the worms

Table 3.2: Redox-sensitive *C. elegans* proteins identified in differential thiol trapping experiment

a. Oxidative stress sensitive proteins					
Protein	**WormBase Accession Number**	**Description**	**Ratio**	**Cys**	**MW (kDa)**
UNC-68	CE41827	Ryanodine receptor ortholog, expressed in body-wall muscle cells and required for normal body tension and locomotion	2.1	91	590.5
CPZ-1	CE36646	Homolog of cathepsin z-like cysteine protease, cyclically expressed in hypodermal cells throughout development and required for normal molting	1.6	14	34.7
RPL-10	CE01543	Large ribosomal subunit L10 protein	2.0	6	24.7
32			2.1		
54			2.1		
61			1.5		
91			2.6		

b. Proteins with a ^{14}C/protein ratio below 0.5

Protein	WormBase Accession Number	Description	Cys	MW (kDa)
PRDX-2	CE32361	Peroxiredoxin-2, thiol specific antioxidant	2	21.8
ALH-1	CE29809	Ortholog to the human mitochondrial gene Aldehyde dehydrogenase 2	5	55.0
C14F11.1	CE02477	Ortholog to Aspartate aminotransferase/Glutamic oxaloacetic transaminase AAT1/GOT2	3	45.6
UNC-60	CE20547	Orthologs of actin depolymerizing factor/cofilin, actin-binding proteins that regulate actin filament dynamics	3	18.3
ACT-4	CE12358	Actin isoform that is most similar to act-2 in amino acid sequence; expressed in body wall and vulval muscles and the spermatheca	6	41.8
R11A5.4	CE12728	Ortholog of Phosphoenolpyruvate carboxykinase.	11	73.4
GLN-3	CE24078	Ortholog to Glutamine synthetase (glutamate-ammonia ligase)	2	36.4
GPD-3	CE07370	Predicted glyceraldehyde 3-phosphate dehydrogenase, affects embryonic viability.	2	36.4
CPL-1	CE16333	Member of the cathepsin L-like cysteine protease family, required for embryonic viability and normal growth; expressed in eggshells and throughout early embryos, accumulates in intestinal cells during late embryogenesis, and expressed in the cuticle, gonad, and pharynx later in development	7	38.1

Protein	WormBase Accession Number	Description	Cys	MW (kDa)
c. Proteins with a ^{14}C/protein ratio between 0.5-2.0				
PDI-2	CE03972	Protein disulfide isomerase (prolyl 4-hydroxylase beta subunit)	4	55.1
PDI-3	CE11570	Protein disulfide isomerase (PDI), required for normal cuticle collagen deposition and, for maintenance of normal body shape; PDI-3 has both PDI and calcium-dependent transglutaminase activity *in vitro*	6	54.9
CRT-1	CE21562	Ortholog of calreticulin (a calcium-binding molecular chaperone of the endoplasmic reticulum); required for normal sperm development, male mating efficiency and hermaphrodite fertility; expression induced by stress	4	45.6
d. Proteins with a ^{14}C/protein ratio above 2.0				
ISP-1	CE17071	Rieske iron sulphur protein (ISP), subunit of the mitochondrial complex III, which catalyses electron transport from ubiquinol to cytochrome c;	4	29.7
T02G5.7	CE04859	Homolog of human Acetyl-CoA acetyltransferase	4	40.7
ZK1307.8	CE15547	Protein kinase C substrate, 80 KD protein, heavy chain	16	58.0
CPR-6	CE04078	Related to the cathepsin L-like cysteine protease family	17	42.4
K02F2.2	CE19022	Ortholog of S-adenosylhomocysteine hydrolase (SAHH), predicted to catalyze the hydrolysis of S-adenosyl-L-homocysteine to adenosine and L-homocysteine.	7	47.5
TTR-16	CE17154	Uncharacterized protein with conserved cysteine	7	14.7

3.1.3 Oxidative stress leads to the rapid overoxidation of *C. elegans* PRDX-2

In addition to the proteins with reversible thiol modifications upon oxidative stress, this analysis also revealed a number of proteins that underwent a dramatic change in protein concentration, such as Phosphoenolpyruvate carboxykinase (R11A5.4) and Glutamine synthetase (GLN-3) (Figure 3.5A). About 50% of Phosphoenolpyruvate carboxykinase and more than 75% of glutamine synthetase GLN-3 was degraded during the 30 min oxidative stress treatment. It has been previously described that both proteins become inactivated by hydrogen peroxide and are most likely being degraded upon the oxidative stress treatment (Fucci et al. 1983).

Additionally, I identified one very abundant protein that showed a dramatic mobility change in response to H_2O_2 -treatment. This protein was identified as the typical 2-Cys peroxiredoxin PRDX-2 of *C. elegans*. PRDX-2 is a member of a highly conserved family of peroxidases identified in bacteria, plants and mammals (Yang et al. 2002) (Section 1.7). The dimeric PRDX-2 converts H_2O_2 to water and during this reduction the peroxidatic cysteine C_P becomes oxidized to C_P-SOH. This sulfenic acid is then resolved by an intermolecular disulfide bond between C_P from the one subunit and the resolving cysteine C_R from the other subunit (Section 1.7.2). Here, I found that more than 70% of the total PRDX-2 population was shifted to a more acidic pI within 30 min of H_2O_2 exposure (Figure 3.5B). It has been shown, that under severe peroxide stress conditions C_P-SOH of typical 2-Cys PRXs reacts with a second H_2O_2 molecule to form sulfinic acid (C_P-SO_2H), an oxidative modification that cannot be reversed by DTT-treatment. This overoxidation, which has been shown to cause a dramatic mobility shift of 2-Cys PRXs on 2D gels, leads to the inactivation of the peroxidase activity (Woo et al. 2003a)

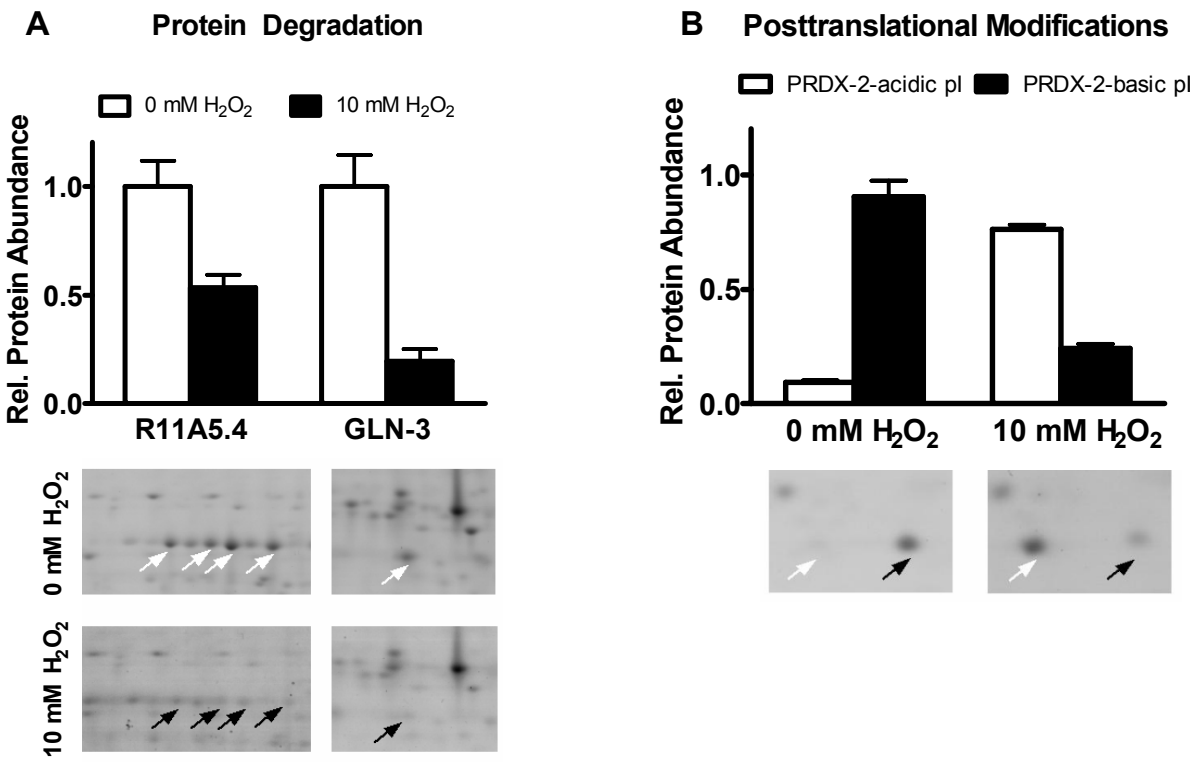

Figure 3.5: H_2O_2 treatment induces protein degradation and posttranslational modifications

2D gel electrophoresis was used to analyze changes in the proteome upon 30 min peroxide treatment. Details of the Coomassie stained 2D gels and the relative protein amounts are shown for ***A)*** *phosphoenolpyruvate carboxykinase (R11A5.4) and glutamine synthetase (GLN-3), which are degraded upon oxidative stress treatment. Phosphoenolpyruvate carboxykinase was present in several isoforms; the relative protein amount is a sum of the different isoforms. A shift in the isoelectric point was found for* ***B)*** *Peroxiredoxin-2 (PRDX-2). More than 75% of the total protein was overoxidized upon H_2O_2 treatment and had a more acidic pI.*

I set out to investigate the nature of the acidic species of PRDX-2 to exclude any other posttranslational modifications, such as phosphorylation as the cause for the shift in the isoelectric point. I performed 2D gel electrophoresis and subsequent immunoblotting using antibodies against a conserved sulfinic acid peptide derived from human PRDX-2. This sulfinic acid antibody reacted with the shifted PRDX-2 species from *C. elegans* (Figure 3.6), which confirmed that high concentrations of

H_2O_2 lead to overoxidation of the peroxidatic cysteine of PRDX-2 to sulfinic acid (SO_2H). This result suggests that PRDX-2 is involved in the initial detoxification of exogenous H_2O_2 in a process that eventually causes the overoxidation of PRDX-2. Noteworthy, PRDX-2's original purification was based on the ability of peroxiredoxins to protect glutamine synthetase from H_2O_2-mediated inactivation and oxidative degradation (Netto et al. 1996). This finding agreed well with the overoxidation results and suggested that short-term treatment of *C. elegans* with sublethal concentrations of H_2O_2 causes the rapid inactivation of PRDX-2's peroxidase activity.

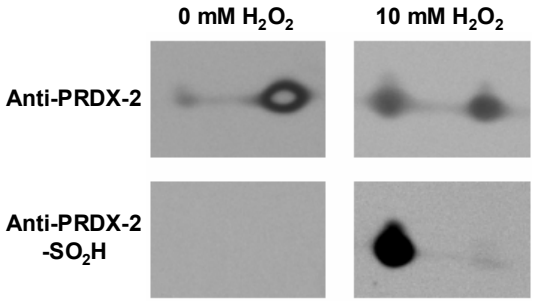

Figure 3.6: Overoxidation of PRDX-2 causes shift in 2D gels

Mobility shift of PRDX-2 in 2D-gels after peroxide stress treatment of C. elegans *correlates with formation of overoxidized PRDX-2 (PRDX-2-SO_2H). Synchronized wild type L4 larvae were either left untreated (0 mM H_2O_2) or were treated with 10 mM H_2O_2 for 30 min in liquid M9 media. Then, the oxidant was removed and aliquots of about 30,000 worms were harvested on TCA. The samples were processed for 2D gel electrophoresis and subsequent immunoblotting using (upper panel) antibodies against* C. elegans *PRDX-2 or (lower panel) antibodies against overoxidized PRDX-2-SO_2H. The partial images of the immunoblotted 2D gels are shown. These data were collected with the help of Maike Thamsen.*

3.2 Peroxide-induced changes in PRDX-2 function

3.2.1 Inactivation of peroxidase activity

To test the effects of overoxidation on PRDX-2's activity *in vitro*, I then overexpressed and purified the His-tagged version of *C. elegans* PRDX-2 from *E. coli* cells to analyze PRDX-2's peroxidase activity in the reduced form as well as in the overoxidized form.

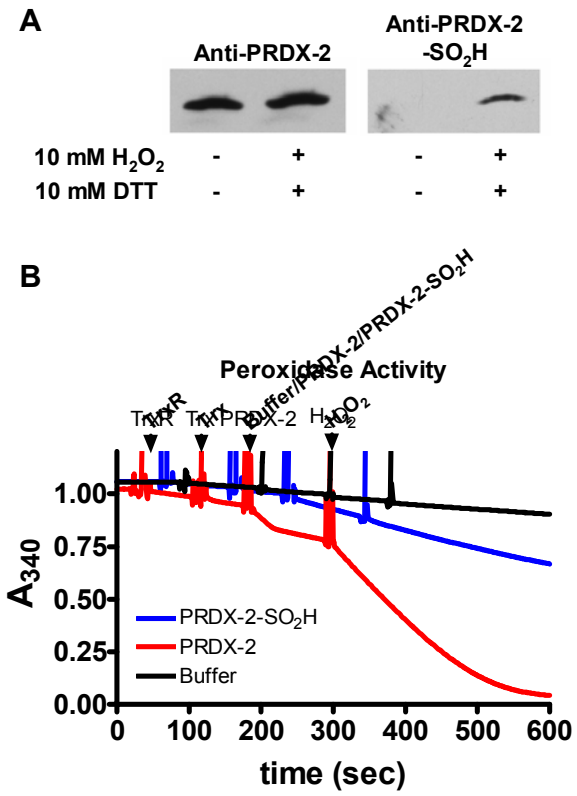

Figure 3.7: Overoxidation of the peroxidatic cysteine of PRDX-2 to sulfinic acid inactivates PRDX-2 as a peroxidase

__A__) Incubation of recombinant PRDX-2 with 10 mM H_2O_2 and 10 mM DTT for 15 min at room temperature lead to the formation of a sulfinic acid species of PRDX2 as shown with the PRDX-2-SO_2H antibody. __B__) Peroxidase activity of PRDX-2 and PRDX-2-SO_2H was determined using the thioredoxin-linked NAPDH assay, in which peroxidase-catalyzed H_2O_2 reduction is monitored as a function of Trx/TrxR-mediated NADPH oxidation. The reaction mixture containing 200 µM NADPH was supplemented with 0.08 µM thioredoxin reductase (TrxR), followed by the addition of 2.5 µM thioredoxin (Trx) and finally 2.5 µM PRDX-2, PRDX-2-SO_2H or equivalent volumes of buffer. The reaction was then started with the addition of 500 µM H_2O_2 and the decrease of NADPH absorption was monitored at 340 nm.

In vitro overoxidation of PRDX-2 was achieved by incubation of PRDX-2 in the presence of 10 mM H_2O_2 and 10 mM DTT. It has been previously shown that overoxidation is only achieved when peroxiredoxins are engaged in the catalytical cycle (Yang et al. 2002). Therefore a reductant, such as DTT or the Trx system (Trx, TrxR, NADPH) together with H_2O_2 has to be present to achieve the overoxidation of

PRX. The sulfinic acid species of PRDX-2 was confirmed by immunoblotting (Figure 3.7A). To determine the activity of overoxidized PRDX-2, the thioredoxin linked NADPH oxidation assay was used (Chae et al. 1994) (Figure 3.7A). In this assay, the NADPH concentration was monitored at 340 nm and decreased substantially during the reduction of H_2O_2 by PRDX-2. The overoxidized PRDX-2 species, however, showed significantly less peroxidase activity. That PRDX-2 showed still some peroxidase activity is probably due to incomplete overoxidation with low molar amounts of DTT. This result confirms that overoxidation of PRDX-2 inactivates the peroxidase activity. It has been suggested that the overoxidation of eukaryotic PRX is a feature that was evolutionarily selected for to allow H_2O_2 to function as a messenger molecule in eukaryotic cells. Recently, it has also been proposed that this change in the redox state of PRX causes a switch in PRX function. Peroxiredoxins from yeast and human PrxII have been shown to have dual activity *in vitro* and act as molecular chaperones under high H_2O_2 concentrations (Jang et al. 2004; Moon et al. 2005).

3.2.2 Peroxide activates PRDX-2 as a molecular chaperone

To assess whether overoxidation converts PRDX-2 into a molecular chaperone, the influence of reduced and overoxidized PRDX-2 on the aggregation of thermally denatured citrate synthase (CS) was tested *in vitro*. Overoxidation of PRDX-2 increased the ability of PRDX-2 to interact with folding intermediates of CS and to slow the aggregation process (Figure 3.8). High molar ratios of overoxidized PRDX-2 to CS (>10:1) were, however, necessary to influence the aggregation process. This result confirms that overoxidation increases the chaperone function of eukaryotic peroxiredoxins but suggests that potential co-chaperones might be missing that regulate substrate binding and affinity of PRDX-2.

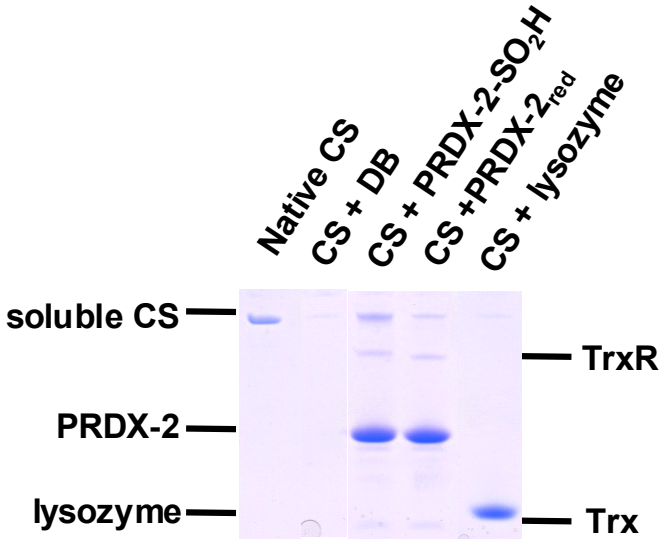

Figure 3.8: Chaperone activity of reduced and overoxidized PRDX-2

Thermal aggregation of 0.5 µm citrate synthase in the presence of either PRDX-2-dialysis buffer (DB), 10 µM PRDX-2$_{red}$, 10 µM PRDX-2-SO$_2$H or 10 µM lysozyme at 43°C was analyzed. The soluble supernatant after 20 min incubation at 43°C is shown. The amount of soluble CS in the native protein sample is shown as control (Figure obtained from Fei Li).

3.3 PRDX-2 is required for oxidative stress protection and recovery in C. elegans

3.3.1 Expression pattern of *C. elegans* PRDX-2

In many organisms peroxiredoxins are highly abundant proteins and present in multiples (Rhee et al. 2005). Three PRX have been identified in *C. elegans* to date (Table 3.3). PRDX-6 (gene Y38C1AA.11) has homology to 1-Cys peroxiredoxins, whereas both, PRDX-2 and PRDX-3 are homologues to typical 2-Cys peroxiredoxins and contain the conserved C_P-motif (FVCP) and C_R-motif (EVCP). The two 2-Cys peroxiredoxins differ most likely in their subcellular localization. PRDX-3 has a mitochondrial signal sequence (WormBase, http://www.wormbase.org, WS193, August 21, 2008). Expression of *C. elegans* PRDX-2, on the other hand, has

previously been reported to be restricted to two pharyngeal neurons (Isermann et al. 2004). Interestingly, I found that PRDX-2 is a highly abundant *C. elegans* protein based on 2D gel analysis (Figure 3.5B). This finding was further confirmed by quantitative western blot analysis, which showed that PRDX-2 constitutes about 0.5% of all soluble proteins in *C. elegans* (Figure 3.9).

Table 3.3: Peroxiredoxins in *C. elegans*

Gene	Sequence name (WormBase)	Function/localization	Size (kDa)	pI	Cys
prdx-2	F09E5.15	Typical 2-Cys peroxiredoxin	21.8	5.63	2
prdx-3	R07E5.2	Mitochondrial typical 2-Cys peroxiredoxin	24.9	7.42	6
prdx-6	Y38C1AA.11	1-Cys peroxiredoxin	25.6	5.11	6

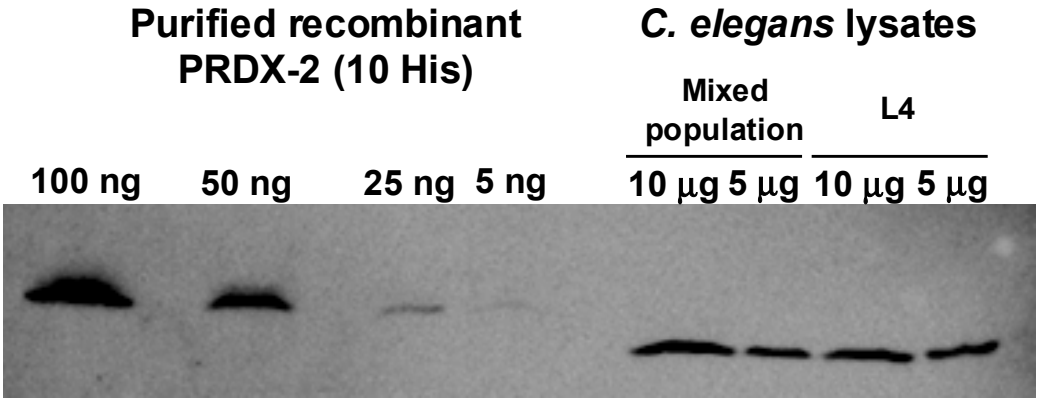

Figure 3.9: PRDX-2 is a high abundance protein in *C. elegans*

Cell lysates from either a mixed population of C. elegans *or synchronized L4 larvae were prepared. The total protein amount was determined with Bradford protein assay and 5 or 10 µg total* C. elegans *protein was applied onto reducing SDS-PAGE. A standard curve with defined concentrations of purified His-tagged* C. elegans *PRDX-2 (5 ng, 25 ng, 50 ng and 100 ng) was used to determine the amount of PRDX-2 in* C. elegans *lysates. The westernblot using antibodies against* C. elegans *PRDX-2 is shown.*

This abundance makes it highly unlikely that PRDX-2 expression is restricted to only two pharyngeal neurons (Isermann et al. 2004) and agreed with other gene expression studies, which suggest that PRDX-2 is a widely expressed protein in *C. elegans* (published online at WormBase: http://www.wormbase.org, release WS193, August 21, 2008). These results were also in excellent agreement with studies in yeast and mammals, where typical 2-Cys peroxiredoxins are considered among the most abundant and ubiquitously expressed proteins (Chae et al. 1999; Jang et al. 2004). The original expression analysis by Isermann et al. was based on a translational GFP-fusion reporter construct (Isermann et al. 2004). The sequence 2 kb upstream of F09E5.15 (*prdx-2*) was used as the promoter sequences, neglecting that PRDX-2 is part of operon CE0P2172 and therefore probably regulated by the promoter of its operon in addition to its own promoter. Good evidence for operon-contained genes comes from the spliced leader (SL) sequence that is added in the different splicing procedures. The spliced leader sequence of the 5' gene is spliced to SL1, whereas the trans-spliced genes further downstream usually contain the SL2 leader sequence. Depending on the distance from the upstream gene, the 3' genes of an operon can also be spliced with the SL1 sequence (Blumenthal). Two typical distances for genes in operons have been reported; if the spacer between the genes is about 100 bp in size, the downstream gene is typically spliced to SL2, if the distance is greater than 300 bp, the downstream gene can be either spliced to SL1 or SL2. The SL1 splicer indicates that this gene might have its own promoter element in the spacer region. The distance of *prdx-2* to downstream *pkc-3* is 535 bp and to upstream F09E5.3 1850 bp (Figure 3.10). For *prdx-2* both, SL1 and SL2 were reported as the SL sequence. Therefore it is likely that *prdx-2* is transcribed by the promoter of the operon in addition to its own (published online at WormBase: http://www.wormbase.org, release WS193, August 21, 2008).

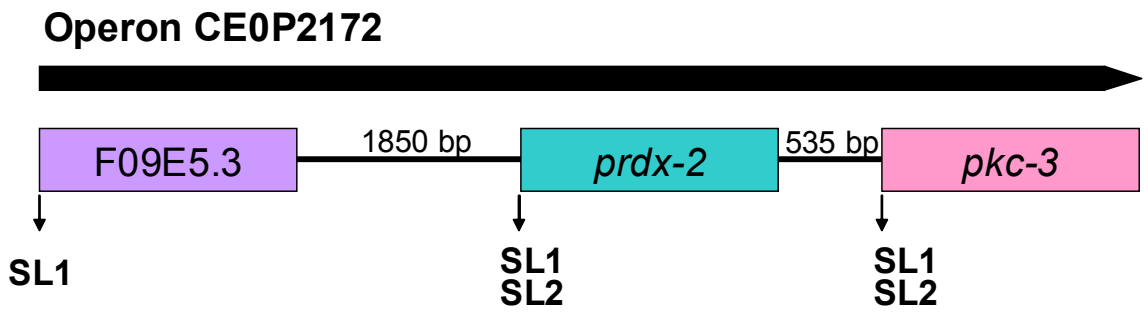

Figure 3.10: Schematic representation of *C. elegans* operon CE0P2172

The PRDX-2 encoding gene is contained in operon CE0P2172. prdx-2 *is downstream of gene F09E5.3 and upstream of* pkc-3*, encoding protein kinase C. The reported spliced leader (SL) sequences indicate that both,* prdx-2 *and* pkc-3 *have their own promoter in addition to the promoter of the operon.*

3.3.2 Characterization of the *prdx-2* phenotype

Isermann and coworkers showed in the same study, that *prdx-2* worms have a reduced brood size at 25°C (Isermann et al. 2004). No differences were found in lifespan, pharyngeal pumping or defecation rate. These behavioral data were collected with the original isolates from the Caenorhabditis Genomic Center. To rule out the possibility that these phenotypes arose from background mutations, I backcrossed the original *prdx-2* strain three times to the N2 wild type strain and re-analyzed the *prdx-2* phenotype in several behavioral assays. Consistent with the previous study, the outcrossed *prdx-2* mutants showed no significant difference in mean lifespan, pharyngeal pumping rate, or fertility span compared to wild type worms (Figure 3.12). However, even though there was no significant difference in the fast movement span of the *prdx-2* worms, the mutant worms displayed a difference in velocity and coordination of movement (Figure 3.11). An automatic worm tracking system was used to assess the worm's velocity. A single worm on day 1 of adulthood

was transferred onto a fresh NGM plate with bacteria and monitored for 10 minutes. Typically, in wild type worms, the stimulus of the transfer will lead to high velocity movement (50 pixel/second) that is followed by a decrease in movement to a basal velocity of about 15 pixel/second (Feng et al. 2006). In contrast, the *prdx-2* worms, did not show an initial increase in velocity but moved steadily with a high basal velocity of 23.7 ± 10.0 pixel/second, a 1.5 fold increase compared to the wild type basal velocity (15.8 ± 10.6 pixel/second). This could indicate that *prdx-2* worms process stimuli or the absence of stimuli differently than wild type worms. Alternatively, their muscular capabilities could be altered. Analysis of the 10 min videos showed that *prdx-2* worms spent more time moving uncoordinatedly than wild type N2 worms. This uncoordinated movement was visualized by the tracks left on the agar of the plate (Figure 3.11) and could alternatively be analyzed by counting the number of body bends.

In addition to differences in movement behavior, progeny production of *prdx-2* worms was significantly altered. Brood size was evaluated on day 1 by counting eggs *in utero*, as well as by counting progeny produced during the whole self-fertile reproductive span and was significantly reduced by about 50%. Interestingly, *prdx-2* worms were only smaller in size once they reached adulthood (Figure 3.12 and Figure 3.16.) There was no significant difference in the length of the worms at the L4 stage; evaluation on day 1, however, revealed a decrease in length of about 25%. This difference in growth, (412 μm for wild type and only 192 μm/ day for *prdx-2* from day 0 to 1) can not be due to a difference in feeding habits since their pharyngeal pumping rates were similar. Interestingly, the same phenotypes (decrease in size, growth rate and progeny production) were observed in peroxide-stress treated wild type worms (Figure 3.12), suggesting that lack of PRDX-2 leads to endogenous oxidative stress.

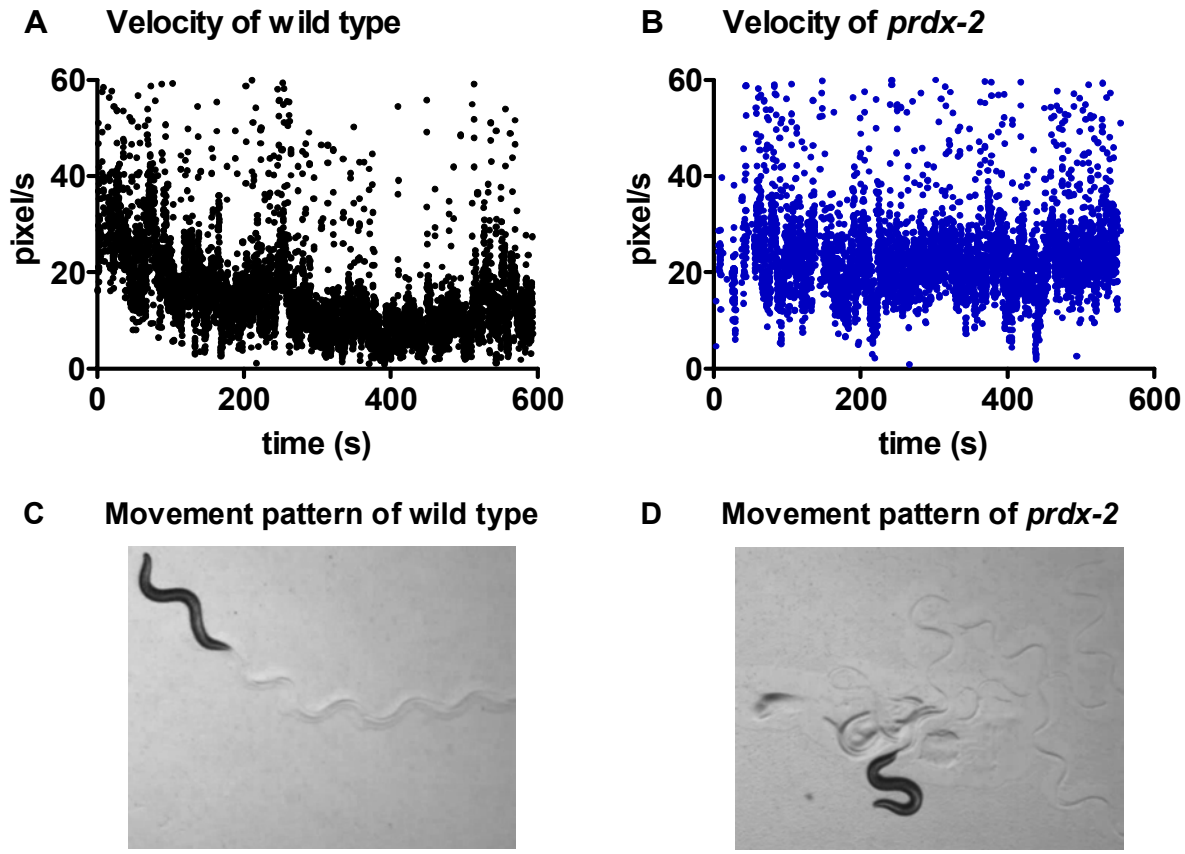

Figure 3.11: Velocity and movement of wild type and *prdx-2* worms at 25°C

Wild type (n=3) and prdx-2 *(n=3) worms on day 1 of adulthood were monitored for their movement behavior using an automated worm tracking system. The average velocity for* ***A)*** *wild type and* ***B)*** prdx-2 *worms is shown over 10 min. A representative picture of the movement behavior of* ***C)*** *wild type and* ***D)*** prdx-2 *worms is shown.*

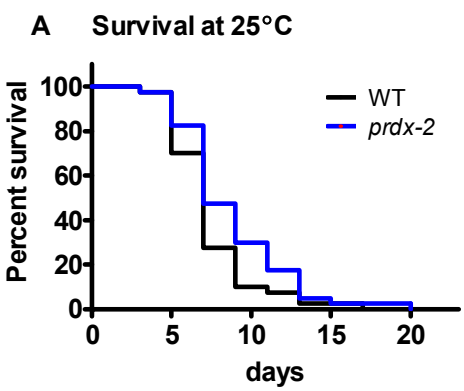
A Survival at 25°C
Percent survival
100
80
60
40
20
0
0
5
10
15
20
days
WT
prdx-2

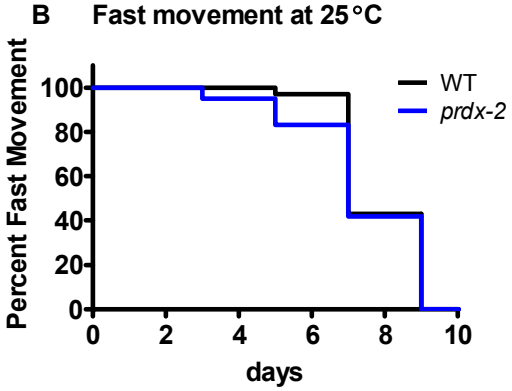
B Fast movement at 25°C
Percent Fast Movement
100
80
60
40
20
0
0
2
4
6
8
10
days
WT
prdx-2

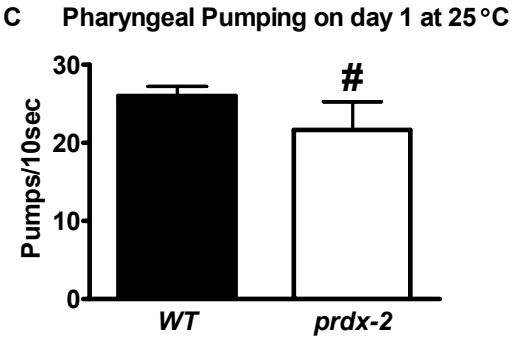
C Pharyngeal Pumping on day 1 at 25°C
Pumps/10sec
30
20
10
0
#
WT
prdx-2

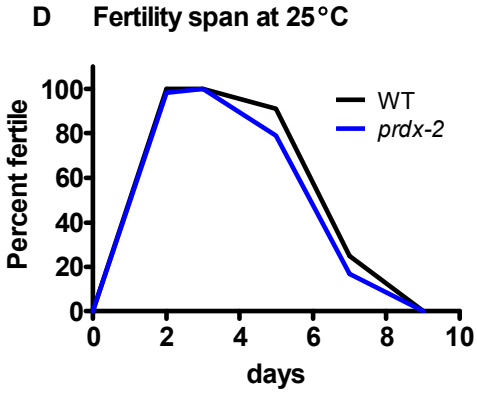
D Fertility span at 25°C
Percent fertile
100
80
60
40
20
0
0
2
4
6
8
10
days
WT
prdx-2

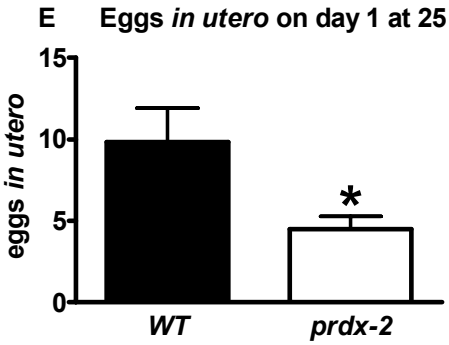
E Eggs in utero on day 1 at 25°C
eggs in utero
15
10
5
0
*
WT
prdx-2

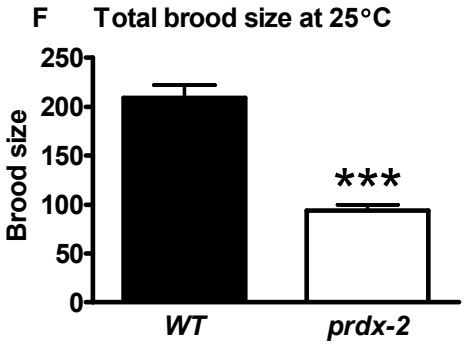
F Total brood size at 25°C
Brood size
250
200
150
100
50
0
***
WT
prdx-2

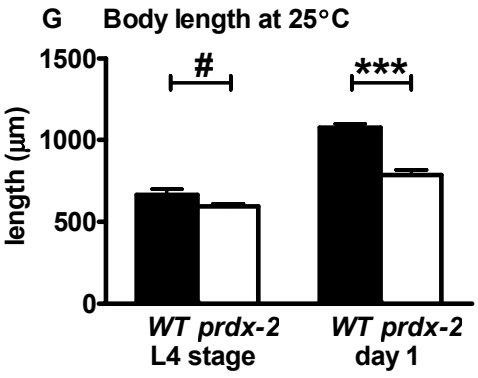
G Body length at 25°C
length (µm)
1500
1000
500
0
#
***
WT prdx-2
L4 stage
WT prdx-2
day 1

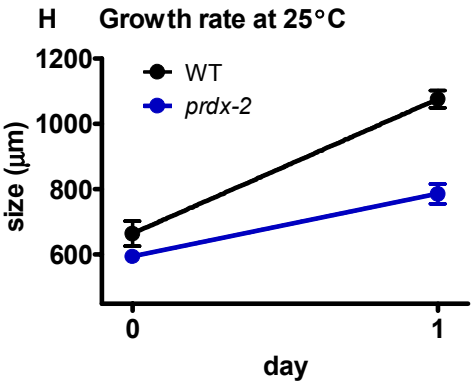
H Growth rate at 25°C
size (µm)
1200
1000
800
600
0
1
day
WT
prdx-2

Figure 3.12: Lifespan and behavior assay of wild type and *prdx-2* worms at 25°C

Synchronized wild type and prdx-2 *worms (n=50) were singled and scored for* ***A)*** *survival,* ***B)*** *fast movement,* ***C)*** *pharyngeal pumping on day 1,* ***D)*** *fertility,* ***E)*** *eggs in utero on day 1 (n=11),* ***F)*** *total brood size during the whole self-fertile reproductive span,* ***G)*** *body length on day 0 and day 1 (n=11) and (H) growth rate.*

Table 3.4: Behavioral parameters for wild type and *prdx-2* mutant worms at 25°C

Behavioral parameter	wild type	*prdx-2*	p-value
Mean lifespan [days]	8.3 ± 0.4	6.5 ± 0.2	> 0.05
Fast movement span [days]	9.5 ± 0.6	6.1 ± 0.2	> 0.05
Pharyngeal pumping [pumps/10 sec]	26.0 ± 1.2	21.7 ± 3.6	> 0.05
Eggs in utero (day 1)	9.8 ± 2.1	4.5 ± 0.8	< 0.05
Total brood size	209.2 ± 12.9	93.8 ± 5.9	< 0.001
Body length (L4) [μm]	663.8 ± 37.3	594.0 ± 16.9	> 0.05
Body length (day 1) [μm]	1076 ± 26.2	786.2 ± 30.6	< 0.001
Growth rate [μm]	411.8 ± 44.8	192.2 ± 42.1	

3.3.3 PRDX-2 provides protection against oxidative stress

In the same study, Isermann and coworkers postulated that PRDX-2 is not involved in the oxidative stress protection of *C. elegans* based on the observation that 5 mM H_2O_2 treatment did not lead to a significant decrease in the survival of *prdx-2* mutants, measured within hours of the oxidative stress treatment. I could show that PRDX-2 is involved in the initial detoxification of exogenous peroxide and that it is a highly abundant protein. This led me to the assumption that PRDX-2 might play a role in the oxidative stress response of *C. elegans*. Because the oxidative stress mediated movement defects (section 3.1.1) appeared to be a more sensitive read-out for oxidative stress than survival assays, I investigated the role of PRDX-2 in the oxidative stress defense of *C. elegans* in the first few days after the stress.

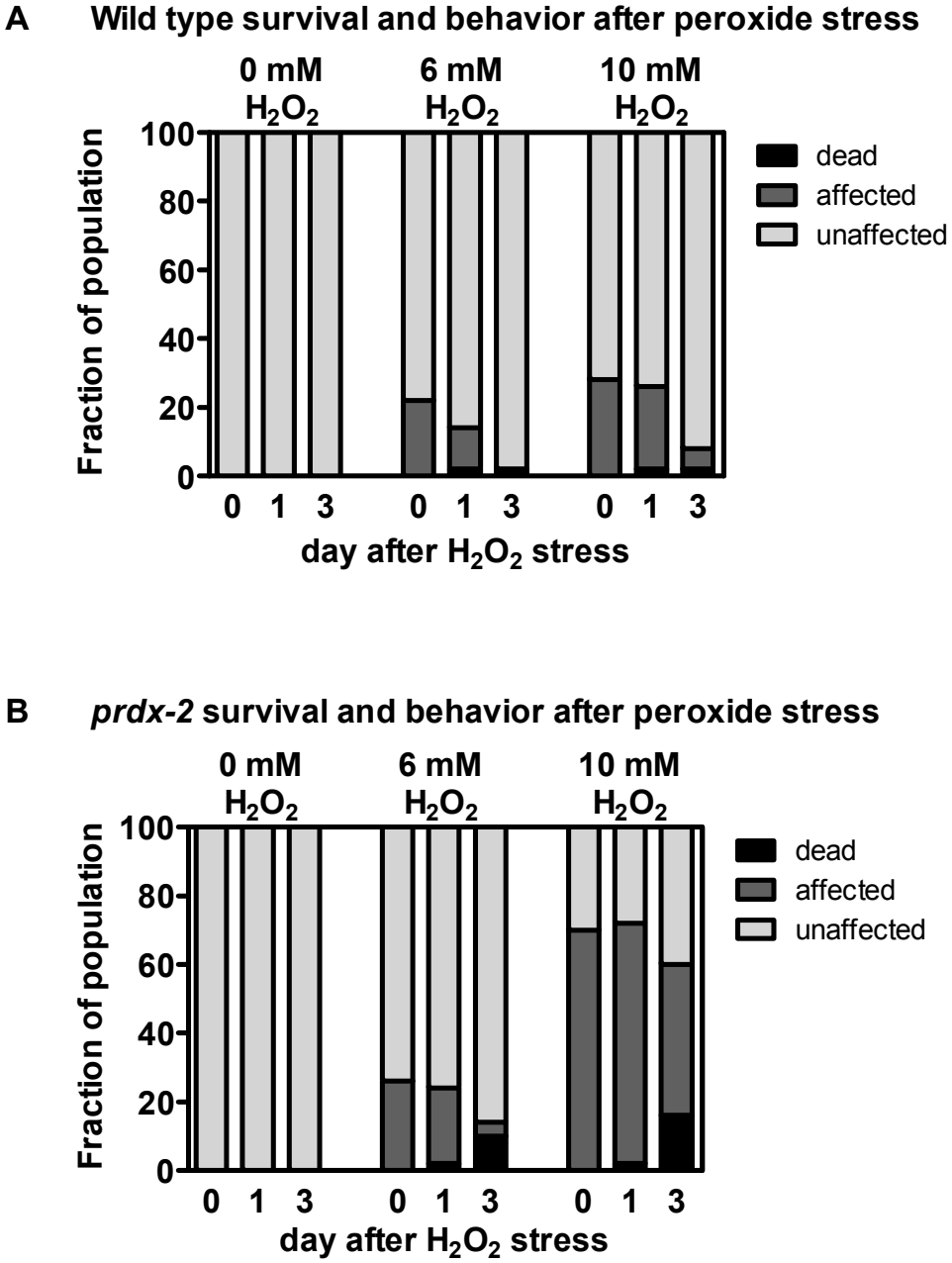

Figure 3.13: Survival and behavior of wild type and *prdx-2* worms after H_2O_2 treatment

A) *Wild type and* ***B)*** prdx-2 *mutant worms were treated with 0, 6 and 10 mM H_2O_2 for 30 min. Then, the oxidant was removed and worms were seeded onto fresh NGM plates using OP50 as food source. Survival and movement of the treated worms was assessed immediately (day 0) as well as 1 and 3 days after the stress treatment.*

Although I did not detect any immediate decrease in the survival rate of H_2O_2 treated *prdx-2* mutants (day 0), a significant increase in the number of worms that died within the first few days after the oxidative stress treatment was clearly detected (Figure 3.13). In addition, at higher H_2O_2 concentrations (10 mM), the *prdx-2* worms were more susceptible to the oxidative stress in means of behavioral defects. Right after the oxidative stress treatment, only 30% of the wild type worms were affected (Figure 3.13A), whereas more than 75% of the *prdx-2* worms moved uncoordinatedly or minimally (Figure 3.13B). This experiment showed that PRDX-2 is indeed important for the protection against oxidative stress. Therefore I analyzed the effects of H_2O_2 treatment using the complete set of behavioral tests that I established. Even though there was increased death of *prdx-2* mutants compared to wild type worms, which translates into a decrease in the minimal lifespan of *prdx-2* mutant worms, there was no statistically significant difference in the mean lifespan of *prdx-2* worms (p-value 0.7121, χ^2 0.6790, non-parametric log rank test) (Figure 3.15A). To better visualize the rate of mortality, I plotted the Gompertz curve of the oxidatively treated *prdx-2* worms (Figure 3.14A). The linear regression reveals that the initial mortality rate of the oxidatively challenged worms was increased compared to untreated controls, as the y-intercept indicates. Interestingly, the rate of aging, expressed as the slope of the regression line, was decreased for the oxidatively stressed worms, yielding equivalent mean lifespans for treated and untreated *prdx-2* worms (Figure 3.14A and Figure 3.15A). Taking a closer look at the data, the increase in initial mortality rate is due to the increased proportion of dead worms on day 2, 3 and 5. The environmental challenge of the oxidative stress treatment leads to this increased death rate. To visualize how much the death rate at this early stage in life is actually increased, I fit the linear regression, not according to the Gompertz law, but as a biphasic mortality rate (Figure 3.14B). The mortality rate in the first days after the 10 mM H_2O_2 stress is

about 6-fold higher than later in life. This result indicates that the peroxide treatment selectively kills the animals that are intrinsically less resistant to oxidative stress. These animals might represent the same animals in the population that die first in a lifespan assay. This is in agreement with longevity mutants that were shown to have increased stress resistance (Larsen 1993). Wild type worms that were treated with H_2O_2 did not display this increase in initial mortality rate, which confirmed that PRDX-2 is crucial for oxidative stress resistance.

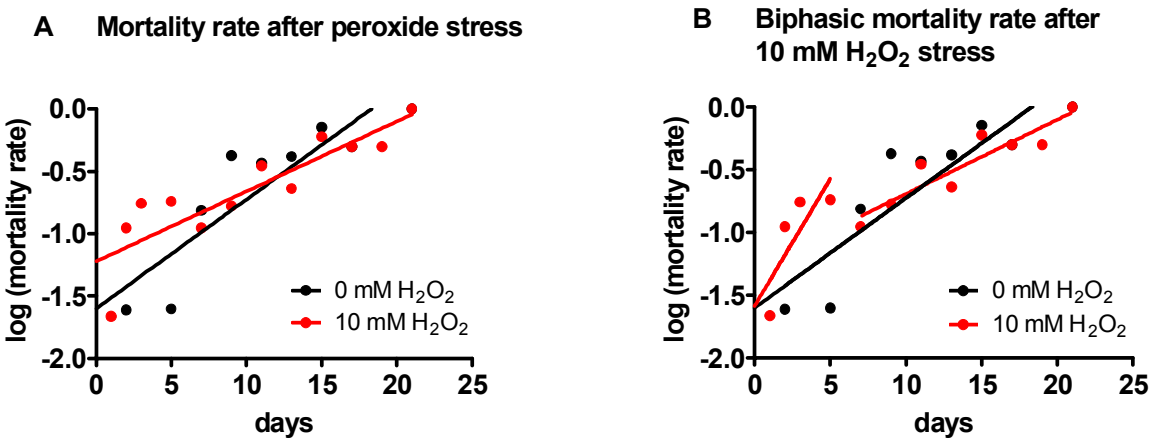

Figure 3.14: Peroxide treatment of *prdx-2* mutants leads to biphasic mortality rate

A) *Survival of* prdx-2 *mutants after short term treatment with 0 and 10 mM H_2O_2 is plotted in a Gompertz curve that expresses mortality rate on a logarithmic scale as a function of the chronological age.* ***B)*** *The Gompertz curve for the* prdx-2 *worms treated with 10 mM H_2O_2 wrorm is divided into two phases.*

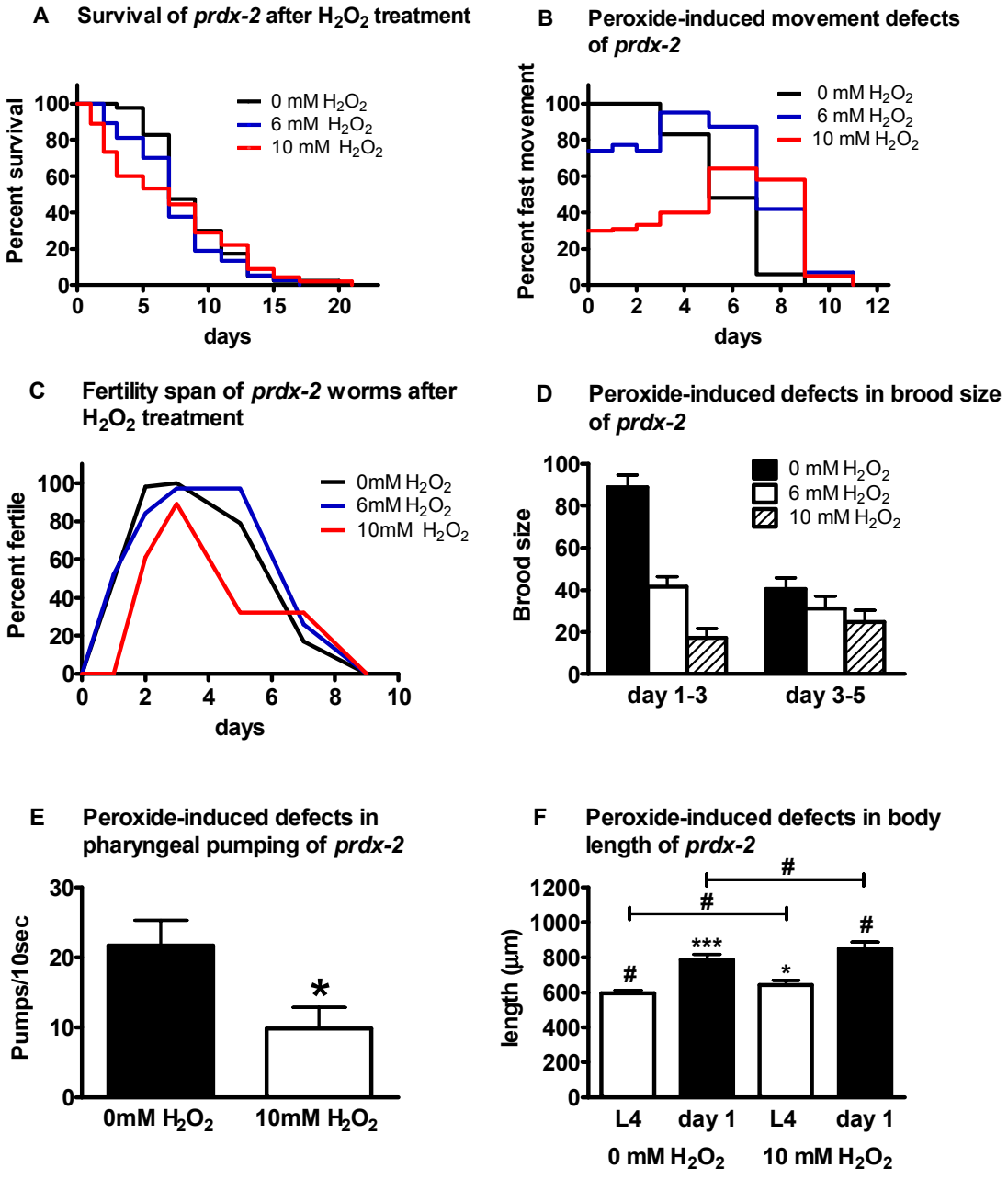

Figure 3.15: prdx-2 worms are highly susceptible to short term H_2O_2 treatment

Synchronized L4 larvae of prdx-2 C. elegans *(day 0 of adulthood) were incubated with 0, 6, and 10 mM H_2O_2 for 30 min in liquid M9 media. The oxidant was washed away and the animals were seeded on fresh NGM plates with OP50 as a food source. 50 worms were singled and scored for **A)** survival and lifespan, **B)** fast movement **C)** fertility span, **D)** progeny production, **E)** pharyngeal pumping on day 1 and **F)** size at 25°C. The symbols above the bars in panel **F)** represent the p-values compared to the size of the respective wild type worms presented in Figure 3.1G (# > 0.05, * < 0.05, *** < 0.001). No significant difference in the mean lifespan of the oxidatively stress treated* prdx-2 *worms was observed (p-value 0.7121, χ^2 0.6790, non-parametric log rank test).*

As shown in Figure 3.15B, the peroxide stress treatment also caused a more severe immediate motility defect in the *prdx-2* mutant strain as compared to wild type *C. elegans* at 10 mM H_2O_2. The increased sensitivity of the mutant worms also became evident when monitoring fertility span and brood-size (Figure 3.15C). The brood size of the oxidatively treated worms was reduced at the assayed peroxide concentrations (Figure 3.15D). It is tempting to speculate that the *prdx-2* worms already suffer from increased oxidative stress under non stress conditions, which leads to the reduction of the brood size (Figure 3.12F). Additional oxidative stress treatment further intensified this defect of the *prdx-2* worms. Progeny production seems to be a highly sensitive process, and a shift in the redox-balance due to the lack of antioxidant proteins might lead to defects in meiosis, egg and sperm production. The severity of the administered oxidative stress treatment then possibly leads to an additional effect.

In contrast to mobility and progeny production of *prdx-2*, neither the size of the *prdx-2* animals (Figure 3.16) nor their growth rate was further reduced. These results suggest that processes that regulate *C. elegans* growth might already be maximally affected by the extent of endogenous oxidative stress that the absence of PRDX-2 causes in these animals. This might either point to differences in the ROS-sensitivity of individual processes in *C. elegans* or, alternatively, might indicate that the extent of ROS-production varies within different *C. elegans* tissues. The fact that lack of PRDX-2 is sufficient to cause visible growth and fertility defects that become noticeable as early as in young adults suggests that large amounts of peroxide are continuously produced but effectively detoxified by the peroxidase in wild type animals.

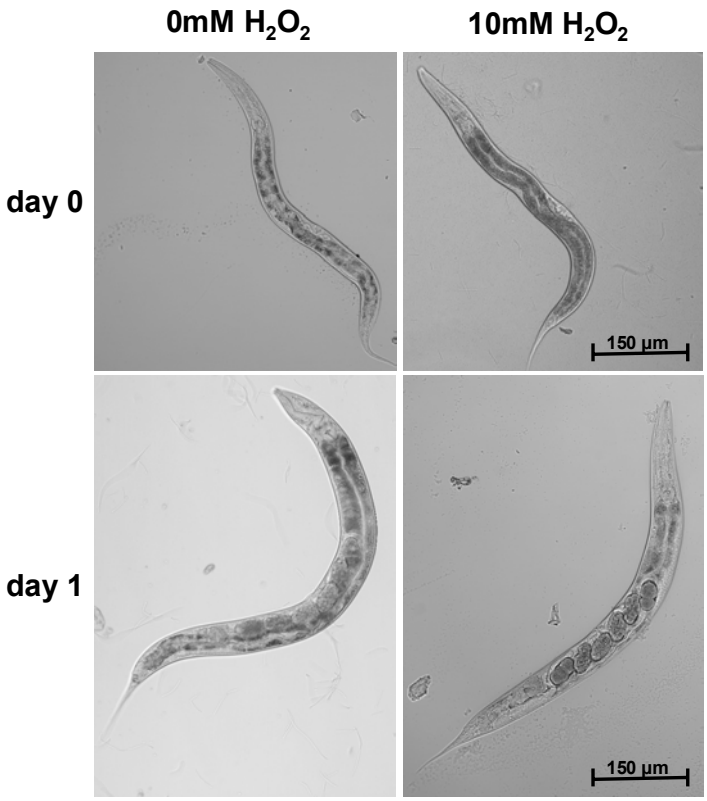

Figure 3.16: H_2O_2 treatment does not reduce body length in *prdx-2 C. elegans* mutants

Synchronized prdx-2 *L4 larvae were subjected to the short-term 10 mM H_2O_2 treatment. Worms were imaged on day 0 and on day 1 after the oxidative stress treatment to assess size and growth rate from L4 stage to day 1 of adulthood*

Most interestingly, the analysis of the fast movement span of *prdx-2* worms after the oxidative stress treatment revealed that the recovery of the worms from the motility defect was severely impaired in the mutant worms (Figure 3.15B). In contrast to wild type worms, which upon treatment with 10 mM H_2O_2 recovered within the first few days after the treatment (Figure 3.1C) most of the affected and surviving *prdx-2* mutant worms did not regain their original fast movement (Figure 3.15B). Similarly, progeny production, which dropped to less than 20% upon oxidative stress treatment as compared to the untreated *prdx-2* mutants, remained low over the complete fertility span of the animals while wild type animals recovered within three days after

the oxidative insult. It remains now to be determined, which of the processes involved in progeny production and development are most sensitive to oxidative stress.

To summarize, I applied the assay that I developed to monitor *C. elegans* for their behavior upon short-term incubation in sublethal concentrations of hydrogen peroxide. This assay enabled me to not only quantify the ability of the nematodes to withstand oxidative stress but also provided me with a measure of how potent the antioxidant systems are that ensure the clearance of the effects of the oxidative stress treatment. The administrations of sublethal H_2O_2 concentrations lead to two aging reminiscent behavioral defects. After the oxidative stress treatment movement was drastically reduced and the worms moved either slowly and in an uncoordinated fashion, or showed only slight head or tail movement. This impaired agility is highly reminiscent of the age-related decline of fast and sinusoidal body movement. The other defect was a decreased brood-size. The inability to produce eggs at the end of the self-fertile reproductive span is another main characteristic of aging nematodes. Interestingly, both behavioral defects caused by the oxidative stress treatment were reversible in the wild type worms. In the *prdx-2* mutant, both of these behavioral defects were more severe than in the wild type worms. The presence of PRDX-2 is crucial for the protection of *C. elegans* against oxidative stress as illustrated by the increased mortality early in life, and by the delayed and insufficient recovery from the oxidative stress treatment in the *prdx-2* strain. Taken together, these data show that *C. elegans* PRDX-2 is important for both, the protection against and the recovery from hydrogen peroxide induced oxidative stress.

3.3.4 Peroxide-induced overoxidation of PRDX-2 is reversible

This study revealed that PRDX-2 is rapidly overoxidized during exogenous peroxide stress treatment presumably during the initial detoxification of high H_2O_2 concentrations (section 3.1.3). This initial detoxification activity of PRDX-2 seems to

play a role in the immediate response of worms to peroxide stress. Interestingly, however, PRDX-2 appears to play a much more significant role in preventing long-term effects of H_2O_2 treatment (Figure 3.1 and Figure 3.15) and to promote recovery of the worms from the stress treatment (Figure 3.15). This was a surprising observation, given that sulfinic acid formation causes the inactivation of PRDX-2's peroxidase activity. It suggested, however, that reduced PRDX-2 is either rapidly regenerated *in vivo* or that either chaperone activity or other, yet to be determined functions of overoxidized PRDX-2 are involved in the recovery process.

To monitor the time course of PRDX-2's *in vivo* regeneration, I exposed *C. elegans* to my short-term peroxide stress treatment and took samples at several time points after the stress. 2D gel electrophoresis was then performed to quantify the amount of overoxidized PRDX-2 *in vivo*. I found that re-appearance of the reduced, peroxidase-active form of PRDX-2 significantly preceded the overall recovery of worms from their stress-induced phenotypes (Figure 3.17). Overoxidized PRDX-2 returned to its low pre-stress levels within about 9 hours of recovery, whereas worms with movement defects required between 24 to 72 hours for full recovery. This result suggested that it is likely the peroxidase activity of PRDX-2 that promotes the recovery of the worms. Analysis of the time course of PRDX-2 regeneration revealed that the decrease in overoxidized PRDX-2 concentration precisely paralleled the re-appearance of reduced PRDX-2 (Figure 3.18). This result made it less likely that regeneration of PRDX-2 is due to new protein synthesis and the selective degradation of overoxidized PRDX-2 but suggested that one or more proteins with sulfinic acid reductase activity exist in *C. elegans* that are responsible for the reduction of overoxidized PRDX-2.

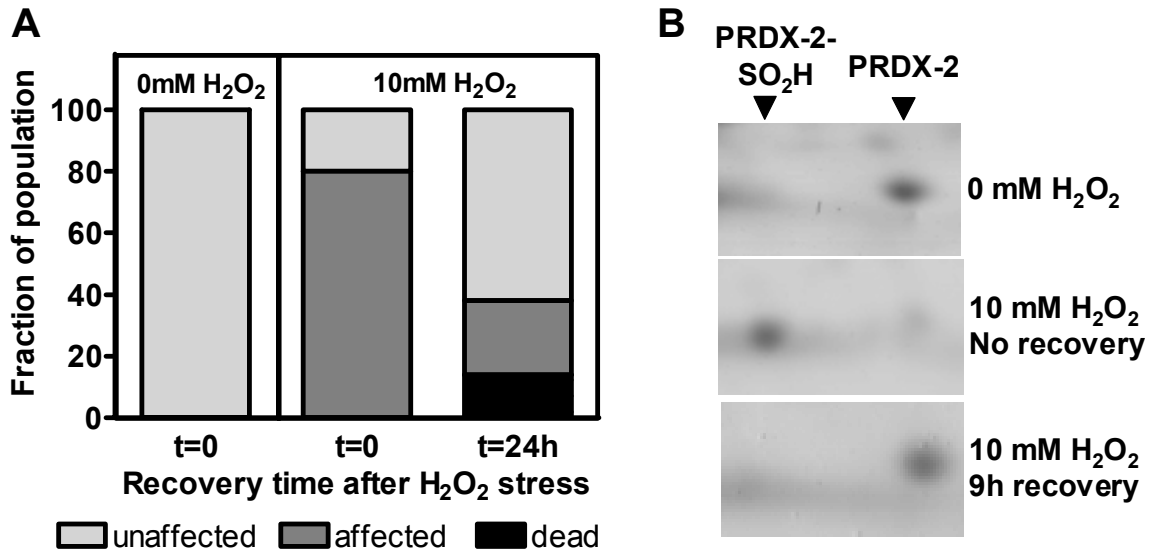

Figure 3.17: PRDX-2 regeneration preceeds recovery from behavioral defects

Synchronized wild type worms were incubated with 0 and 10 mM H_2O_2 for 30 min in liquid M9 media on day 0 of adulthood. The oxidant was washed away and a portion of the worms were harvested on TCA and processed for 2D gel electrophoresis. This constitutes timepoint 0 of recovery. ***A)*** *50 of the remaining worms were singled and scored for movement and survival after the 24h recovery time at 25°C.* ***B)*** *Details of 2D gels are shown. The upper panel shows the control group, for the middle panel worms were used that were treated with 10 mM H_2O_2 and the same population is shown after 9h of recovery time in the lower panel.*

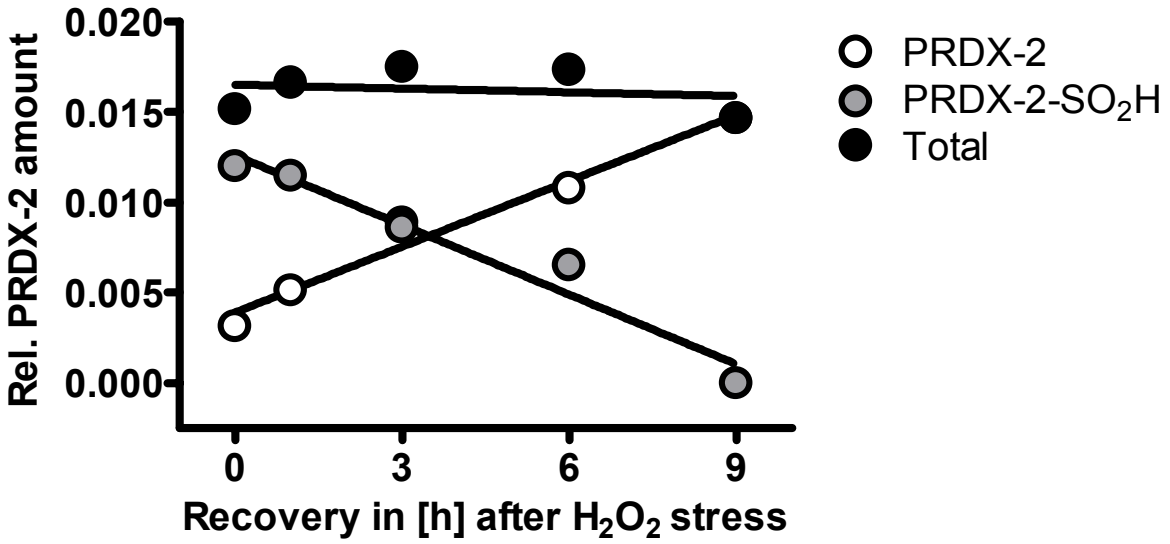

Figure 3.18: Regeneration of reduced, peroxidase-active PRDX-2

Synchronized wild type L4 larvae were incubated with 10 mM H_2O_2 for 30 min in liquid M9 media on day 0 of adulthood. The oxidant was removed and a portion of the worms were harvested on TCA and directly processed for 2D gel electrophoresis. The remaining animals were seeded onto fresh NGM plates with OP50 as a food source and allowed to recover at 25°C. At the indicated time points, aliquots were taken and again processed for 2D gel analysis. The relative cellular amounts of reduced PRDX-2 and overoxidized PRDX-2-SO2H were quantified from the 2D gels using the Delta 2D software.

Protein sulfinic acids cannot be reduced by the typical oxidoreductases such as thioredoxin or glutaredoxin, and were long thought to be irreversible. Recently, Biteau et al discovered Sulfiredoxin (SRX), the responsible enzyme for the ATP-dependent sulfinic acid reduction in yeast (Biteau et al. 2003). Even though SRX constitute a family of proteins conserved in lower and higher eukaryotes, they are absent from *C. elegans.* However, one *C. elegans* protein, Y74C9A.5, shares extensive homology to sestrin, a protein, which has recently been reported to regenerate overoxidized peroxiredoxin in human tissue cultures (Budanov et al. 2004). Based on the homology of Y74C9A.5 to human sestrin, we decided to rename the gene *sesn-1* and

the protein SESN-1. To determine whether this sestrin homologue is responsible for the reduction of peroxiredoxin's sulfinic acid we obtained and outcrossed the Y74C9A.5 knockout strain. To analyse the extent of sulfinic acid formation in the sestrin (Y74C9A.5) worms, I conducted immunoblotting using an antibody specific for Prx-SO_2H. Under non stress condition, we found PRDX-2 in the overoxidized form in the Y74C9A worms (Figure 3.19), which suggests that sestrin is required to keep PRDX-2 in its reduced peroxidase active form.

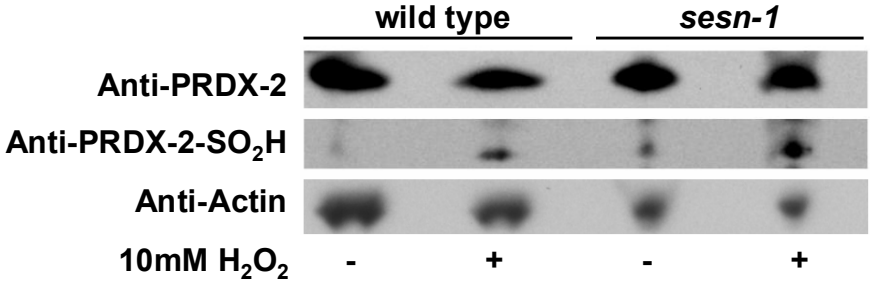

Figure 3.19: PRDX-2 is overoxidized under non-stress conditions in *sesn-1* mutants

Mixed populations of wild type and sesn-1 *worms were incubated in 0 and 10 mM H_2O_2 for 30 min in liquid M9 media. After the oxidative stress treatment, reducing loading buffer was added to the worms and they were boiled for 30 min for lysis prior to SDS-PAGE. Subsequent immunoblotting was performed with antibodies specific against PRDX-2-SO_2H, PRDX-2 and actin respectively, which are shown here.*

This result suggested that *sesn-1* mutant worms have a diminished capability of regenerating reduced PRDX-2. This result was confirmed, when we analyzed the recovery of PRDX-2-SO_2H upon H_2O_2 treatment in *sesn-1* mutant worms (Figure 3.20). Even 9 hours after the stress treatment, *sesn-1* worms still contained more than 65% of PRDX-2 in the overoxidized state, while less than 25% of overoxidized PRDX-2 was detected in wild type *C. elegans*. The appearance of reduced PRDX-2 in the *sesn-1* strains can be most likely attributed to new protein biosynthesis and the

selective degradation of overoxidized PRDX-2, although yet to be identified additional enzymes with sulfinic acid reductase activity cannot be excluded. These results strongly suggest that *C. elegans* Y74C9A.5 (*sesn-1*) is involved in the reduction of PRDX-2's sulfinic acid and in the regeneration of reduced, peroxidase-active PRDX-2.

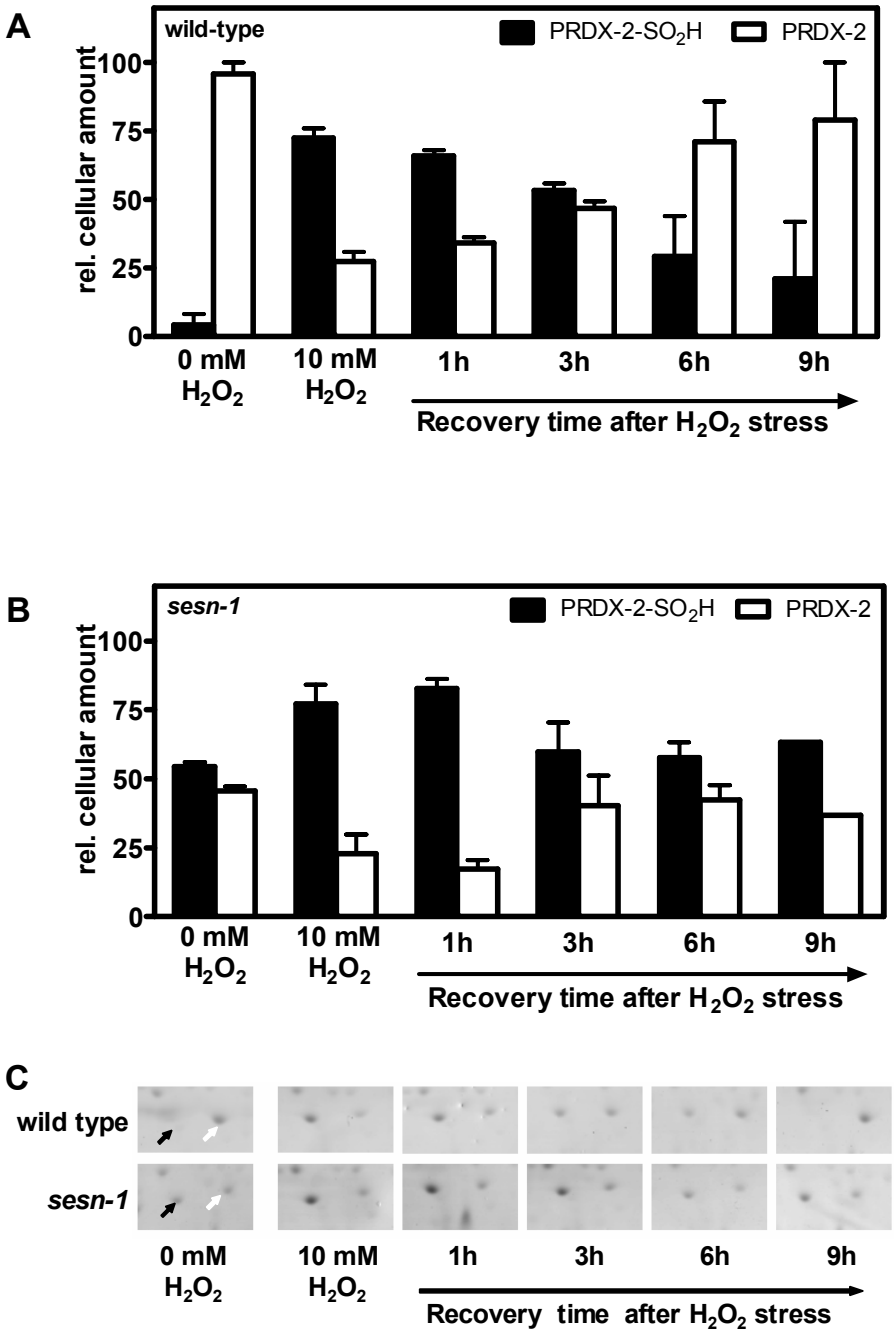

Figure 3.20: Regeneration of peroxidase-active PRDX-2 is a SESN-1-dependent process *in vivo*

Synchronized wild type L4 larvae or sesn-1 *L4 larvae were either left untreated (0 mM H_2O_2) or were treated with 10 mM H_2O_2 for 30 min in liquid M9 media. Then, the oxidant was removed and an aliquot of ~ 30,000 worms was harvested on TCA and processed for 2D gel electrophoresis (10 mM H_2O_2). The remaining animals were seeded on fresh NGM plates with OP50 as a food source and allowed to recover for the indicated time points at 25°C. Quantification of relative amounts of reduced PRDX-2 and overoxidized PRDX-2-SO_2H in* ***A)*** *wild type or* ***B)*** sesn-1 *are based on 2D-gel analysis using Delta2D software. Details of a representative set of 2D gels are shown in* ***C)****. The average of three experiments is shown.*

The finding that unstressed *sesn-1* mutant worms accumulate overoxidized PRDX-2 even in the absence of additional oxidative stress suggested that *C. elegans* larvae even under regular growth conditions are exposed to endogenous peroxide levels that are high enough to cause the overoxidation of PRDX-2's active site cysteine. These conclusions agreed well with the previous observations that *prdx-2* mutants lacking the ability to constantly detoxify intracellular peroxide exert oxidative-stress like phenotypes.

3.3.5 Characterization of the *sesn-1* phenotype

S*esn-1* deficient mutants contain very similar total amounts of PRDX-2 protein compared to wild type strains (Figure 3.21) but accumulate large proportions of PRDX-2 in the overoxidized, peroxidase-inactive form (Figure 3.19). The comparison of the phenotypes of *sesn-1* and *prdx-2* mutant worms might provide me with the ability to investigate the role of PRDX-2's overoxidation on the *in vivo* function of 2-Cys peroxiredoxins and might allow me to distinguish between peroxidase-dependent and independent functions of PRDX-2 in *C. elegans*.

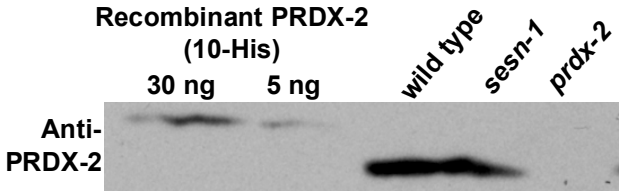

Figure 3.21: PRDX-2 is expressed at similar levels in wild type and *sesn-1* mutants

Mixed populations of wild type, sesn-1 *and* prdx-2 *worms were boiled for 30 min for lysis in reducing loading buffer and the proteins separated by SDS-PAGE. As a control, 30 and 5 ng purified recombinant PRDX-2 was loaded. Subsequent immunoblotting was performed with an antibody specific against* C. elegans *PRDX-2 and shown here.*

I, therefore cultivated the *sesn-1* mutants and found that neither size, growth rate, activity span, fertility span nor lifespan differed compared to the wild type worms. Sestrin deficient worms reproducibly showed a reduced brood size, this trend however was not significant in comparison to the wild type control.

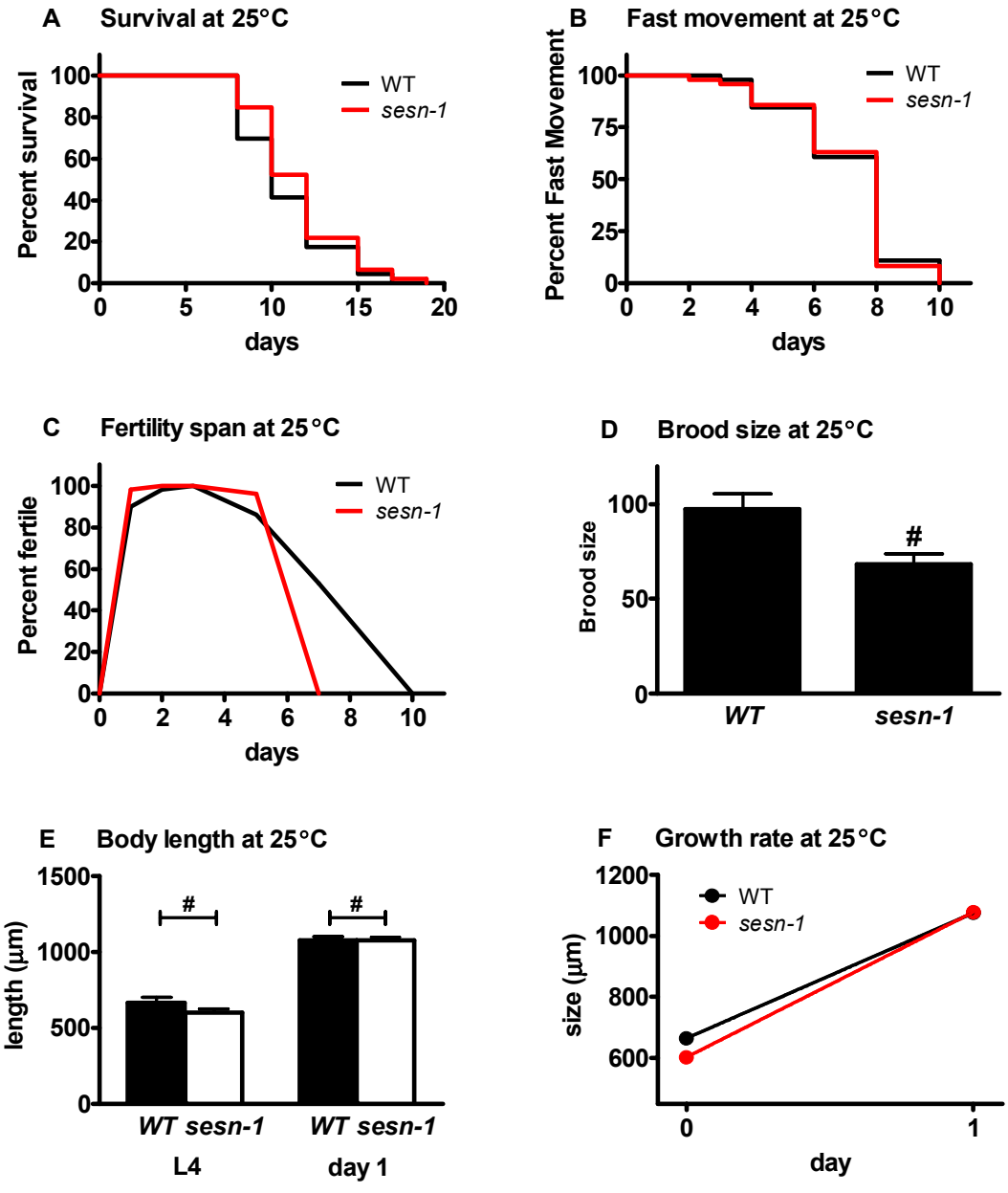

Figure 3.22: Lifespan and behavior assay of wild type and *sesn-1* worms at 25°C

Synchronized wild type and sesn-1 *worms (n=50) were singled and scored for* ***A)*** *survival,* ***B)*** *fast movement,* ***C)*** *fertility,* ***D)*** *brood size,* ***E)*** *size on day 0 and day 1 (n=11) and* ***F)*** *growth rate.*

These results suggest that the remaining amounts of peroxidase-active PRDX-2 in *sesn-1* worms might be sufficient to detoxify endogenously produced peroxide and to prevent significant endogenous oxidative stress. Alternatively, however, peroxidase-independent functions of PRDX-2 might play a role and might, at least in part, be responsible for the observed phenotypes of *prdx-2* mutant worms.

3.3.6 Sestrin is important for the antioxidant defense in *C. elegans*

To investigate how *sesn-1* mutants deal with additional exogenous oxidative stress, I treated the *sesn-1* mutant worms with 10 mM H_2O_2 for 30 min and analyzed survival, motility, fertility and growth rate (Figure 3.23 and Figure 3.24) and compared them directly to wild type and *prdx-2* mutants.

I found that the lack of sestrin clearly rendered *C. elegans*' more susceptible to the oxidative stress treatment than wild type worms (Figure 3.23). The oxidative stress sensitivity of *sesn-1* was however not as pronounced as of *prdx-2* mutants. The increased vulnerability of the *sesn-1* worms could be due to the lack of peroxidase activity of completely overoxidized PRDX-2. Reduction of progeny production seems to be one of the most sensitive read-out for stressfull conditions. Oxidatively stressed sesn-1 mutants produced about the same amount of offspring as *prdx-2* worms (p-value > 0.05 in Kruskal-Wallace test) (Figure 3.23F). *Sesn-1* mutants, however, produced more progeny under non-stress conditions and thus the decrease in progeny production was more pronounced than in the wild type worms as well as the *prdx-2* worms. It is conceivable that sestrin does not only reduce sulfinic acids from peroxiredoxins but has other substrates and or functions that could contribute to maintaining physiological processes upon oxidative stress.

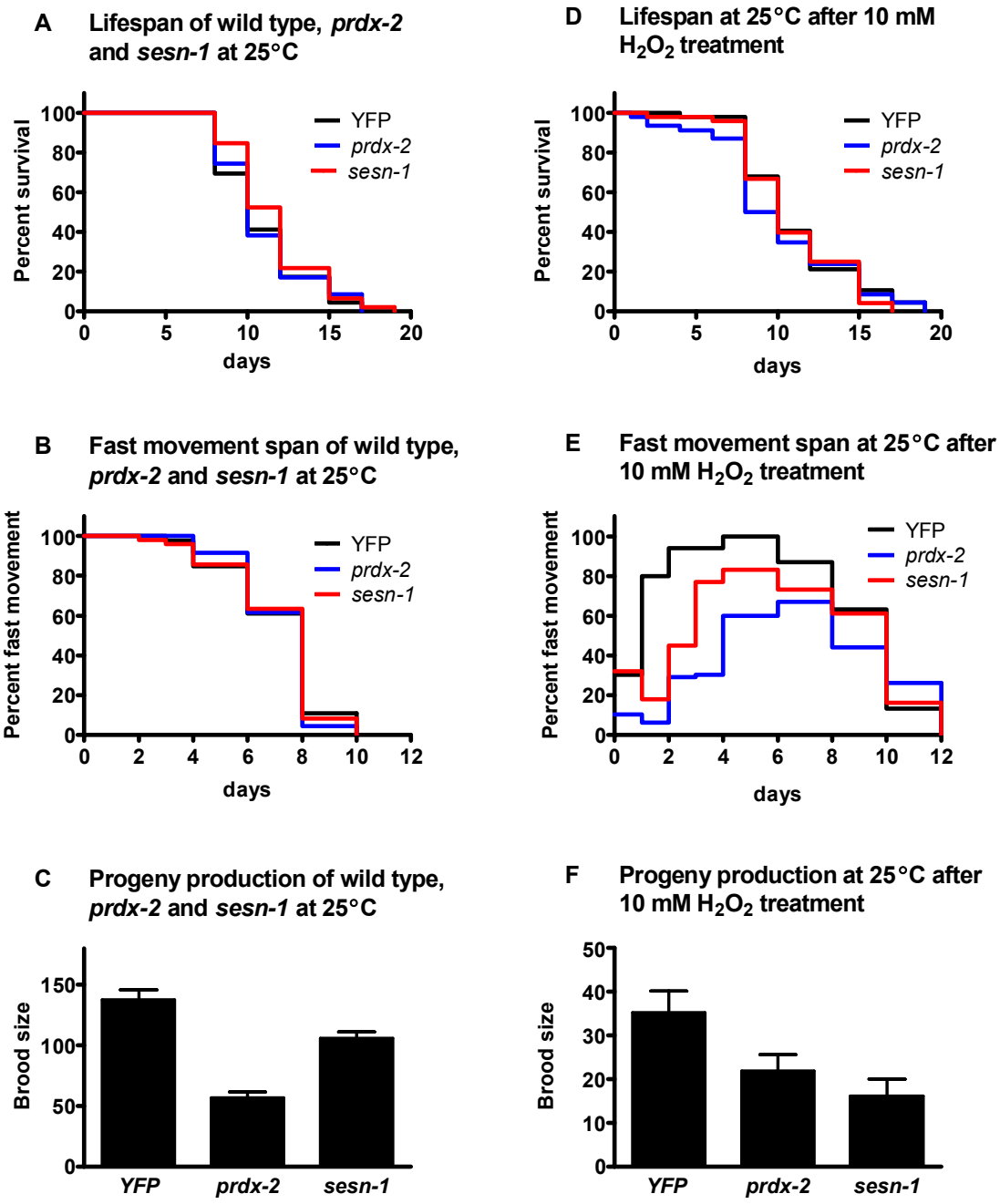

Figure 3.23: Comparison of wild type, *prdx-2* and *sesn-1* worms after peroxide stress at 25°C

For the 25°C lifespan and oxidative stress survival experiment prdx-2 *worm were mixed with wild type YFP worms, as well as* sesn-1 *with YFP worms and incubated with 0 and 10 mM* H_2O_2 *for 30 min in liquid M9 media on day 0 of adulthood. The oxidant was washed away and the animals were seated on fresh NGM plates with OP50 as a food source. 50 worms were singled and scored for movement, progeny production and survival for the subsequent days at 25°C.* ***A)*** *Lifespan and survival of the assayed worms at 25°C and* ***D)*** *after 10 mM* H_2O_2 *treatment at 25°C. Fast movement and brood size of the untreated worms* ***B)*** *and* ***C)*** *and the animals treated with 10 mM* H_2O_2 ***E)*** *and* ***F)*** *is shown.*

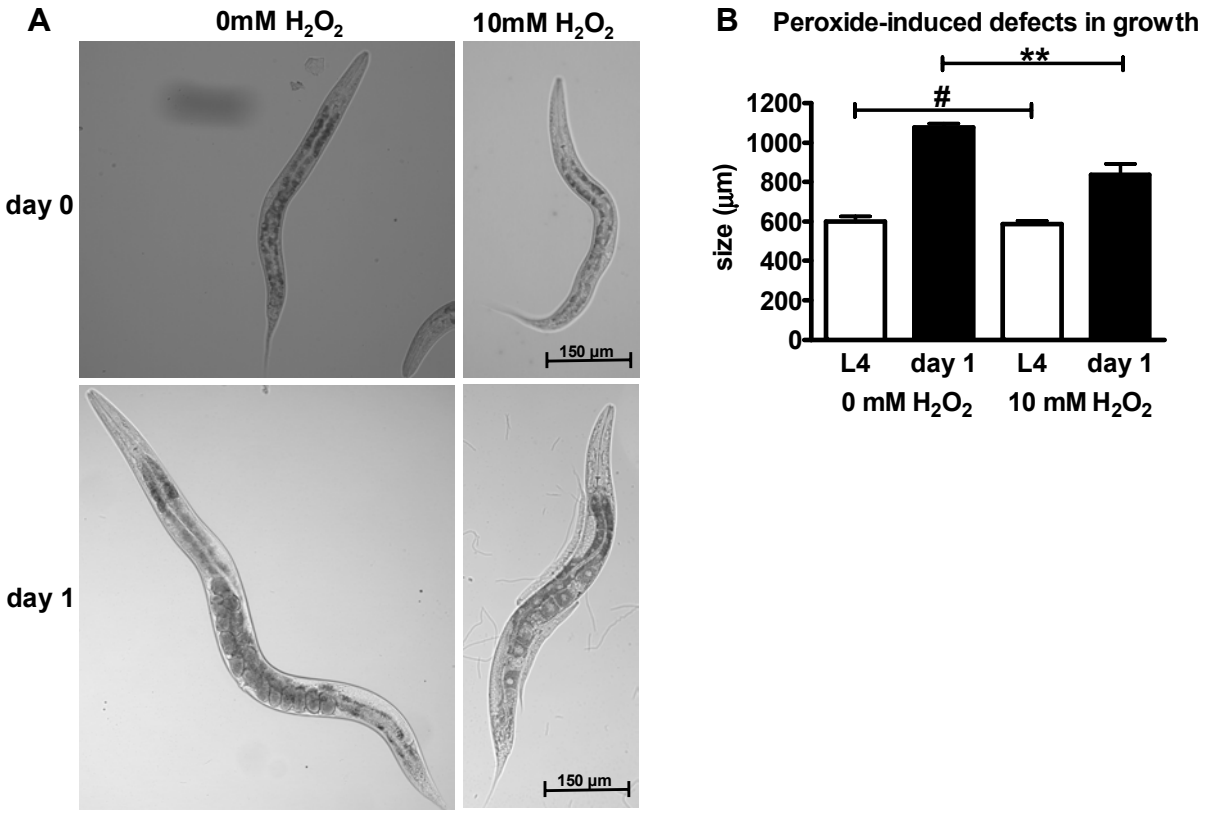

Figure 3.24: Peroxide stress leads to reduced growth rate of *sesn-1* worms

Synchronized sesn-1 *L4 larvae were subjected to the short-term 10 mM H_2O_2 treatment.* ***A)*** *Worms were imaged on day 0 and on day 1 after the oxidative stress treatment to assess* ***B)*** *size and growth rate from L4 stage to day 1 of adulthood*

The other sensitive read-out for the effects of oxidative stress is the recovery of fast and coordinated movement. The recovery of the *sesn-1* worms was clearly impaired and incomplete but better compared to *prdx-2* worms (Figure 3.23). Therefore I decided to analyze the behavior of wild type, *prdx-2* and *sesn-1* worms after the oxidative stress treatment in more detail. Of the wild type worms that showed oxidative stress-induced mobility defects, more than 90% resumed normal mobility within 2 days after the treatment (Figure 3.25A) and less than 5% showed delayed motility defects (Figure 3.25C). This result clearly reiterated our previous results showing that wild type *C. elegans* harbor potent antioxidant systems that quickly

repair and further prevent oxidative damage. In contrast, however, less than 30% of the surviving *prdx-2* mutants recovered from the initial movement defect (Figure 3.25B). Moreover, nearly 50% of the worms that appeared to be initially unaffected by the peroxide treatment showed delayed movement defects that became evident only 24-48 hours after the treatment (Figure 3.25C). These results indicated that lack of PRDX-2 lengthens the exposure of cellular macromolecules to the damaging effects of peroxide stress, thereby causing mobility defects even in animals that were initially unaffected by the treatment. Analysis of the *sesn-1* mutant worm revealed that both recovery as well as the prevention of delayed peroxide-stress effects strongly depends on the regeneration of peroxidase-active PRDX-2. Recovery studies showed that the initially affected *sesn-1* worms regained their original mobility but at a rate that was significantly slower than observed in wild type worms (Figure 3.25B). This recovery is presumably dependent on the *de novo* synthesis of reduced, peroxidase-active PRDX-2. Delayed mobility defects were initially very similar in *sesn-1* worms as compared to *prdx-2* mutants but became less pronounced at later time points indicating that *sesn-1* worms are eventually able to recover. These results suggested that the observed effects are due to the slow regeneration of peroxidase-active PRDX-2, which reduces the ability of *sesn-1* mutants to quickly clear intracellular peroxide (Figure 3.25C). They furthermore demonstrated that PRDX-2 plays an important role in the detoxification of ROS and protects *C. elegans* against the lethal effects of oxidative stress.

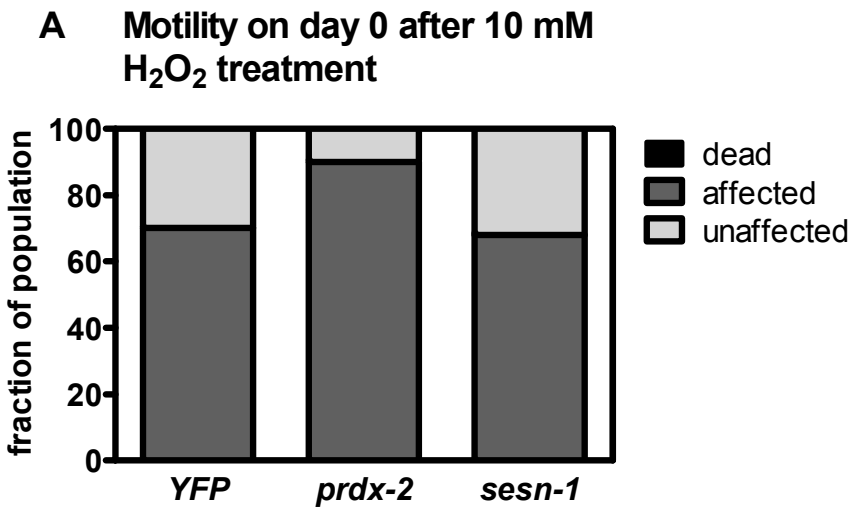
A
Motility on day 0 after 10 mM H_2O_2 treatment
fraction of population
100
80
60
40
20
0
YFP
prdx-2
sesn-1
dead
affected
unaffected

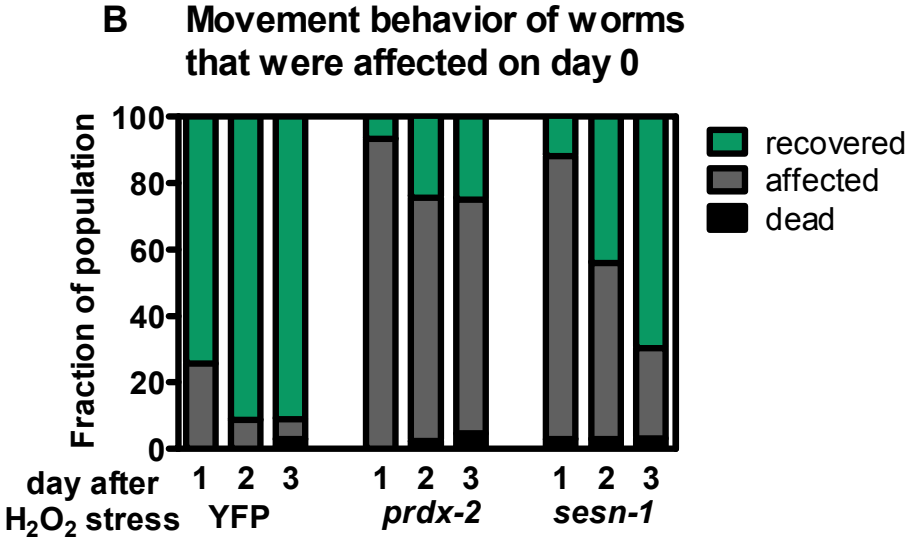
B
Movement behavior of worms that were affected on day 0
Fraction of population
100
80
60
40
20
0
day after H_2O_2 stress
1 2 3
YFP
prdx-2
sesn-1
recovered
affected
dead

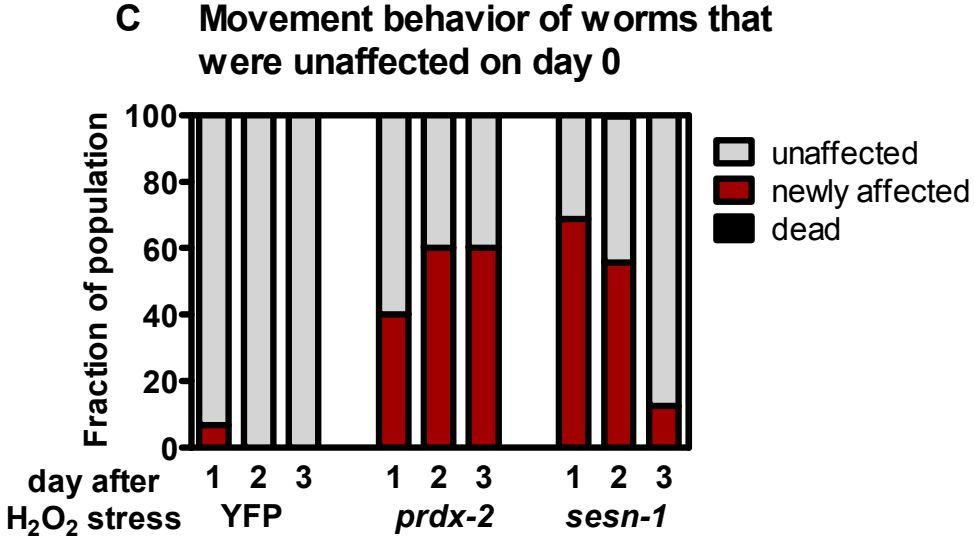
C
Movement behavior of worms that were unaffected on day 0
Fraction of population
100
80
60
40
20
0
day after H_2O_2 stress
1 2 3
YFP
prdx-2
sesn-1
unaffected
newly affected
dead

Figure 3.25: PRDX-2 is involved in H_2O_2-stress protection and recovery of *C. elegans*

Wild type, prdx-2 *and* sesn-1 *mutant worms were treated with 10 mM H_2O_2 for 30 min. Then, the oxidant was removed and worms were seeded onto fresh NGM plates using OP50 as food source.* ***A)*** *The movement of the treated worms was assessed immediately (day 0) as well as 1, 2 and 3 days after the stress treatment.* ***B)*** *Recovery of worms from oxidative stress-mediated movement defects. The movement of stress-treated worms that showed B- or C-movement on day 0 was monitored over the subsequent days.* ***C)*** *Assessment of delayed movement defects. Movement of stress-treated worms that showed A-movement on day 0 was assessed for their movement on day 1. The same worms were scored for their behavior on the subsequent days.*

3.4 Lack of PRDX-2 shortens C. elegans lifespan at lower cultivation temperature

The free radical theory of aging states that intracellular ROS accumulation causes the age-associated decline observed in older organisms. Phenotypical analysis of *prdx-2* mutant animals suggested that these animals suffer from increased peroxide stress. Yet, lifespan assays conducted at 25°C failed to reveal any defects in longevity (Figure 3.23A) (Isermann et al. 2004). To investigate whether there is a lifespan defect at different cultivation conditions, I analyzed the lifespan of *prdx-2* and *sesn-1* mutants at a lower temperature.

I found that the lifespan of PRDX-2 deficient worms at 15°C was reduced by about 40% ($P < 0.001$) (Figure 3.26). No significant effect of the *sesn-1* mutation was observed in the lifespan of *C. elegans* at 15°C (Figure 3.26). I obtained very similar results when I monitored the movement span of wild type and mutant worms at 15°C and found that the fast movement span of *prdx-2* mutants worms was substantially reduced compared to wild type worms ($P<0.001$) and *sesn-1* mutants (Figure 3.26B). Moreover, some of the phenotypes of the *prdx-2* mutant, such as reduced brood size, appeared to be further intensified when the animals were kept at lower cultivation

temperatures (Figure 3.26C). These studies revealed that the detoxifying activity of PRDX-2 contributes to the lifespan of wild type *C. elegans* at lower cultivation temperatures, raising the possibility that the antioxidant properties of PRDX-2 make this highly abundant peroxidase a general anti-aging protein.

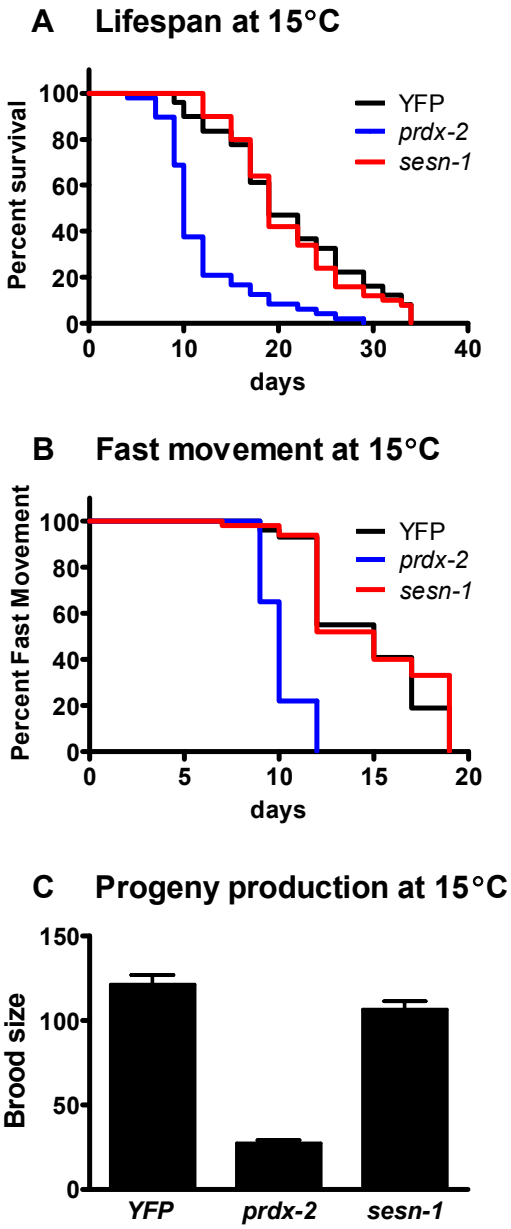

Figure 3.26: *prdx-2* deletion mutants have shortened lifespan at 15°C

Synchronized wild type, prdx-2 *and* sesn-1 *mutant worms (n=50) were singled and scored for* ***A)*** *survival* ***B)*** *fast movement and* ***C)*** *progeny production. The* prdx-2 *mutants are significantly short-lived, less active and produce fewer offspring (p-values < 0.001). Lifespan measurements were repeated at least three times per strain and a representative result is shown.*

Although the role of ROS as lifespan determining factor has been studied extensively since the free radical theory of aging was first formulated (Harman 1956), no direct proof or disproof for this hypothesis has been provided yet. In *C. elegans*, use of catalase/superoxide mimetics have resulted in conflicting results concerning their life extending effects (Melov et al. 2000; Keaney et al. 2004; Collins et al. 2008). Moreover, neither disruption of *sod-1* (cytosolic MnZnSOD) or *sod-2* (mitochondrial MnSOD) expression nor deletion of *ctl-1*, encoding the cytosolic catalase, have been shown to cause any detrimental effect on the lifespan of *C. elegans* (Petriv and Rachubinski 2004; Yang et al. 2007). Peroxisomal catalase CTL-2 seems to be the only other ROS-detoxifying enzyme in *C. elegans*, whose deletion significantly decreases the lifespan of *C. elegans* by about 16% (Petriv and Rachubinski 2004). Noteworthy, *ctl-2* mutants were reported to exert progeric phenotypes (*i.e.* reduced brood size) that are reminiscent of the phenotypes we observed in the *prdx-2* mutant. The lifespan of the *ctl-2* mutants has only been measured at 20°C. It will be interesting to determine whether the lifespan shortening effect of the *ctl-2* deletion will be similar to the effects of the *prdx-2* mutation and also more pronounced at lower cultivation temperatures. But why do *prdx-2* mutants reveal lifespan defects at lower cultivation temperature and not at higher? The effect of temperature on the longevity of organisms is thought to be caused by changes in the metabolic rates (for review (Van Voorhies 2002). While the metabolic rate of worms is overall reduced at 15°C, the lifetime metabolic output of these worms is higher at 15°C than at 25°C (Van Voorhies and Ward 1999). This discrepancy in metabolic rate and lifetime output raises the question as to when and how the reduction of metabolic rate occurs at 25°C. Do nematodes reared at 25°C reduce their metabolic rate at a certain time point in life or even switch to anaerobic energy production (Holt and Riddle 2003; Rea and Johnson 2003)? Both would significantly reduce H_2O_2 production and might

explain why PRDX-2 is no longer required to protect against oxidative stress. Alternatively, it is also conceivable that the high specific activity of H_2O_2-detoxifying enzymes (e.g. CTL-2) is sufficient for peroxide detoxification at high cultivation temperatures but that a potential temperature-induced decrease in enzyme activity might require compensation by the highly abundant PRDX-2 peroxidase activity at lower temperatures. Finally, expression of compensatory proteins in *prdx-2* deletion mutants at 25°C but not at lower temperatures might be responsible for the observed differences.

As Rich Miller stated, a shortened lifespan does not prove accelerated aging (Miller 2004). To analyze the rate of aging, I plotted the Gompertz curve of the lifespan data of *prdx-2* and wild type worms at 15°C (Figure 3.27). The linear regression reveals that the initial mortality rate, indicated by the y-intercept, of the *prdx-2* worms was significantly ($P < 0.0001$) increased compared to untreated controls. The rate of aging, expressed as the slope of the regression line, was unchanged ($P = 0.7989$). This suggests that the *prdx-2* worms are facing greater life challenges at 15°C than the wild type worms, but do not have an accelerated aging rate. The loss of PRDX-2 therefore already has a tremendous impact on the worms at the beginning of the adulthood at 15°C. It is possible that the damaging effects of accumulating ROS in the *prdx-2* mutants are high from the beginning of adulthood and cause the increased initial mortality rate. It would be interesting to see, whether this increased challenge of *prdx-2* worms at 15°C would lead to increased killing of *prdx-2* upon additional exogenously induced oxidative stress. It is, however, still conceivable that nematodes reared at 15°C die from different sources than accumulating ROS species. The similarity between the progeric phenotypes observed in *prdx-2* mutants and wild type *C. elegans* treated with exogenous peroxide-stress strongly implicates, however, that

the severe oxidative stress in the absence of *prdx-2* causes the premature death of the animals.

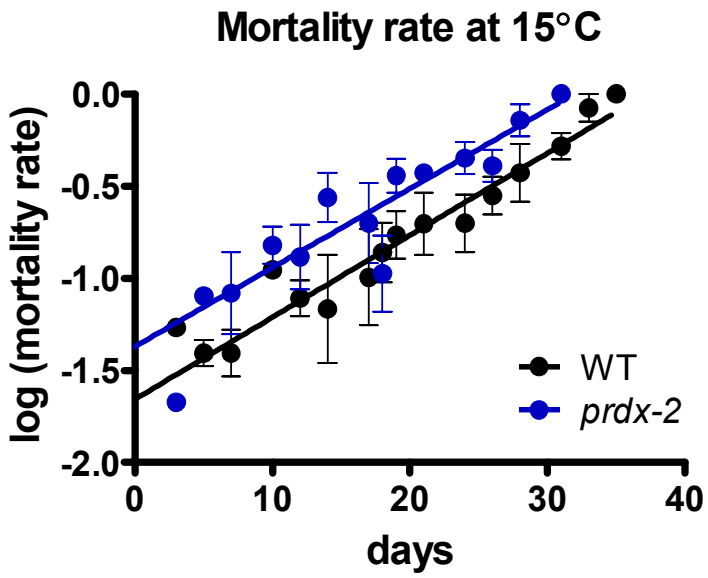

Figure 3.27: Mortality rate of *prdx-2* and wild type worms at 15°C

The average of four independent lifespan experiments of prdx-2 and wild type worms reared at 15°C is plotted in a Gompertz curve that expresses mortality rate on a logarithmic scale as a function of the chronological age.

The importance of peroxiredoxins became also apparent in studies with *prx-1*$^{-/-}$ knockout mice, which were found to die prematurely either from severe hemolytic anemia or malignant cancer (Lee et al. 2003; Neumann et al. 2003; Wang et al. 2003; Egler et al. 2005). Mice lacking other antioxidant enzymes, such as catalase or glutathione peroxidase do not suffer from any of these pathologies, further illustrating the importance of peroxiredoxins (for review (Muller et al. 2007)). These results suggest that the antioxidant activity of peroxiredoxins protects against ROS generation in erythrocytes and functions in tumor suppression in aging animals.

3.5 Loss of PRDX-2 leads to changes in redox-balance

I was able to show that *prdx-2* knockout worms have a substantial lifespan decrease at 15°C, and are highly susceptible to oxidative stress, suggesting that PRDX-2 plays an important cytoprotective role in *C. elegans*. To test the effects of ROS accumulation in *prdx-2* mutants, I wanted to determine whether the loss of PRDX-2 leads to an overall perturbance in the redox-balance in *C. elegans*. I therefore compared oxidation status of proteins of *prdx-2* knockout worms with proteins of wild type worms using our novel OxICAT technique. This quantitative proteomic method employs two chemically identical affinity tags, that only differ in their molecular mass (Leichert et al. 2008). Similar to the differential thiol trapping technique, all *in vivo* reduced cysteines in a cell lysate are labeled with light ^{12}C-ICAT reagent and all *in vivo* oxidized cysteines in the very same sample are labeled with heavy ^{13}C-ICAT reagent. Peptides containing the differentially labeled cysteines will yield distinct peaks in the mass spectrum (peak doublets) that are 9 Da apart and whose relative ion intensities represent the relative abundance of the oxidized and reduced protein species in the cell lysate (Figure 3.28). Oxidation-sensitive proteins can be identified *in vivo* by detecting changes in the ratio of heavy to light labeled peptides in the different samples.

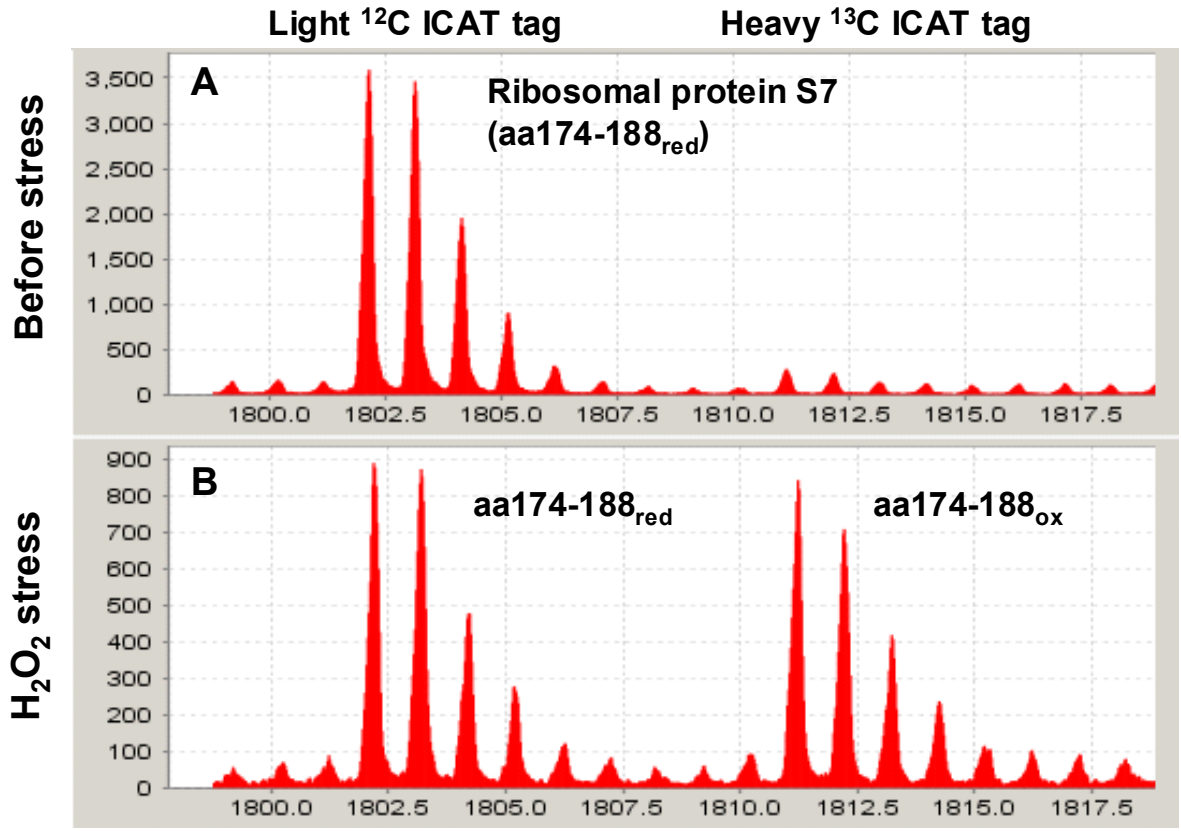

Figure 3.28: Visualizing oxidative thiol modifications in wild type worms upon peroxide stress using OxICAT

Synchronized L4 larvae of wild type C. elegans *were incubated with 0 (before stress) or 6 mM H_2O_2 for 30 min. After the oxidant was washed away, the animals were processed for OxICAT analysis. A representative peak doublet of a peptide is shown that shows an increase in oxidation status upon peroxide stress treatment.* ***A)*** *Under control conditions, the tryptic peptide 174-188 of ribosomal protein S7 is only 7.3% oxidized, and thus mainly light ICAT reagent was incorporated.* ***B)*** *Under oxidative stress conditions (6mM H_2O_2), the same peptide is 46.9% oxidized and therefore equally incorporated the heavy ICAT reagent.*

Table 3.5: Peroxide stress leads to oxidatively modified proteins in wild type *C. elegans*

WormBase Accession	Protein	Percentage oxidized		Ratio
		0 mM H_2O_2	6 mM H_2O_2	
Lipid and Carbohydrate Metabolism				
CE30646	Fructose-bisphosphate aldolase	17.8	50.2	2.8
CE30654	Enoyl-CoA hydratase/isomerase, (beta-oxidation)	12.9	30.4	2.4
CE04809	Phosphoglucomutase	13.9	27.6	2.2
CE23521	Malate synthase (Glyoxylate cycle)	20.5	44.1	2.1
Protein Synthesis				
CE06360	Ribosomal protein S7	7.3	46.9	6.5
CE11024	60S ribosomal protein L7 endopeptidase activity, (active site cysteine)	6.3	21.6	3.4
CE15900	Elongation Factor 2	6.0	20.1	3.4
CE13968	60S ribosomal protein L11	23.3	68.3	2.9
CE27398	60S ribosomal protein L7A	12.6	30	2.4
CE02560	Elongation Factor 4	6.8	16.4	2.4
Cellular Structure				
CE16197	Beta-Tubulin	11.4	33.8	3.0
Muscular Function				
CE09349	Major Myosin Class II heavy chain	16.6	39.7	2.4
Protein Transport				
CE26971	Karyopherin (importin) beta 3, Nuclear Transport Factor of ribosomal proteins	14.5	42.6	2.9
CE14954	Transport protein Sec 61, alpha subunit	11.6	29.5	2.5
Protein Folding				
CE25494	Chaperonin complex component TCP-1 theta subunit (CCT-8)	12.0	33.6	2.8
P09446	Hsp70	12.1	53.2	4.4
Energy Generation				
CE29950	F0F1-type ATP synthase, beta subunit	10.8	41	3.8
Q9XW92	Vacuolar ATP synthase	28.8	69.7	2.2
Other				
CE23530	Vigilin, high density lipoprotein	12.2	45.9	3.8
CE32024	Conserved protein unknown function	11.3	34.9	3.1
CE20901	Vitellogenin (Yolk protein)	27.5	61.9	2.2
CE03959	S'adenosylmethionine synthetase	13.3	27.3	2.1

Peptides that were found to be oxidized in *prdx-2* worms are shaded in grey.

In a first control experiment, I compared untreated wild type worms with wild type worms that were subjected to exogenous peroxide-stress to identify oxidative stress sensitive marker proteins. I found more than 50 peptides in wild type worms that showed substantially increased levels of oxidative protein modifications upon exogenous hydrogen peroxide treatment. The functions of the 20 proteins, which were identified with MS/MS analysis, were mainly grouped into lipid and carbohydrate metabolism, protein synthesis, transport and cell structure (Table 3.5). Many of the oxidized cysteines of the peptides were found to be highly conserved and some play a functional role. These proteins serve as excellent marker proteins to test, whether *prdx-2* deficient *C. elegans* mutants suffer from endogenous peroxide stress. Synchronized L4 larvae of wild type animals as well as *prdx-2* mutants were collected and processed for OxICAT analysis. I found at least 26 peptides in *prdx-2*, whose oxidation status was increased at least 1.5 fold compared to the wild type worms. Of the 16 identified proteins (Table 3.6), 6 were also found to be oxidized in wild type animals upon oxidative stress treatment. The OxICAT method is unique, because it allows the quantification of the extent of the thiol-oxidation. I can therefore compare the values of the oxidized fraction of the control groups in the two independent experiments presented here. Curiously, all peptides of untreated wild type control worms in the peroxide stress experiment were higher when compared to the wild type worms in the strain comparison experiment with *prdx-2*. This variation between two similarly treated groups of wild type worms across two different experiments can probably be attributed to one major difference in the experimental procedure. To exclude the possibility of airoxidation of thiol-containing proteins, I processed the samples in the study comparing *prdx-2* to wild type worms in the anaerobic chamber. Air-oxidation is most likely the reason for the higher basal oxidation levels of the untreated wild type control group in the peroxide stress experiment.

Table 3.6: Endogenous oxidative stress in *prdx-2* worms leads to oxidative modifications of proteins

WormBase Accession	Protein	Percentage oxidized		Ratio
		wild type	*prdx-2*	
Protein Synthesis				
CE30779	40S ribosomal protein S21 (RPS-21)	2.12	5.19	2.44
CE16012	40S ribosomal protein S26 (RPS-26)	16.73	26.08	1.56
CE13968	60S ribosomal protein L11 (RPL-11)	13.07	26.22	2.01
CE11024	60S ribosomal protein L7 (RPL-7)	1.16	3.44	2.96
CE27398	60S ribosomal protein L7a	5.44	8.21	1.51
CE15900	Elongation Factor 2	0.74	2.68	3.60
CE01270	Elongation Factor 1-alpha	1.96	4.98	2.54
Protein Degradation				
CE03482	Ubiquitin-conjugating enzyme E2 2 (Ubiquitin-protein ligase 2) LET-70	14.60	25.49	1.75
Cellular Structure				
CE05953	Putative cuticle collagen 155	22.45	63.49	2.83
CE17563	Tubulin alpha-2 chain	4.98	9.99	2.01
CE17563	Papilin precursor	1.59	3.54	2.23
Muscular Function				
Q27371	Troponin T	10.85	19.25	1.77
CE09349	Major Myosin Class II heavy chain	8.16	13.88	1.70
Protein transport				
CE14954	Transport protein Sec61, alpha subunit	0.07	5.13	74.97
Energy Generation				
CE29950	F0F1-type ATP synthase, beta subunit	3.35	10.82	3.24
Other				
CE23470	Ras GTPase activating protein (GAP-2)	21.38	34.36	1.61

Peptides that were found to be oxidized upon peroxide-stress in wild type worms are shaded in grey.

Nevertheless, comparison of the fold change values of the thiol-oxidation status allows the conclusion that the loss of PRDX-2 induces endogenous oxidative stress conditions that lead to oxidative protein modifications. All of the proteins with oxidative thiol modifications potentially contribute to the physiological defects upon exogenous and endogenous oxidative stress. The proteins that were oxidized in

prdx-2 mutant worms, as well as wild type worms treated with hydrogen peroxide could potentially explain the similarities in the behavioral defects of these two groups under the same conditions. F_0F_1-ATP synthetase was one of the proteins that were oxidized upon peroxide treatment in wild type worms as well as in non-stress treated *prdx-2* worms. It has been shown that hydrogen peroxide leads to the inactivation of ATP-Synthetase and thereby decreases ATP production (Lippe et al. 1991). It will be interesting to see whether *prdx-2* worms have reduced ATP levels compared to wild type worms. Reduced energy levels could be the underlying cause for the reduced growth rate and body length of *prdx-2* worms. The other class of proteins that were highly oxidatively modified, were proteins involved in protein biosynthesis. Protein biosynthesis is a tightly regulated process and is usually cued by energy and nutrient levels. This regulation is important to shift animals from growth and nutrient utilization to states of cell maintenance and stress resistance. It is possible that oxidative stress is an additional signal to regulate and inhibit protein translation to allow the cells to cope with the stress. In addition, I found that both *prdx-2* worms and peroxide treated wild type animals have increased oxidation of major myosin class II heavy chain. Studies on intact muscles have shown that contractile function of muscles may be strongly influenced by the cellular redox balance (Crowder and Cooke 1984; Andrade et al. 1998). Especially hydrogen peroxide has been shown to change the force of the myosin fibers. Short exposure to H_2O_2, leads to an increase in the contraction force of intact frog muscle fibers, while a longer exposure leads to a decline in contractility (Oba et al. 1996). It is tempting to speculate, that the movement defects observed in oxidatively treated nematodes are at least partially induced by intracellular peroxide concentrations. In addition, the uncoordinated movement of *prdx-2* worms could be due to the extended exposure of endogenously produced hydrogen peroxide on body wall muscle cells.

These preliminary data show that endogenous peroxide stress accumulates already in young adults and is high enough to lead to oxidative protein modifications if the antioxidant capabilities of the cells are perturbed. The proteins that were found to be highly sensitive to oxidative modifications have the clear potential to serve as biomarkers for oxidative damage and might even be involved in lifespan determination.

4 Summary

In the last 15-20 years, the aging field has made tremendous progress in identifying important longevity pathways and genes involved in lifespan determination (Guarente and Kenyon 2000). Still, very little is known about the underlying cause of aging and the biochemical effects of the mutations that result in lifespan expansion. One potential cause of aging is the accumulation of oxidative damage to biomolecules (Johnson, Sinclair et al. 1999). The major drawback in analyzing the role of oxidative stress in aging organisms is the inability to define whether and when oxidative stress becomes physiologically relevant. Here, I demonstrate that *C. elegans* encounters high intracellular concentrations of peroxide even at early stages of life and harbors effective antioxidant systems that protect *C. elegans* against oxidative stress. This result suggests that the age-related decline of organisms is, at least in part, induced by endogenous peroxide stress.

During the characterization of oxidative stress-specific changes in *C. elegans* I made the important observation that exogenous oxidative stress mimics many of the known age-related effects. I then determined the proteins that are specifically modified by oxidative stress and studied their role in oxidative stress defense and lifespan. I discovered that at least one of our identified redox-sensitive proteins, the highly abundant typical 2-Cys peroxiredoxin PRDX-2 plays a major role in the oxidative stress defense of *C. elegans*. I show that knockout mutants of *prdx-2* are more oxidative stress sensitive than wild type worms and unable to recover from exogenous peroxide stress. Moreover, PRDX-2-deficient worms exert phenotypes that closely resemble changes that I identified as oxidative-stress specific defects of *C. elegans*, and which are very reminiscent of age-related changes. These results indicate that *prdx-2* mutant worms suffer from severe endogenous peroxide stress.

The reduced capability of *prdx-2* mutant worms to clear intracellular peroxide apparently becomes lifespan determining at lower cultivation temperature as *prdx-2* mutants show a 40% reduction in their adult lifespan at 15°C. These results suggest that intracellular accumulation of peroxide leads to age-associated phenotypes and affects lifespan of *C. elegans*.

This study illustrates how a combination of proteomics, biochemistry and classical genetics can be used as an alternative approach to gain insights into the role of endogenous oxidative stress in *C. elegans* aging. 2D gel analysis and subsequent biochemical analysis revealed that the active site cysteine of PRDX-2 is highly susceptible for sulfinic acid formation during peroxide stress. By identifying the protein responsible for the regeneration of overoxidized PRDX-2 in *C. elegans* (*i.e.,* sestrin) and acquiring the respective knockout strain (*sesn-1*), there is now an excellent *in vivo* read-out for endogenous H_2O_2-stress conditions in *C. elegans*. Even young animals are exposed to intracellular peroxide levels that are high enough to cause PRDX-2 overoxidation, explaining the requirement for effective antioxidant systems that protect *C. elegans* against endogenous oxidative stress.

To date, PRDX-2 is only the second ROS-detoxifying enzyme besides the peroxisomal catalase (CTL-2), whose deletion causes progeric phenotypes and a lifespan shortening effect in *C. elegans.* In contrast, deletion of either one of the two major superoxide dismutases failed to cause major phenotypical changes in worms (5). These results reflect well the very distinct chemical properties and reactivities of these two major physiological oxidants, which are often used inter-changeable in aging research. They serve as first evidence that peroxide might play a significantly more important role than superoxide in determining the lifespan of *C. elegans* and possibly other organisms. This finding has the clear potential to fundamentally

change the view of oxidative stress in aging and to influence the development of new antioxidant strategies.

5 Zusammenfassung

In den letzten 15-20 Jahren hat die Alterungsforschung enorme Fortschritte gemacht, wichtige Gene und Signalwege zu identifizieren, die mit Langlebigkeit verknüpft sind (Guarente and Kenyon 2000). Es ist jedoch immer noch wenig bekannt über die Ursachen der Alterung und über die biochemischen Auswirkungen der Mutationen die zur Verlängerung der Lebensdauer führen. Eine mögliche Ursache der Alterung ist die Anhäufung oxidativer Schäden von Biomolekülen (Johnson, Sinclair et al. 1999). Die Untersuchung der Auswirkung von oxidativem Stress auf alternde Organismen wird dadurch erschwert, dass es unmöglich ist zu definieren, ob und wann oxidativer Stress physiologisch relevant ist. Hier konnte ich zeigen, dass es in *C. elegans* schon in frühen Lebensstadien zu hohen intrazellulären Wasserstoff-peroxidkonzentrationen kommt und dass effektive Systeme vorhanden sind, die *C. elegans* vor oxidativem Stress schützen. Dieses Ergebnis zeigt, dass altersbedingte Veränderungen wenigstens zum Teil durch endogenen Peroxid-stress ausgelöst werden. Während der Charakterisierung der durch oxidativen Stress hervorgerufenen Veränderungen in *C. elegans* machte ich die wichtige Beobachtung, dass exogener oxidativer Stress ähnliche Auswirkung hat wie altersbedingte Veränderungen, die in *C. elegans* vorkommen.

Anschliessend habe ich die Proteine ermittelt, die spezifisch durch Wasserstoff-peroxid modifiziert wurden und habe ihre Rolle im Schutz vor oxidativem Stress und für Langlebigkeit untersucht. Eines der vier redox-sensitiven Proteine, die ich entdeckt habe, ist das reichlich vorhandende typische 2-Cys Peroxiredoxin PRDX-2, dass eine wichtige Rolle in der Verteidigung gegen oxidativen Stress spielt. Die Deletionsmutanten für *prdx-2* sind empfindlicher gegenüber oxidativem Stress als der Wildtyp und sind nicht fähig sich von den Effekten des Wasserstoffperoxids zu

erholen. Ausserdem erinnern die Phenotypen der *prdx-2* Würmer an die Effekte die ich als spezifisch für oxidativen Stress identifizert habe und die den alterungsbedingten Veränderungen ähnlich sind. Diese Ergebnisse weisen darauf hin, dass die *prdx-2* Mutanten erheblichem endogen Wasserstoffperoxidstress ausgesetzt sind. Die verringerte Kapazität der *prdx-2* Würmer das intrazelluläre Wasserstoffperoxid abzubauen beeinträchtigt die Lebenszeit der Würmer bei niedrigen Kultivierungstemperaturen, da diese Mutanten eine Verringerung der Lebensdauer von etwa 40% bei 15°C haben. Das könnte darauf hinweisen, dass die Ansammlung vom intrazellulären Wasserstoffperoxid zu den alterungsähnlichen Phenotypen führt und die Lebensdauer von *C. elegans* beeinflusst.

Anschliessende 2D gel Analysen und biochemische Charakteriserung zeigte, dass das katalytische Cystein von PRDX-2 empfindlich für Oxidierung zur Sulfinsäure ist. Mittels der Identifizierung des Proteins, das für die Regenerierung der reduzierten PRDX-2 in *C. elegans* verantwortlich ist (i.e. sestrin) und der Deletionsmutante (*sesn-1*) ist es nun möglich abzulesen, ob es in *C. elegans* zu intrazellulärem Wasserstoffperoxidstress kommt. Schon in frühen Lebensstadien sind die Wasserstoffperoxidkonzentrationen hoch genug um PRDX-2 zur Sulfinsäure zu oxidieren, was die Notwendigkeit effektiver Systeme zur Bekämpfung von oxidativem Stress in *C. elegans* erklärt. Diese Studie zeigt, dass Wasserstoffperoxid eine wichtige Rolle für die Bestimmung der Lebensdauer in *C. elegans* spielt und kann möglicherweise auch die Entwicklung neuer Antioxidant-Strategien beeinflussen.

6 Supplementary Section

6.1 Publications

i. Marianne Ilbert, Caroline Kumsta, Ursula Jakob
Cellular Responses to Oxidative Stress
In: Oxidative Folding of Cysteine-rich Peptides and Proteins
Editors: Johannes Buchner, Luis Moroder
In Press

ii. Caroline Kumsta, Maike Thamsen, Ursula Jakob
Effects of Oxidative Stress on Multicellular Organisms
Submitted to Genes and Development

iii. Caroline Kumsta and Ursula Jakob
The diverse family of redox-regulated chaperones
Manuscript in preparation

6.2 Presentations and congress contributions

01/2008	13th Annual Midwest Stress Response and Molecular Chaperone Meeting, Northwestern University, Evanston, IL Poster Presentation: ***Caenorhabditis elegans'*** **Peroxiredoxin-2 plays a crucial role in the resistance against oxidative stress** Caroline Kumsta, Oliver Lorenz, Maike Thamsen, Ursula Jakob

09/2007 Biology of Aging, Stockholm, Sweden

Poster Presentation:

***Caenorhabditis elegans'* Peroxiredoxin-2 plays a crucial role in the resistance against oxidative stress**

Caroline Kumsta, Oliver Lorenz, Maike Thamsen, Ursula Jakob

04/2007 Geriatrics Research Symposium, University of Michigan, Ann Arbor, MI

Poster Presentation:

Monitoring Proteomic Changes upon Oxidative stress in *C. elegans*

Caroline Kumsta, Lars Leichert, Florian Gehrke, Ursula Jakob

02/2007 12th Annual Midwest Stress Response and Molecular Chaperone Meeting, Northwestern University, Evanston, IL

Poster Presentation:

Monitoring Proteomic Changes upon Oxidative stress in *C. elegans*

Caroline Kumsta, Lars Leichert, Florian Gehrke, Ursula Jakob

11/2006 Annual Meeting of the Cellular and Molecular Biology Graduate Program, University of Michigan, Ann Arbor, MI

Poster Presentation:

Role of Oxidative Stress in *C. elegans* aging

Caroline Kumsta and Ursula Jakob

10/2006 Molecular Genetics of Aging, Cold Spring Harbor, NY

Participant

09/2006	BIF North America Meeting, Woods Hole, MA, September 2006 Talk: **Role of Oxidative Stress in *C. elegans* aging** Caroline Kumsta and Ursula Jakob
11/2005	Northwestern University, Evanston, IL Talk: **Monitoring oxidative stress in *C. elegans*** Caroline Kumsta and Ursula Jakob
2003	Molecular Genetics of Bacteria and Phages Meeting, University of Wisconsin, Madison, WI Poster Presentation: **Catalytic mechanism and substrate binding site of RrmJ, a heat shock inducible methyltransferase** Jutta Hager, Caroline Kumsta, Bart Staker, Marc Saper, Ursula Jakob

7 Acknowledgements

I would like to thank several people, without whom this thesis wouldn't have been possible. First of all, I thank my 'Doktormutter' Ursula Jakob, who initiated this work, and secondly my external 'Doktorvater' Johannes Buchner for making my stay in Michigan possible.

I thank all the members of the Jakob lab, especially Marianne Ilbert and Sara Eiseler: Without your support, your inspiration and, especially, your companionship these last years wouldn't have been half as enjoyable. Thank you for all the craziness and fun in and outside the lab. I will never forget your spirit and pranks, and, just for you two, I managed to put the words "chicken" and "frog" in my thesis! Good luck finding them!

In addition, I thank Nicolas Brandes: I enjoyed your helpful insights in our discussions about OxICAT and other things, I appreciate your honesty and sense of humor, and without question I call you my most teutonic friend.

I am grateful to Lars Leichert who was invaluable for 2D gel analysis, differential thiol trapping, OxICAT analysis and any other scientific discussion. I thank Florian Gehrke, our bioinformatician who made OxICAT analysis applicable to us and who also wrote a little script for my automatic worm scanning suite!

I am especially grateful to Maike Thamsen, who worked closely with me in the last year and did a lot of work with the sestrin mutants. You were invaluable for counting progeny, running 2D gels and many lifespan experiments. Thank you for your helping hand. I also thank all the other students that worked with me over the years: Sonja Nieratschker, Oliver Lorenz, Andreas Minsinger and Fei Li. Andreas and Fei were especially helpful with the *in vitro* characterization of PRDX-2.

I thank my other lab members Daniela Knöfler and Winnie Chen for fruitful discussions and help of any kind. I have special gratitude also for all the work studies,

especially Kyle Robertson and Chris Tobin, who kept us stocked up with everything we needed. I also thank Jim Bardwell and his lab members, especially Tim Tapley, Linda Foit and Inga Sliskovic for their various inputs, scientific and otherwise.

The University of Michigan provided an optimal research environment, and many people contributed to this thesis. I thank Györgyi Csankovszki for the use of her microscopes, the back-up supplies, and her advice. Her graduate students Karishma Sadikot and Emily Petty were very helpful when I had questions about any *C. elegans* technique. But most importantly, I am grateful to Martha Snyder who provided a helping hand any time needed, endless support and friendship.

I am grateful to Allen Hsu and Shawn Xu, also from the University of Michigan worm community, for providing me with an injection scope and the worm tracker system.

I also thank Rick Morimoto from Northwestern University and his postdoc James West for helping me get familiarized with *C. elegans* as a model organism.

I am grateful to the Boehringer Ingelheim Fonds for financial support and all the helpful seminars and resources.

I thank John Perkowski, the bright spot in my life, for his endless support and help. You make everything possible and you inspire me.

Meinem Bruder Robert und insbesondere meinen Eltern, Jitka und Stanislav, bin ich unendlich dankbar für die grenzenlose Unterstützung. Ihr wart und seid mir immer nah und Worte können meiner Dankbarkeit nicht nahekommen.

8 References

Adachi, H., Fujiwara, Y., and Ishii, N. 1998. Effects of oxygen on protein carbonyl and aging in *Caenorhabditis elegans* mutants with long (*age-1*) and short (mev-1) life spans. *J Gerontol A Biol Sci Med Sci* **53**(4): B240-244.

Aliev, G., Smith, M.A., Seyidov, D., Neal, M.L., Lamb, B.T., Nunomura, A., Gasimov, E.K., Vinters, H.V., Perry, G., LaManna, J.C., and Friedland, R.P. 2002. The role of oxidative stress in the pathophysiology of cerebrovascular lesions in Alzheimer's disease. *Brain Pathol* **12**(1): 21-35.

Alphey, M.S., Bond, C.S., Tetaud, E., Fairlamb, A.H., and Hunter, W.N. 2000. The structure of reduced tryparedoxin peroxidase reveals a decamer and insight into reactivity of 2Cys-peroxiredoxins. *J Mol Biol* **300**(4): 903-916.

Altun Z.F., H.D.H. 2002-2006. WormAtlas. In.

-. 2005a. Alimentary System - Rectum and Anus. In *WormAtlas*.

-. 2005b. Alimentary System - The pharynx. In *WormAtlas*.

Andrade, F.H., Reid, M.B., Allen, D.G., and Westerblad, H. 1998. Effect of hydrogen peroxide and dithiothreitol on contractile function of single skeletal muscle fibres from the mouse. *J Physiol* **509 (Pt 2)**: 565-575.

Apel, K. and Hirt, H. 2004. Reactive oxygen species: metabolism, oxidative stress, and signal transduction. *Annual review of plant biology* **55**: 373-399.

Apfeld, J. and Kenyon, C. 1999. Regulation of lifespan by sensory perception in *Caenorhabditis elegans*. *Nature* **402**(6763): 804-809.

Aracena-Parks, P., Goonasekera, S.A., Gilman, C.P., Dirksen, R.T., Hidalgo, C., and Hamilton, S.L. 2006. Identification of cysteines involved in S-nitrosylation, S-glutathionylation, and oxidation to disulfides in ryanodine receptor type 1. *The Journal of biological chemistry* **281**(52): 40354-40368.

Biteau, B., Labarre, J., and Toledano, M.B. 2003. ATP-dependent reduction of cysteine-sulphinic acid by S. cerevisiae sulphiredoxin. *Nature* **425**(6961): 980-984.

Blanc, A., Pandey, N.R., and Srivastava, A.K. 2003. Synchronous activation of ERK 1/2, p38mapk and PKB/Akt signaling by H2O2 in vascular smooth muscle cells: potential involvement in vascular disease (review). *Int J Mol Med* **11**(2): 229-234.

Blokhina, O., Virolainen, E., and Fagerstedt, K.V. 2003. Antioxidants, oxidative damage and oxygen deprivation stress: a review. *Ann Bot (Lond)* **91 Spec No**: 179-194.

Blumenthal, T. Trans-splicing and operons. In *WormBook* (ed. T.C.e.R. Community). WormBook.

Bolanowski, M.A., Russell, R.L., and Jacobson, L.A. 1981. Quantitative measures of aging in the nematode *Caenorhabditis elegans*. I. Population and longitudinal studies of two behavioral parameters. *Mech Ageing Dev* **15**(3): 279-295.

Bowie, A. and O'Neill, L.A. 2000. Oxidative stress and nuclear factor-kappaB activation: a reassessment of the evidence in the light of recent discoveries. *Biochem Pharmacol* **59**(1): 13-23.

Brenner, S. 1974. The genetics of *Caenorhabditis elegans*. *Genetics* **77**(1): 71-94.

Bryk, R., Lima, C.D., Erdjument-Bromage, H., Tempst, P., and Nathan, C. 2002. Metabolic enzymes of mycobacteria linked to antioxidant defense by a thioredoxin-like protein. *Science* **295**(5557): 1073-1077.

Budanov, A.V., Sablina, A.A., Feinstein, E., Koonin, E.V., and Chumakov, P.M. 2004. Regeneration of peroxiredoxins by p53-regulated sestrins, homologs of bacterial AhpD. *Science* **304**(5670): 596-600.

Chae, H.Z., Chung, S.J., and Rhee, S.G. 1994. Thioredoxin-dependent peroxide reductase from yeast. *The Journal of biological chemistry* **269**(44): 27670-27678.

Chae, H.Z., Kim, H.J., Kang, S.W., and Rhee, S.G. 1999. Characterization of three isoforms of mammalian peroxiredoxin that reduce peroxides in the presence of thioredoxin. *Diabetes research and clinical practice* **45**(2-3): 101-112.

Chang, T.S., Jeong, W., Woo, H.A., Lee, S.M., Park, S., and Rhee, S.G. 2004. Characterization of mammalian sulfiredoxin and its reactivation of hyperoxidized peroxiredoxin through reduction of cysteine sulfinic acid in the active site to cysteine. *The Journal of biological chemistry* **279**(49): 50994-51001.

Cheng, C.L., Gao, T.Q., Wang, Z., and Li, D.D. 2005. Role of insulin/insulin-like growth factor 1 signaling pathway in longevity. *World J Gastroenterol* **11**(13): 1891-1895.

Chiocchetti, A., Zhou, J., Zhu, H., Karl, T., Haubenreisser, O., Rinnerthaler, M., Heeren, G., Oender, K., Bauer, J., Hintner, H., Breitenbach, M., and Breitenbach-Koller, L. 2007. Ribosomal proteins Rpl10 and Rps6 are potent regulators of yeast replicative life span. *Experimental gerontology* **42**(4): 275-286.

Collins, J.J., Huang, C., Hughes, S., and Kornfeld, K. 2008. The measurement and analysis of age-related changes in *Caenorhabditis elegans*. *WormBook*: 1-21.

Counter, C.M., Avilion, A.A., LeFeuvre, C.E., Stewart, N.G., Greider, C.W., Harley, C.B., and Bacchetti, S. 1992. Telomere shortening associated with chromosome instability is arrested in immortal cells which express telomerase activity. *Embo J* **11**(5): 1921-1929.

Crowder, M.S. and Cooke, R. 1984. The effect of myosin sulphydryl modification on the mechanics of fibre contraction. *J Muscle Res Cell Motil* **5**(2): 131-146.

Dean, R.T., Fu, S., Stocker, R., and Davies, M.J. 1997. Biochemistry and pathology of radical-mediated protein oxidation. *Biochem J* **324 (Pt 1)**: 1-18.

Delaunay, A., Pflieger, D., Barrault, M.B., Vinh, J., and Toledano, M.B. 2002. A thiol peroxidase is an H2O2 receptor and redox-transducer in gene activation. *Cell* **111**(4): 471-481.

Deneke, S.M. 2000. Thiol-based antioxidants. *Curr Top Cell Regul* **36**: 151-180.

Egler, R.A., Fernandes, E., Rothermund, K., Sereika, S., de Souza-Pinto, N., Jaruga, P., Dizdaroglu, M., and Prochownik, E.V. 2005. Regulation of reactive oxygen species, DNA damage, and c-Myc function by peroxiredoxin 1. *Oncogene* **24**(54): 8038-8050.

Ellis, H.R. and Poole, L.B. 1997. Novel application of 7-chloro-4-nitrobenzo-2-oxa-1,3-diazole to identify cysteine sulfenic acid in the AhpC component of alkyl hydroperoxide reductase. *Biochemistry* **36**(48): 15013-15018.

Fairbanks, G., Steck, T.L., and Wallach, D.F. 1971. Electrophoretic analysis of the major polypeptides of the human erythrocyte membrane. *Biochemistry* **10**(13): 2606-2617.

Feng, Z., Li, W., Ward, A., Piggott, B.J., Larkspur, E.R., Sternberg, P.W., and Xu, X.Z. 2006. A *C. elegans* model of nicotine-dependent behavior: regulation by TRP-family channels. *Cell* **127**(3): 621-633.

Finkel, T. and Holbrook, N.J. 2000. Oxidants, oxidative stress and the biology of ageing. *Nature* **408**(6809): 239-247.

Fomenko, D.E. and Gladyshev, V.N. 2003. Identity and functions of CxxC-derived motifs. *Biochemistry* **42**(38): 11214-11225.

Fratelli, M., Gianazza, E., and Ghezzi, P. 2004. Redox proteomics: identification and functional role of glutathionylated proteins. *Expert Rev Proteomics* **1**(3): 365-376.

Fucci, L., Oliver, C.N., Coon, M.J., and Stadtman, E.R. 1983. Inactivation of key metabolic enzymes by mixed-function oxidation reactions: possible implication in protein turnover and ageing. *Proceedings of the National Academy of Sciences of the United States of America* **80**(6): 1521-1525.

Garigan, D., Hsu, A.L., Fraser, A.G., Kamath, R.S., Ahringer, J., and Kenyon, C. 2002. Genetic analysis of tissue aging in *Caenorhabditis elegans*: a role for heat-shock factor and bacterial proliferation. *Genetics* **161**(3): 1101-1112.

Gerstbrein, B., Stamatas, G., Kollias, N., and Driscoll, M. 2005. In vivo spectrofluorimetry reveals endogenous biomarkers that report healthspan and dietary restriction in *Caenorhabditis elegans*. *Aging Cell* **4**(3): 127-137.

Glantz, S.A. 2005. How to analyze survival data. in *Primer of Biostatistics* pp. 413-440. McGraw-Hill.

Goel, N.S. and Ycas, M. 1976. The error catastrophe hypothesis and aging. *J Math Biol* **3**(2): 121-147.

Guarente, L. and Kenyon, C. 2000. Genetic pathways that regulate ageing in model organisms. *Nature* **408**(6809): 255-262.

Harman, D. 1956. Aging: a theory based on free radical and radiation chemistry. *J Gerontol* **11**(3): 298-300.

Hattori, F. and Oikawa, S. 2007. Peroxiredoxins in the central nervous system. *Subcell Biochem* **44**: 357-374.

Hayflick, L. 2000. The future of ageing. *Nature* **408**(6809): 267-269.

Headlam, H.A., Gracanin, M., Rodgers, K.J., and Davies, M.J. 2006. Inhibition of cathepsins and related proteases by amino acid, peptide, and protein hydroperoxides. *Free radical biology & medicine* **40**(9): 1539-1548.

Hekimi, S. and Guarente, L. 2003. Genetics and the specificity of the aging process. *Science* **299**(5611): 1351-1354.

Herndon, L.A., Schmeissner, P.J., Dudaronek, J.M., Brown, P.A., Listner, K.M., Sakano, Y., Paupard, M.C., Hall, D.H., and Driscoll, M. 2002. Stochastic and genetic factors influence tissue-specific decline in ageing *C. elegans*. *Nature* **419**(6909): 808-814.

Hillar, A., Peters, B., Pauls, R., Loboda, A., Zhang, H., Mauk, A.G., and Loewen, P.C. 2000. Modulation of the activities of catalase-peroxidase HPI of Escherichia coli by site-directed mutagenesis. *Biochemistry* **39**(19): 5868-5875.

Hirotsu, S., Abe, Y., Okada, K., Nagahara, N., Hori, H., Nishino, T., and Hakoshima, T. 1999. Crystal structure of a multifunctional 2-Cys peroxiredoxin heme-binding protein 23 kDa/proliferation-associated gene product. *Proc Natl Acad Sci U S A* **96**(22): 12333-12338.

Hodgkin, J. and Barnes, T.M. 1991. More is not better: brood size and population growth in a self-fertilizing nematode. *Proc Biol Sci* **246**(1315): 19-24.

Hofmann, B., Hecht, H.J., and Flohe, L. 2002. Peroxiredoxins. *Biological chemistry* **383**(3-4): 347-364.

Holt, S.J. and Riddle, D.L. 2003. SAGE surveys *C. elegans* carbohydrate metabolism: evidence for an anaerobic shift in the long-lived dauer larva. *Mechanisms of ageing and development* **124**(7): 779-800.

Honda, Y. and Honda, S. 1999. The *daf-2* gene network for longevity regulates oxidative stress resistance and Mn-superoxide dismutase gene expression in *Caenorhabditis elegans*. *Faseb J* **13**(11): 1385-1393.

Hope, I.A. 1999. in *C elegans - A practical approach*
pp. 62-63. Oxford University Press, Oxford, UK.

Hoshi, T. and Heinemann, S. 2001. Regulation of cell function by methionine oxidation and reduction. *J Physiol* **531**(Pt 1): 1-11.

Hosono, R., Sato, Y., Aizawa, S.I., and Mitsui, Y. 1980. Age-dependent changes in mobility and separation of the nematode *Caenorhabditis elegans*. *Exp Gerontol* **15**(4): 285-289.

Hsu, A.L., Feng, Z., Hsieh, M.Y., and Xu, X.Z. 2008. Identification by machine vision of the rate of motor activity decline as a lifespan predictor in *C. elegans*. *Neurobiol Aging*.

Huang, C., Xiong, C., and Kornfeld, K. 2004. Measurements of age-related changes of physiological processes that predict lifespan of *Caenorhabditis elegans*. *Proceedings of the National Academy of Sciences of the United States of America* **101**(21): 8084-8089.

Hughes, S.E., Evason, K., Xiong, C., and Kornfeld, K. 2007. Genetic and pharmacological factors that influence reproductive aging in nematodes. *PLoS Genet* **3**(2): e25.

Imlay, J.A. 2003. Pathways of oxidative damage. *Annual review of microbiology* **57**: 395-418.

Isermann, K., Liebau, E., Roeder, T., and Bruchhaus, I. 2004. A peroxiredoxin specifically expressed in two types of pharyngeal neurons is required for

normal growth and egg production in *Caenorhabditis elegans*. *Journal of molecular biology* **338**(4): 745-755.

Jakob, U., Muse, W., Eser, M., and Bardwell, J.C. 1999. Chaperone activity with a redox switch. *Cell* **96**(3): 341-352.

Jang, H.H., Lee, K.O., Chi, Y.H., Jung, B.G., Park, S.K., Park, J.H., Lee, J.R., Lee, S.S., Moon, J.C., Yun, J.W., Choi, Y.O., Kim, W.Y., Kang, J.S., Cheong, G.W., Yun, D.J., Rhee, S.G., Cho, M.J., and Lee, S.Y. 2004. Two enzymes in one; two yeast peroxiredoxins display oxidative stress-dependent switching from a peroxidase to a molecular chaperone function. *Cell* **117**(5): 625-635.

Jefferies, H., Coster, J., Khalil, A., Bot, J., McCauley, R.D., and Hall, J.C. 2003. Glutathione. *ANZ J Surg* **73**(7): 517-522.

Jonsson, T.J. and Lowther, W.T. 2007. The peroxiredoxin repair proteins. *Subcell Biochem* **44**: 115-141.

Kang, S.W., Chang, T.S., Lee, T.H., Kim, E.S., Yu, D.Y., and Rhee, S.G. 2004. Cytosolic peroxiredoxin attenuates the activation of Jnk and p38 but potentiates that of Erk in Hela cells stimulated with tumor necrosis factor-alpha. *J Biol Chem* **279**(4): 2535-2543.

Keaney, M., Matthijssens, F., Sharpe, M., Vanfleteren, J., and Gems, D. 2004. Superoxide dismutase mimetics elevate superoxide dismutase activity in vivo but do not retard aging in the nematode *Caenorhabditis elegans*. *Free radical biology & medicine* **37**(2): 239-250.

Kenyon, C. 2001. A conserved regulatory system for aging. *Cell* **105**(2): 165-168.

Kinnula, V.L., Lehtonen, S., Sormunen, R., Kaarteenaho-Wiik, R., Kang, S.W., Rhee, S.G., and Soini, Y. 2002. Overexpression of peroxiredoxins I, II, III, V, and VI in malignant mesothelioma. *The Journal of pathology* **196**(3): 316-323.

Kirkwood, T.B. and Austad, S.N. 2000. Why do we age? *Nature* **408**(6809): 233-238.

Kirkwood, T.B. and Holliday, R. 1979. The evolution of ageing and longevity. *Proc R Soc Lond B Biol Sci* **205**(1161): 531-546.

Klass, M., Nguyen, P.N., and Dechavigny, A. 1983. Age-correlated changes in the DNA template in the nematode *Caenorhabditis elegans*. *Mech Ageing Dev* **22**(3-4): 253-263.

Kovacic, P. and Jacintho, J.D. 2001. Mechanisms of carcinogenesis: focus on oxidative stress and electron transfer. *Current medicinal chemistry* **8**(7): 773-796.

Krapfenbauer, K., Engidawork, E., Cairns, N., Fountoulakis, M., and Lubec, G. 2003. Aberrant expression of peroxiredoxin subtypes in neurodegenerative disorders. *Brain research* **967**(1-2): 152-160.

Kyselova, P., Zourek, M., Rusavy, Z., Trefil, L., and Racek, J. 2002. Hyperinsulinemia and oxidative stress. *Physiological research / Academia Scientiarum Bohemoslovaca* **51**(6): 591-595.

Larsen, P.L. 1993. Aging and resistance to oxidative damage in *Caenorhabditis elegans*. *Proc Natl Acad Sci U S A* **90**(19): 8905-8909.

Lee, T.H., Kim, S.U., Yu, S.L., Kim, S.H., Park, D.S., Moon, H.B., Dho, S.H., Kwon, K.S., Kwon, H.J., Han, Y.H., Jeong, S., Kang, S.W., Shin, H.S., Lee, K.K., Rhee, S.G., and Yu, D.Y. 2003. Peroxiredoxin II is essential for sustaining life span of erythrocytes in mice. *Blood* **101**(12): 5033-5038.

Leichert, L.I., Gehrke, F., Gudiseva, H.V., Blackwell, T., Ilbert, M., Walker, A.K., Strahler, J.R., Andrews, P.C., and Jakob, U. 2008. Quantifying changes in the thiol redox proteome upon oxidative stress in vivo. *Proc Natl Acad Sci U S A*.

Leichert, L.I. and Jakob, U. 2004. Protein thiol modifications visualized in vivo. *PLoS Biol* **2**(11): e333.

-. 2006. Global methods to monitor the thiol-disulfide state of proteins in vivo. *Antioxid Redox Signal* **8**(5-6): 763-772.

Link, A.J., Robison, K., and Church, G.M. 1997. Comparing the predicted and observed properties of proteins encoded in the genome of Escherichia coli K-12. *Electrophoresis* **18**(8): 1259-1313.

Lippe, G., Comelli, M., Mazzilis, D., Sala, F.D., and Mavelli, I. 1991. The inactivation of mitochondrial F1 ATPase by H2O2 is mediated by iron ions not tightly bound in the protein. *Biochemical and biophysical research communications* **181**(2): 764-770.

Liu, B., Chen, Y., and St Clair, D.K. 2008. ROS and p53: a versatile partnership. *Free Radic Biol Med* **44**(8): 1529-1535.

Macmillan-Crow, L.A. and Cruthirds, D.L. 2001. Invited review: manganese superoxide dismutase in disease. *Free Radic Res* **34**(4): 325-336.

Maryon, E.B., Saari, B., and Anderson, P. 1998. Muscle-specific functions of ryanodine receptor channels in *Caenorhabditis elegans*. *Journal of cell science* **111 (Pt 19)**: 2885-2895.

McDonagh, B. and Sheehan, D. 2008. Effects of oxidative stress on protein thiols and disulphides in Mytilus edulis revealed by proteomics: actin and protein disulphide isomerase are redox targets. *Mar Environ Res* **66**(1): 193-195.

McGhee. 1999. Biochemistry of *C. elegans*. in *A practical approach: C elegans* (ed. I.A. Hope). Oxford University Press, Oxford.

Medawar, P.B. 1952. *An Unsolved Problem of Biology*. HK Lewis & Co., London.

Medvedev, Z.A. 1990. An attempt at a rational classification of theories of ageing. *Biol Rev Camb Philos Soc* **65**(3): 375-398.

Melov, S., Ravenscroft, J., Malik, S., Gill, M.S., Walker, D.W., Clayton, P.E., Wallace, D.C., Malfroy, B., Doctrow, S.R., and Lithgow, G.J. 2000. Extension of life-span with superoxide dismutase/catalase mimetics. *Science (New York, NY* **289**(5484): 1567-1569.

Michiels, C., Raes, M., Toussaint, O., and Remacle, J. 1994. Importance of Se-glutathione peroxidase, catalase, and Cu/Zn-SOD for cell survival against oxidative stress. *Free Radic Biol Med* **17**(3): 235-248.

Miller, R.A. 2004. 'Accelerated aging': a primrose path to insight? *Aging cell* **3**(2): 47-51.

Moon, J.C., Hah, Y.S., Kim, W.Y., Jung, B.G., Jang, H.H., Lee, J.R., Kim, S.Y., Lee, Y.M., Jeon, M.G., Kim, C.W., Cho, M.J., and Lee, S.Y. 2005. Oxidative stress-dependent structural and functional switching of a human 2-Cys peroxiredoxin isotype II that enhances HeLa cell resistance to H2O2-induced cell death. *J Biol Chem* **280**(31): 28775-28784.

Moore, R.B., Mankad, M.V., Shriver, S.K., Mankad, V.N., and Plishker, G.A. 1991. Reconstitution of Ca(2+)-dependent K+ transport in erythrocyte membrane vesicles requires a cytoplasmic protein. *J Biol Chem* **266**(28): 18964-18968.

Muller, F.L., Lustgarten, M.S., Jang, Y., Richardson, A., and Van Remmen, H. 2007. Trends in oxidative aging theories. *Free radical biology & medicine* **43**(4): 477-503.

Naskalski, J.W. 1994. Oxidative modification of protein structures under the action of myeloperoxidase and the hydrogen peroxide and chloride system. *Ann Biol Clin (Paris)* **52**(6): 451-456.

Netto, L.E.S., Chae, H.Z., Kang, S.W., Rhee, S.G., and Stadtman, E.R. 1996. Removal of hydrogen peroxide by thiol-specific antioxidant enzyme (TSA) is involved with its antioxidant properties. TSA possesses thiol peroxidase activity. *The Journal of biological chemistry* **271**(26): 15315-15321.

Neumann, C.A., Krause, D.S., Carman, C.V., Das, S., Dubey, D.P., Abraham, J.L., Bronson, R.T., Fujiwara, Y., Orkin, S.H., and Van Etten, R.A. 2003. Essential role for the peroxiredoxin Prdx1 in erythrocyte antioxidant defence and tumour suppression. *Nature* **424**(6948): 561-565.

Oba, T., Koshita, M., and Yamaguchi, M. 1996. H2O2 modulates twitch tension and increases Po of Ca2+ release channel in frog skeletal muscle. *Am J Physiol* **271**(3 Pt 1): C810-818.

Olshansky, S.J. and Carnes, B.A. 1997. Ever since Gompertz. *Demography* **34**(1): 1-15.

Pachler, K., Karl, T., Kolmann, K., Mehlmer, N., Eder, M., Loeffler, M., Oender, K., Hochleitner, E.O., Lottspeich, F., Bresgen, N., Richter, K., Breitenbach, M., and Koller, L. 2004. Functional interaction in establishment of ribosomal integrity between small subunit protein rpS6 and translational regulator rpL10/Grc5p. *FEMS Yeast Res* **5**(3): 271-280.

Petriv, O.I. and Rachubinski, R.A. 2004. Lack of peroxisomal catalase causes a progeric phenotype in *Caenorhabditis elegans*. *The Journal of biological chemistry* **279**(19): 19996-20001.

Poole, L.B., Reynolds, C.M., Wood, Z.A., Karplus, P.A., Ellis, H.R., and Li Calzi, M. 2000. AhpF and other NADH:peroxiredoxin oxidoreductases, homologues of low Mr thioredoxin reductase. *European journal of biochemistry / FEBS* **267**(20): 6126-6133.

Rea, S. and Johnson, T.E. 2003. A metabolic model for life span determination in *Caenorhabditis elegans*. *Developmental cell* **5**(2): 197-203.

Reaume, A.G., Elliott, J.L., Hoffman, E.K., Kowall, N.W., Ferrante, R.J., Siwek, D.F., Wilcox, H.M., Flood, D.G., Beal, M.F., Brown, R.H., Jr., Scott, R.W., and Snider, W.D. 1996. Motor neurons in Cu/Zn superoxide dismutase-deficient mice develop normally but exhibit enhanced cell death after axonal injury. *Nat Genet* **13**(1): 43-47.

Rhee, S.G., Chae, H.Z., and Kim, K. 2005. Peroxiredoxins: a historical overview and speculative preview of novel mechanisms and emerging concepts in cell signaling. *Free Radic Biol Med* **38**(12): 1543-1552.

Rodriguez-Aguilera, J.C., Gavilan, A., Asencio, C., and Navas, P. 2005. The role of ubiquinone in *Caenorhabditis elegans* longevity. *Ageing Res Rev* **4**(1): 41-53.

Rose, M. and Charlesworth, B. 1980. A test of evolutionary theories of senescence. *Nature* **287**(5778): 141-142.

Sampayo, J.N., Gill, M.S., and Lithgow, G.J. 2003. Oxidative stress and aging--the use of superoxide dismutase/catalase mimetics to extend lifespan. *Biochem Soc Trans* **31**(Pt 6): 1305-1307.

Schrader, M. and Fahimi, H.D. 2006. Peroxisomes and oxidative stress. *Biochim Biophys Acta* **1763**(12): 1755-1766.

Schroder, E., Littlechild, J.A., Lebedev, A.A., Errington, N., Vagin, A.A., and Isupov, M.N. 2000. Crystal structure of decameric 2-Cys peroxiredoxin from human erythrocytes at 1.7 A resolution. *Structure* **8**(6): 605-615.

Seo, M.S., Kang, S.W., Kim, K., Baines, I.C., Lee, T.H., and Rhee, S.G. 2000. Identification of a new type of mammalian peroxiredoxin that forms an intramolecular disulfide as a reaction intermediate. *J Biol Chem* **275**(27): 20346-20354.

Stadtman, E.R. 2001. Protein oxidation in aging and age-related diseases. *Ann N Y Acad Sci* **928**: 22-38.

Stadtman, E.R., Starke-Reed, P.E., Oliver, C.N., Carney, J.M., and Floyd, R.A. 1992. Protein modification in aging. *Exs* **62**: 64-72.

Stiernagle, T. Maintenance of *C. elegans*. In *WormBook* (ed. T.C.e.R. Community). WormBook.

Stone, J.R. and Yang, S. 2006. Hydrogen peroxide: a signaling messenger. *Antioxid Redox Signal* **8**(3-4): 243-270.

Storz, G. and Imlay, J.A. 1999. Oxidative stress. *Current opinion in microbiology* **2**(2): 188-194.

Taub, J., Lau, J.F., Ma, C., Hahn, J.H., Hoque, R., Rothblatt, J., and Chalfie, M. 1999. A cytosolic catalase is needed to extend adult lifespan in *C. elegans* daf-C and *clk-1* mutants. *Nature* **399**(6732): 162-166.

-. 2003. A cytosolic catalase is needed to extend adult lifespan in *C. elegans* daf-C and *clk-1* mutants. *Nature* **421**(6924): 764.

Towbin, H., Staehelin, T., and Gordon, J. 1979. Electrophoretic transfer of proteins from polyacrylamide gels to nitrocellulose sheets: procedure and some applications. *Proc Natl Acad Sci U S A* **76**(9): 4350-4354.

Van Voorhies, W.A. 2002. The influence of metabolic rate on longevity in the nematode *Caenorhabditis elegans*. *Aging cell* **1**(2): 91-101.

Van Voorhies, W.A. and Ward, S. 1999. Genetic and environmental conditions that increase longevity in *Caenorhabditis elegans* decrease metabolic rate. *Proceedings of the National Academy of Sciences of the United States of America* **96**(20): 11399-11403.

Veal, E.A., Findlay, V.J., Day, A.M., Bozonet, S.M., Evans, J.M., Quinn, J., and Morgan, B.A. 2004. A 2-Cys peroxiredoxin regulates peroxide-induced oxidation and activation of a stress-activated MAP kinase. *Mol Cell* **15**(1): 129-139.

Wan, X.Y. and Liu, J.Y. 2008. Comparative proteomics analysis reveals an intimate protein network provoked by hydrogen peroxide stress in rice seedling leaves. *Mol Cell Proteomics* **7**(8): 1469-1488.

Wang, X., Phelan, S.A., Forsman-Semb, K., Taylor, E.F., Petros, C., Brown, A., Lerner, C.P., and Paigen, B. 2003. Mice with targeted mutation of peroxiredoxin 6 develop normally but are susceptible to oxidative stress. *The Journal of biological chemistry* **278**(27): 25179-25190.

Williams, G. 1957. Pleiotropy, natural selection and the evolution of senescence. in *Evolution*, pp. 398-411.

Wong, C., Sridhara, S., Bardwell, J.C., and Jakob, U. 2000. Heating greatly speeds Coomassie blue staining and destaining. *Biotechniques* **28**(3): 426-428, 430, 432.

Woo, H.A., Chae, H.Z., Hwang, S.C., Yang, K.S., Kang, S.W., Kim, K., and Rhee, S.G. 2003a. Reversing the inactivation of peroxiredoxins caused by cysteine sulfinic acid formation. *Science* **300**(5619): 653-656.

Woo, H.A., Kang, S.W., Kim, H.K., Yang, K.S., Chae, H.Z., and Rhee, S.G. 2003b. Reversible oxidation of the active site cysteine of peroxiredoxins to cysteine sulfinic acid. Immunoblot detection with antibodies specific for the hyperoxidized cysteine-containing sequence. *J Biol Chem* **278**(48): 47361-47364.

Wood, Z.A., Poole, L.B., Hantgan, R.R., and Karplus, P.A. 2002. Dimers to doughnuts: redox-sensitive oligomerization of 2-cysteine peroxiredoxins. *Biochemistry* **41**(17): 5493-5504.

Wood, Z.A., Poole, L.B., and Karplus, P.A. 2003a. Peroxiredoxin evolution and the regulation of hydrogen peroxide signaling. *Science* **300**(5619): 650-653.

Wood, Z.A., Schroder, E., Robin Harris, J., and Poole, L.B. 2003b. Structure, mechanism and regulation of peroxiredoxins. *Trends in biochemical sciences* **28**(1): 32-40.

Wu, D., Rea, S.L., Yashin, A.I., and Johnson, T.E. 2006. Visualizing hidden heterogeneity in isogenic populations of *C. elegans*. *Exp Gerontol* **41**(3): 261-270.

Yan, L.J. and Sohal, R.S. 2001. Analysis of oxidative modification of proteins. *Curr Protoc Protein Sci* **Chapter 14**: Unit14 14.

Yang, K.S., Kang, S.W., Woo, H.A., Hwang, S.C., Chae, H.Z., Kim, K., and Rhee, S.G. 2002. Inactivation of human peroxiredoxin I during catalysis as the result of the oxidation of the catalytic site cysteine to cysteine-sulfinic acid. *The Journal of biological chemistry* **277**(41): 38029-38036.

Yang, W., Li, J., and Hekimi, S. 2007. A Measurable increase in oxidative damage due to reduction in superoxide detoxification fails to shorten the life span of long-lived mitochondrial mutants of *Caenorhabditis elegans*. *Genetics* **177**(4): 2063-2074.

Yochem, J. Nomarski images for learning the anatomy, with tips for mosaic analysis. In *WormBook* (ed. T.C.e.R. Community). WormBook.

Zima, A.V. and Blatter, L.A. 2006. Redox regulation of cardiac calcium channels and transporters. *Cardiovascular research* **71**(2): 310-321.